

FRUCTOOLIGOSACCHARIDE SYNTHESIS BY IMMOBILIZED INULOSUCRASE
FROM *Lactobacillus reuteri* 121 AND IMPROVEMENT OF PRODUCT PATTERN USING
SITE-DIRECTED MUTAGENESIS



A Dissertation Submitted in Partial Fulfillment of the Requirements
for the Degree of Doctor of Philosophy in Biochemistry and Molecular Biology

Department of Biochemistry

Faculty of Science

Chulalongkorn University

Academic Year 2019

Copyright of Chulalongkorn University

การสังเคราะห์ฟรุกโตโอลิโกแซ็กคาไรด์โดยอิมูโนโกลูโคสแบบตรึงจาก *Lactobacillus reuteri* 121
และปรับปรุงรูปแบบผลิตภัณฑ์โดยการกลายเฉพาะตำแหน่ง



วิทยานิพนธ์นี้เป็นส่วนหนึ่งของการศึกษาตามหลักสูตรปริญญาวิทยาศาสตรดุษฎีบัณฑิต
สาขาวิชาชีวเคมีและชีววิทยาโมเลกุล ภาควิชาชีวเคมี
คณะวิทยาศาสตร์ จุฬาลงกรณ์มหาวิทยาลัย
ปีการศึกษา 2562
ลิขสิทธิ์ของจุฬาลงกรณ์มหาวิทยาลัย

Thesis Title	FRUCTOOLIGOSACCHARIDE SYNTHESIS BY IMMOBILIZED INULOSUCRASE FROM <i>Lactobacillus reuteri</i> 121 AND IMPROVEMENT OF PRODUCT PATTERN USING SITE- DIRECTED MUTAGENESIS
By	Mr. Thanapon Charoenwongpaiboon
Field of Study	Biochemistry and Molecular Biology
Thesis Advisor	Assistant Professor MANCHUMAS PROUSOONTORN, Ph.D.
Thesis Co Advisor	Assistant Professor RATH PICHYANGKURA, Ph.D.

Accepted by the Faculty of Science, Chulalongkorn University in Partial
Fulfillment of the Requirement for the Doctor of Philosophy

..... Dean of the Faculty of Science
(Professor POLKIT SANGVANICH, Ph.D.)

DISSERTATION COMMITTEE

..... Chairman
(Associate Professor TEERAPONG BUABOOCHA, Ph.D.)

..... Thesis Advisor
(Assistant Professor MANCHUMAS PROUSOONTORN,
Ph.D.)

..... Thesis Co-Advisor
(Assistant Professor RATH PICHYANGKURA, Ph.D.)

..... Examiner
(Associate Professor KUAKARUN KRUSONG, Ph.D.)

..... Examiner
(Assistant Professor KANOKTIP PACKDIBAMRUNG, Ph.D.)

..... External Examiner
(Emeritus Professor PIAMSOOK PONGSAWASDI, Ph.D.)

ธนพล เจริญวงษ์ไพฑูลย์ : การสังเคราะห์ฟรุกโตโอลิโกแซ็กคาไรด์โดยอินูลูซูเครสแบบตรึง
จาก *Lactobacillus reuteri* 121 และปรับปรุงรูปแบบผลิตภัณฑ์โดยการกลายเฉพาะ
ตำแหน่ง. (FRUCTOOLIGOSACCHARIDE SYNTHESIS BY IMMOBILIZED
INULOSUCRASE FROM *Lactobacillus reuteri* 121 AND IMPROVEMENT OF
PRODUCT PATTERN USING SITE-DIRECTED MUTAGENESIS) อ.ที่ปรึกษาหลัก : ผศ. ดร.
มัญชุมาส เพราะสุนทร, อ.ที่ปรึกษาร่วม : ผศ. ดร.รัฐ พิชญางกูร

ฟรุกโตโอลิโกแซ็กคาไรด์ชนิดอินูลิน (IFOS) เป็นสารพรีไบโอติกที่รู้จักกัน สามารถสังเคราะห์
ได้จากซูโครสโดยใช้เอนไซม์อินูลูซูเครส (E.C. 2.4.1.9) จากแบคทีเรีย อย่างไรก็ตาม การใช้อินูลูซูเครสใน
การสังเคราะห์ IFOS มีข้อจำกัดบางอย่าง เนื่องจากอินูลูซูเครสยังสามารถสังเคราะห์พอลิแซ็กคาไรด์
และมีความเสถียรน้อยกว่าเอนไซม์ที่ได้จากรา เพื่อลดข้อจำกัดดังกล่าว งานวิจัยนี้ได้ทำการปรับปรุงอินูลู
ซูเครสโดยใช้เทคนิคการตรึงเอนไซม์และการทำวิศวกรรมเอนไซม์ ในขั้นแรกทำการตรึงอินูลูซูเครส
จาก *Lactobacillus reuteri* 121 บนบีตาโคโตซานชนิดใหม่ที่มีความสามารถในการตรึงเอนไซม์ได้
ปริมาณมาก โดยใช้กลูตาราลดีไฮด์เป็นตัวเชื่อมโยง จากผลการทดลองแสดงให้เห็นว่าทั้งเอนไซม์อิสระ
และตรึงรูปทำงานได้ดีที่สุดที่ pH 5.5 ขณะที่อุณหภูมิที่เอนไซม์ตรึงทำงานได้ดีที่สุดเปลี่ยนจาก 50 เป็น
60 องศาเซลเซียส นอกจากนี้พบว่า เอนไซม์ตรึงมีความเสถียรมากกว่าเอนไซม์อิสระ และสามารถใช้งานได้
ได้อย่างน้อย 12 ครั้ง จากนั้นทำการปรับปรุงรูปแบบผลิตภัณฑ์ของอินูลูซูเครสโดยการกลายเฉพาะ
ตำแหน่ง จากการวิเคราะห์ผลิตภัณฑ์ แสดงให้เห็นว่าตำแหน่งกลายส่งผลอย่างมากต่อขนาดความยาว
ของ IFOS สุดท้ายนี้ได้นำอินูลูซูเครสกลาย (R483A) มาตรึงด้วยวิธี cross-linked enzyme
aggregates โดยเอนไซม์ตรึงรูปนี้มีความเสถียรที่เทียบต่อความเป็นกรด-ด่าง และอุณหภูมิเมื่อเทียบกับ
เอนไซม์อิสระ จากการศึกษาจะเห็นว่าไม่เพียงแต่จะได้เอนไซม์ชนิดใหม่ที่ผลิตโอลิโกแซ็กคาไรด์ แต่
ยังให้ข้อมูลเกี่ยวกับความสัมพันธ์ระหว่างโครงสร้างและหน้าที่ และกลไกการเกิดผลิตภัณฑ์ของอินูลู
เครส อีกด้วย

สาขาวิชา	ชีวเคมีและชีววิทยาโมเลกุล	ลายมือชื่อนิสิต
ปีการศึกษา	2562	ลายมือชื่อ อ.ที่ปรึกษาหลัก
		ลายมือชื่อ อ.ที่ปรึกษาร่วม

5772008023 : MAJOR BIOCHEMISTRY AND MOLECULAR BIOLOGY

KEYWORD: inulosucrase, fructooligosaccharide, immobilized enzyme, enzyme engineering

Thanapon Charoenwongpaiboon : FRUCTOOLIGOSACCHARIDE SYNTHESIS BY IMMOBILIZED INULOSUCRASE FROM *Lactobacillus reuteri* 121 AND IMPROVEMENT OF PRODUCT PATTERN USING SITE-DIRECTED MUTAGENESIS.
Advisor: Asst. Prof. MANCHUMAS PROUSOONTORN, Ph.D. Co-advisor: Asst. Prof. RATH PICHYANGKURA, Ph.D.

Inulin-type fructooligosaccharides (IFOS) are well-known prebiotics which can be produced from sucrose using bacterial inulosucrase (E.C. 2.4.1.9). However, the use of inulosucrase for IFOS synthesis has some limitations because it also synthesizes some polysaccharides and exhibits lower stability than the fungal enzymes. To overcome these limitations, improvement of inulosucrase was made by using enzyme immobilization and enzyme engineering. First, inulosucrase from *Lactobacillus reuteri* 121 was immobilized on a novel, high capacity core-shell chitosan beads using glutaraldehyde as a cross-linker. The results showed that both immobilized and free inulosucrase had the same optimum pH (5.5), while the optimum temperature was shifted from 50 to 60°C. In addition, the immobilized biocatalyst was more stable than the free enzyme, and could be reused for at least 12 cycles. The product pattern of inulosucrase was then improved by site-directed mutagenesis. Product characterization revealed that the mutation essentially affected the degree of polymerization (DP) of IFOS. Finally, the selected mutated inulosucrase (R483A) was immobilized by cross-linked enzyme aggregates (CLEAs). This CLEAs exhibited excellent pH and thermostability compared to that of the free enzyme. This study not only provides the novel enzyme producing oligosaccharides, but also renders the information about structure-function relationship and product formation mechanism of inulosucrase.

Field of Study: Biochemistry and Molecular Biology Student's Signature

Academic Year: 2019 Advisor's Signature

Co-advisor's Signature

ACKNOWLEDGEMENTS

I would like to express my sincere appreciation to my thesis advisor, Asst. Prof. Dr. Manchumas Prousoontorn and my co-advisor, Asst. Prof. Dr. Rath Pichyangkura, who always provide helpful, valuable, and motivated suggestions during my PhD study. I would also like to greatly thank all member of 709 Lab and Starch and Cyclodextrin Research Unit for their mentorship and helpful assistance to this research, especially in the experimental investigations. Additionally, I would like to acknowledge Prof. Dr. Robert A. Field and RAF members at John Innes Centre, UK, for generous support. I would also like to thank Dr Karan Wangpaiboon, who always gives useful comments and helpful mentorship.

Finally, I would like to thank the Science Achievement Scholarship of Thailand (SAST) for a Ph.D. scholarship. Supports from the Overseas Research Experience Scholarship for Graduate Student and Faculty of Science, Chulalongkorn University are also acknowledged. Research at the JIC is supported by the UK BBSRC Institute Strategic Program on Molecules from Nature - Products and Pathways [BBS/E/J/000PR9790] and the John Innes Foundation.

TABLE OF CONTENTS

	Page
ABSTRACT (THAI).....	iii
ABSTRACT (ENGLISH).....	iv
ACKNOWLEDGEMENTS.....	v
TABLE OF CONTENTS.....	vi
LIST OF FIGURES.....	xi
LIST OF TABLES.....	xiv
CHAPTER I.....	1
INTRODUCTION.....	1
1.1 Research rationality.....	1
1.2 Background and significance of research problem.....	2
1.3 Objectives.....	6
CHAPTER II.....	7
IMMOBILIZATION OF INULOSUCRASE FROM <i>Lactobacillus reuteri</i> 121 ON NOVEL, HIGH CAPACITY, CHITOSAN BEADS USING GLUTARALDEHYDE AS A CROSS LINKER.....	7
2.1 Abstract.....	8
2.2 Introduction.....	9
2.3 Experimental.....	11
2.3.1 Materials.....	11
2.3.2 Enzyme expression and purification.....	11
2.3.3 Preparation of HGBs, DBs, and CSBs.....	11
2.3.4 Characterization of chitosan beads.....	12

2.3.5 Immobilization of inulosucrase on HGBs and CSBs	14
2.3.6 Enzymatic activity assay	14
2.3.7 Effects of pH and temperature on the activity of free and immobilized inulosucrase.....	14
2.3.8 Sugar analysis.....	15
2.3.9 Batch production of IFOS using immobilized inulosucrase.....	15
2.3.10 IFOS synthesis in a continuous fixed-bed bioreactor with immobilized inulosucrase.....	16
2.4 Results and discussion	16
2.4.1 Expression and purification of inulosucrase	16
2.4.2 Preparation and characterization of HGBs, DBs, and CSBs	17
2.4.3 Immobilization of inulosucrase on HGBs and CSBs	21
2.4.4 Effects of pH and temperature on the activity of free and immobilized inulosucrase.....	25
2.4.5 IFOS synthesis in batch mode on INU-CSBs	29
2.4.6 IFOS synthesis in a continuous fixed-bed bioreactor on INU-CSBs	31
2.5 Conclusion	33
CHAPTER III	34
IDENTIFICATION OF OLIGOSACCHARIDE BINDING SITE OF INULOSUCRASE BY SITE- DIRECTED MUTAGENESIS	34
3.1 Abstract	35
3.2 Introduction.....	36
3.3 Materials and methods	39
3.3.1 Molecular techniques	39
3.3.2 Enzyme expression and purification	39

3.3.3 Enzyme activity assay and biochemical characterization.....	40
3.3.4 FOS production and sugar analysis	41
3.3.5 Kinetic study	41
3.3.6 Investigation of enzyme-saccharide interaction	42
3.3.7 Identification of catalytically competent binding conformations.....	42
3.4 Results	43
3.4.1 Structural analysis of LrInu and selection of mutation sites	43
3.4.2 Enzyme activity and biochemical characterization of inulosucrase with single mutations	47
3.4.3 Kinetic parameters of wild-type and mutant LrInu	48
3.4.4 Effect of mutation on FOS profiles	51
3.4.5 Identification of catalytically competent binding conformation	53
3.5 Discussion.....	56
3.6 Conclusion	62
CHAPTER IV	63
IMPROVEMENT OF PRODUCT PATTERN OF INULOSUCRASE BY RATIONAL SITE- DIRECTED MUTAGENESIS	63
4.1 Abstract	64
4.3 Materials and methods	65
4.3.1 Model construction and binding free energy calculation	65
4.3.2 Construction, expression and purification of inulosucrase	66
4.3.3 Enzyme activity assay and biochemical characterisation.....	66
4.3.4 Enzyme kinetic	67
4.3.5 FOSs synthesis and characterisation.....	67

4.4 Results and discussion	68
4.4.1 Rational protein design.....	68
4.2 Introduction.....	73
4.4.2 Activity and kinetic study of inulosucrase variants	74
4.4.3 Synthesis of FOSs by engineered inulosucrase	76
4.5 Conclusion	80
CHAPTER V	81
IMMOBILIZATION OF MUTANT INULOSUCRASE	81
5.1 Abstract	82
5.2 Introduction.....	83
5.3 Materials and Methods	84
5.3.1 Expression and purification of inulosucrase mutant	84
5.3.2 Enzyme activity assay	85
5.3.3 Preparation of cross-linked inulosucrase aggregates	85
5.3.4 Biochemical characterization of free and CLEAs R483A-LrInu.....	86
5.3.5 Oligosaccharide synthesis and analysis	86
5.3.6 Operational stability	87
5.4 Results and discussion	87
5.4.1. Preparation of immobilized inulosucrase mutant	87
5.4.2. Biochemical characterization of free and immobilized R483A-LrInu	90
5.4.3. IFOS synthesis using free and immobilized R483A-LrInu.....	91
5.4.4 Operational stability of R483A-LrInu CLEAs.....	95
5.5 Conclusion	96
CHAPTER VI	97

CONCLUSION 97

REFERENCES 99

APPENDIX..... 1

VITA..... 16



LIST OF FIGURES

Figure 1. The countries that exported the highest dollar value worth of sugar during 2018.....	2
Figure 2. Synthesis of inulin type fructooligosaccharide using inulosucrase.....	3
Figure 3. The methods of enzyme immobilization.	4
Figure 4. The approaches for enzyme engineering.....	5
Figure 5. Preparation of HGBs, DBs, and CSBs.....	13
Figure 6. Inulosucrase purification profile by DEAE toyopearl chromatography.	17
Figure 7. Light microscope magnification of dried and core-shell chitosan beads.....	18
Figure 8. BSA isotherm on DBs, HGBs and CSBs of the Langmuir model.....	20
Figure 9. SEM micrographs of HGBs, DBs and CSBs at magnification 10,000x.	21
Figure 10. Effects of pH and glutaraldehyde and enzyme concentrations on the immobilized activity and activity yield of immobilized inulosucrase.....	23
Figure 11. Volumetric activity of inulosucrase on immobilized HGBs and CSBs	24
Figure 12. Homology modeling of inulosucrase of <i>Lactobacillus reuteri</i> 121 by means of Swissmodel	25
Figure 13. Biochemical characterization of free and immobilized inulosucrase	27
Figure 14. Effects of pH and temperature on stability of free and immobilized inulosucrase.....	28
Figure 15. An HPAEC chromatogram of standard sugars, IFOS synthesized by INU-CSBs and free inulosucrase.	30
Figure 16. Batch reusability of INU-CSBs for IFOS synthesis.....	31
Figure 17. Continuous production of IFOS by immobilized inulosucrase in the fixed-bed reactor	32
Figure 18. Proposed molecular mechanism of levansucrase and inulosucrase.....	37

Figure 19. SDS PAGE of purified wild-type and mutant inulosucrase.....	40
Figure 20. Rational design of target residues for mutagenesis.....	45
Figure 21. Amino acid sequence alignment of Lrlnu from <i>L. reuteri</i> 121 and other FTFs in GH68	46
Figure 22. Specific activities of wild-type and mutant Lrlnu at 50°C.....	47
Figure 23. Optimum pH and temperature of wild-type and mutant inulosucrase.....	48
Figure 24. Graphs of relationship between initial velocity (V) and sucrose concentration for wild-type and mutant inulosucrase.....	50
Figure 25. Analysis of mutants FOS profiles by TLC and HPLC.....	52
Figure 26. TLC of FOS products synthesized from double mutant inulosucrase.	52
Figure 27. HPAEC-PAD chromatograms of wild-type and mutant FOS.....	53
Figure 28. Prediction of a catalytically competent binding conformation of fructosyl nystose (GF4) by molecular docking.	55
Figure 29. Schematic representation of proposed inulosucrase mechanism.	60
Figure 30. the FOS profile of N414A and N419A of Lrlnu analyzed by HPAEC.....	61
Figure 31. Schematic display of enzyme engineering for modulation of the size of oligosaccharide produced by glycosyltransferase.	69
Figure 32. The predicted catalytically competent binding conformations of wild type, R483A, R483F, R483Y and R483W variants by Rosetta.....	71
Figure 33. Analysis of the H/T activity.....	75
Figure 34. Effect of pH on initial velocity of wild-type and variant inulosucrase.	77
Figure 35. TLC analysis and MALDI-TOF MS spectra of FOS products synthesised by the wild-type and variant Lrlnu.....	79
Figure 36. The product specificity of wild-type and variant inulosucrase	80
Figure 37. Precipitation of R483A-Lrlnu with different precipitating agents.....	88

Figure 38. Effect of glutaraldehyde concentration, pH, incubation time and Triton-X100 treatment on the recovered activity of CLEAs.....	89
Figure 39. Effect of pH and temperature on the activity of free and CLEAs R483A-LrInu.....	91
Figure 40. Effect of pH and temperature on the stability of free and CLEAs R483A-LrInu.....	91
Figure 41. (A) TLC analysis of IFOS profiles synthesized by free and immobilized inulosucrase, (B) HPAEC chromatogram of standard sugars and IFOS synthesized by free and immobilized inulosucrase, (C) IFOS compositions analyzed by HPLC with Asahipak NH2P-50 4E column.....	93
Figure 42. MALDI-TOF analysis of IFOS synthesized by free and immobilized inulosucrase.....	94
Figure 43. Production of IFOS by R483A-LrInu CLEAs.....	95
Figure 44. Operational stability of R483A-LrInu CLEAs.....	96

LIST OF TABLES

Table 1 Inulosucrase purification data by DEAE toyopearl chromatography.	17
Table 2 Diameter of CSBs and DBs	19
Table 3 BSA adsorption analysis of HGBs, DBs, and CSBs	20
Table 4 Apparent kinetic constants of WT and mutant LrInu.....	49
Table 5 The average values of predicted binding free energy ($\Delta G_{\text{binding}}$) of GF4 in the active sites of the wild-type and variant LrInu containing a fructosyl-D272 intermediate (Fru-WT, Fru-R483A, Fru-R483F, Fru-R483Y and Fru-R483W) calculated by Rosetta.....	72
Table 6 Specific activity and kinetic parameters of WT and variant inulosucrase.....	74



CHAPTER I

INTRODUCTION

1.1 Research rationality

Since Thailand is the 2nd largest sucrose exporter in the world, the transformation of sucrose to high value oligosaccharides is very attractive (Figure 1). Many studies showed that sucrose can be used as a raw material for the synthesis of many bioactive sugars [1]. Inulin-type fructooligosaccharides (IFOS) can be synthesized from sucrose using transfructosylation activity of inulosucrase [2]. Synthesis of IFOS using inulosucrase has an advantage over β -fructofuranosidase, the enzyme commonly used for IFOS synthesis, since it possesses higher transfructosylation activity. In addition, bacterial inulosucrase can produce a broader range of oligo-fructose than that of fungal enzymes. Nonetheless, the use of inulosucrase for FOS synthesis had shown some limitations because this enzyme was poorly stable and produced some polysaccharides. In this study, the stability and product pattern of inulosucrase were improved using two strategies: enzyme immobilization and site-directed mutagenesis. To improve its stability and reusability, inulosucrase from *Lactobacillus reuteri* 121 was immobilized on novel chitosan beads using glutaraldehyde as a cross-linker. Then, the product pattern of inulosucrase was modulated using rational site-directed mutagenesis in which the target amino acid residues were selected based on 3D structure of homology modelling and bioinformatics analysis. These mutated enzymes were expected to synthesize higher yield of FOS without polysaccharides.

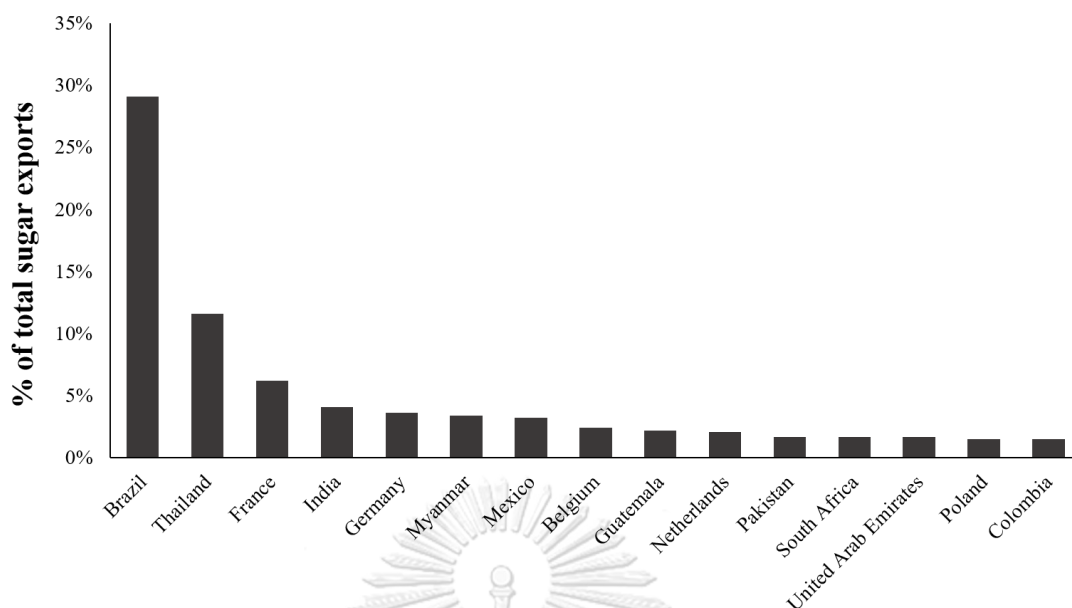


Figure 1. The countries that exported the highest dollar value worth of sugar during 2018 (<http://www.worldstopexports.com/sugar-exports-country>).

1.2 Background and significance of research problem

Inulin type fructooligosaccharides (IFOS) are oligofructose in which fructosyl residues are covalently linked by a β -2,1 glycosidic linkage. IFOS are well known as good prebiotics as they are indigestible by the human gastrointestinal tract [3]. IFOS have also been used as a low-calorie sweetener since they provide only a small amount of energy [4]. Furthermore, IFOS also stimulate immune response [5-7], improve mineral adsorption [8], and decrease levels of serum cholesterol, triacylglycerols and phospholipids [9].

Generally, IFOS were synthesized from sucrose using a β -fructofuranosidase (E.C. 3.2.1.26) derived from fungal species such as *Aspergillus niger* [10, 11], *Aspergillus japonicase* [12-14], *Aspergillus kawachii* [15], and *Aspergillus oryzae* [16]. However, the use of fungal enzymes for IFOSs is limited since they usually synthesize a short chain of IFOS with a degree of polymerization (DP) 2-4 and prefer hydrolysis to transfructosylation. Inulosucrase (E.C. 2.4.1.9) is a bacterial fructosyltransferase which was found in only some bacteria such as *Leuconostoc citreum* [17], *Lactobacillus*

reuteri [2], *Lactobacillus johnsonii* [18], *Lactobacillus gasseri* [19-21], and *Streptomyces viridochromogenes* [22]. This enzyme synthesizes IFOS and fructan (called “inulin”) using sucrose as a substrate (Figure 2). The synthesis of IFOSs using bacterial inulosucrase has an advantage over fungal β -fructofuranosidase because it possesses high transglycosylation activity and thus is suitable for an acceptor reaction. Nonetheless, the stability of this bacterial fructosyltransferase (inulosucrase) is lower than that of the fungal enzyme, and inulosucrase also produces polyfructose which is less reactive than oligofructose.

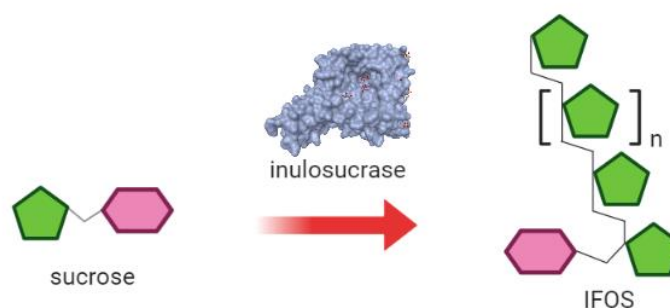


Figure 2. Synthesis of inulin type fructooligosaccharide using inulosucrase [23].

To overcome these problems, inulosucrase can be prepared as immobilized form or engineered by mutagenesis. The stability of enzyme can be improved using enzyme immobilization, a method that enzyme is attached to insoluble supports via covalent or non-covalent interaction (Figure 3). For covalent immobilization, the enzyme molecules are covalently linked to the supports using bi-functional cross-linking agents. This technique provides a very highly stable biocatalyst and prevents the enzyme leakage during the reaction. An enzyme support is a crucial part for immobilization. In general, the material used as a support for enzyme immobilization is divided into 2 groups: inorganic and organic supports. Inorganic supports, such as glass, silica gel, alumina, metal oxides and other silica-based materials, are considered as material of choice because they usually have thermal and mechanical resistance, and they are also resistant to microbial contamination. However, inorganic materials showed some limitations, such as limited biocompatibility and various geometrical

shapes were difficult to synthesize. Due to these reasons, some organic materials are also applied for the immobilization of various enzymes.

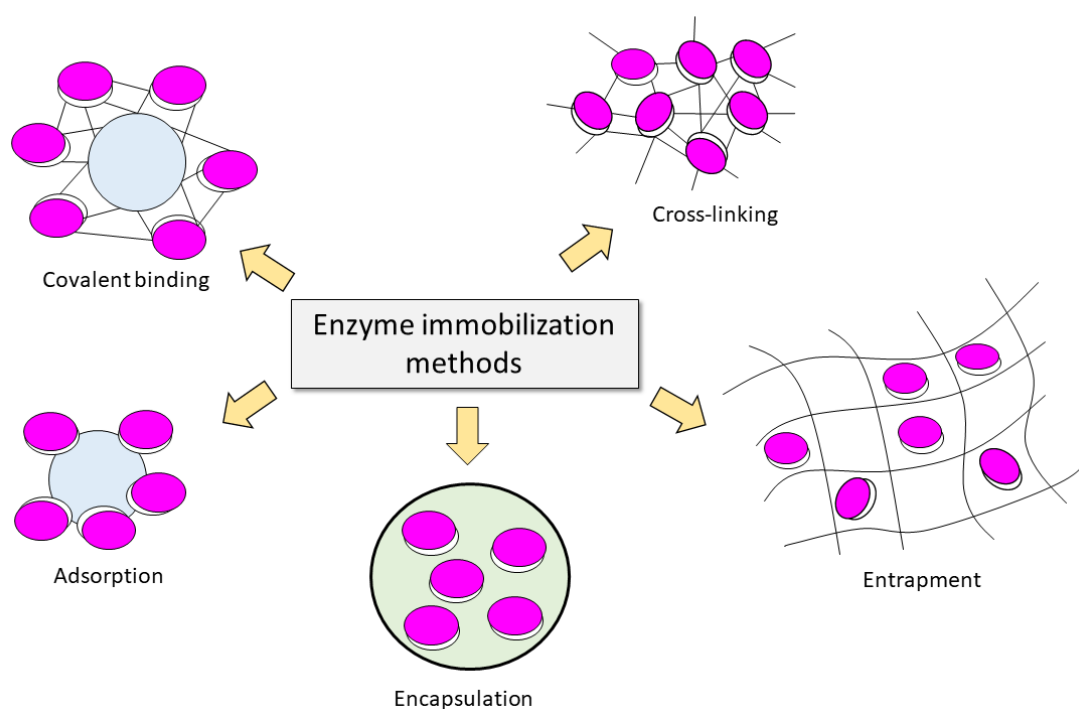


Figure 3. The methods of enzyme immobilization.

Although the properties of enzymes can be improved by immobilization, the product specificity of enzyme is difficult to improve by this technique. On the other hand, the specificity of the enzyme can be improved by enzyme engineering in which amino acid residues of the enzyme was changed by site-directed mutagenesis (Figure 4). To select the target amino acid residues, the crystal structure data and the information concerning structure-function relationship of the target enzymes are needed. Thus, molecular insight into the mechanism of inulosucrase is crucial. Many studied have shown that mutation at some specific residues of carbohydrate modifying enzymes can regulate the size of saccharide they produced. Previous studies have shown that mutation at conserved amino acid residues of *L. reuteri* 121 inulosucrase

involved in the size of oligosaccharide products. However, those mutated enzymes still synthesized the polymer which limited the IFOS production.

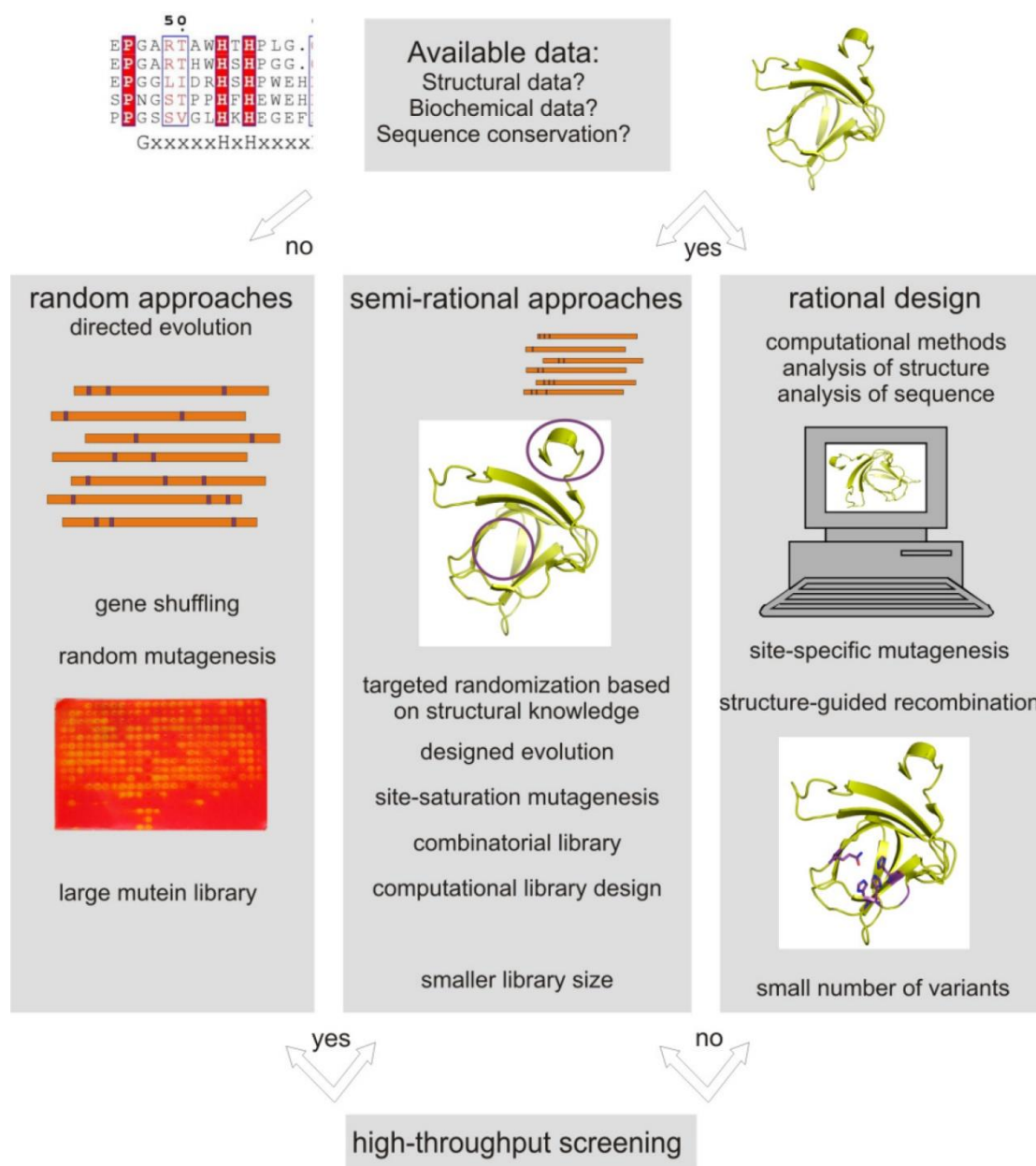


Figure 4. The approaches for enzyme engineering [24].

Our research group is interested in carbohydrate modifying enzymes, especially “sucrase” which inulosucrase belongs to. Since Thailand is the 2nd largest cane sugar (sucrose) exporter in the world, the transformation of low-price cane sugar to valuable

sugar (such as FOS) is very attractive. In this research, we focused on the production of IFOS from sucrose using inulosucrase. The stability and specificity of inulosucrase were improved using two strategies: enzyme immobilization and site-directed mutagenesis. To improve enzyme stability, Inulosucrase from *Lactobacillus reuteri* 121 was immobilized on novel chitosan beads using glutaraldehyde as a cross linker. To achieve the highest efficiency of immobilized biocatalysts, the immobilization condition such as pH, glutaraldehyde concentration and enzyme concentration was optimized. After that, the product pattern of inulosucrase was altered by rational site-directed mutagenesis. The IFOS pattern derived from mutated enzyme was characterized and compared to that of wild-type enzyme. Finally, the engineered biocatalyst was further applied for the synthesis of IFOS.

1.3 Objectives

To prepare the immobilized inulosucrase by covalent immobilization technique

To biochemically characterize the immobilized inulosucrase and compare to that of the free enzyme

To synthesize the oligosaccharides using the immobilized enzyme

To improve the product pattern using site-directed mutagenesis technique

CHAPTER II
IMMOBILIZATION OF INULOSUCRASE FROM *Lactobacillus reuteri* 121
ON NOVEL, HIGH CAPACITY, CHITOSAN BEADS USING GLUTARALDEHYDE
AS A CROSS LINKER

Highly porous core-shell chitosan beads with superb immobilization
efficiency for *Lactobacillus reuteri* 121 inulosucrase and production of inulin-
type fructooligosaccharides

Thanapon Charoenwongpaiboon^a, Karan Wangpaiboon^a, Rath Pichyangkura^a
and Manchumas Prousoontorn^a

^a Department of Biochemistry, Faculty of Science, Chulalongkorn University,
Payathai Road, Bangkok 10330, Thailand

Published in RSC advances (2018), 8(30), 17008-17016

จุฬาลงกรณ์มหาวิทยาลัย
CHULALONGKORN UNIVERSITY

2.1 Abstract

With the aim to overcome the limitations of hydrogel chitosan beads (HGBs), various types of chitosan, core–shell chitosan beads (CSBs), and dried chitosan beads (DBs) were synthesized. Physical and chemical properties were compared with those of HGBs. CSBs were proved to be an effective support because they displayed higher stability and capacity over the HGBs, and thus, were selected for enzyme immobilization. Recombinant inulosucrase (INU) from *Lactobacillus reuteri* 121 was immobilized on CSBs using glutaraldehyde as a cross-linker. Immobilized biocatalysts (INU-CSBs) were then used for the synthesis of inulin-type fructooligosaccharide (IFOS). Biochemical characterization revealed that the optimum pH of both INU-CSBs and free enzyme was unaltered at 5.5 whereas the optimum temperature of INU-CSBs shifted from 50 °C to 60 °C. Moreover, pH stability and thermostability of INU-CSBs significantly improved. For batch synthesis of IFOS, INU-CSBs retained approximately 45% of their initial catalytic activity after being reused for 12 cycles. IFOS was also continuously synthesized in a fixed-bed bioreactor for a reaction duration of at least 30 h. The high efficiency of INU-CSBs makes them very attractive for industrial applications.

2.2 Introduction

Inulin-type fructooligosaccharides (IFOSs) are oligomers of fructose in which fructose residues are covalently linked *via* a $\beta(2\rightarrow1)$ glycosidic linkage. IFOSs are well known as good prebiotics because they are indigestible by the human gastrointestinal tract [3] and thus provide only a small amount of energy [4]. Normally, IFOSs are produced *via* enzymatic activity of β -fructofuranosidase (E.C. 3.2.1.26) derived from various fungal species such as *Aspergillus niger* [10, 11], *Aspergillus japonicus* [12-14], *Aspergillus aculeatus* [25, 26], *Aspergillus awamori* [27], *Aspergillus kawachii* [15], and *Aspergillus oryzae* [16]. Nonetheless, the use of fungal enzymes had been shown to have some limitations because they prefer hydrolysis to transfructosylation, and most of the fungal enzymes specifically synthesize only a short chain of IFOS with a degree of polymerization (DP) in the range of 2–4.

Inulosucrase (E.C. 2.4.1.9) is a bacterial fructosyltransferase that can synthesize IFOS from sucrose. Inulosucrase has been identified in only a few bacterial species such as *Leuconostoc citreum* [17], *Lactobacillus reuteri* [2], *Lactobacillus johnsonii* [18], *Lactobacillus gasserii* [19-21], and *Streptomyces viridochromogenes* [22]. Structural analysis shows that bacterial inulosucrases have low structural similarity when compared to fungal β -fructofuranosidase. In contrast, they are closely related to levansucrase (E.C. 2.4.1.10), another type of fructosyltransferase, which synthesizes mainly $\beta(2\rightarrow6)$ levan-type fructooligosaccharides. Production of IFOS using inulosucrase has an advantage over fungal β -fructofuranosidase because it provides high-molecular-weight inulin and longer chains of IFOS. In addition, inulosucrase possesses high transglycosylation activity and thus is suitable for an acceptor reaction. Nevertheless, the stability of bacterial fructosyltransferase is lower than that of the fungal enzyme.

To increase the stability of a biocatalyst, the enzyme can be prepared in an immobilized form. Glutaraldehyde-mediated immobilization is a method where an enzyme and support, in some cases an enzyme and enzyme, are covalently linked by means of glutaraldehyde as a cross-linker [28]. The formation of a covalent bond is irreversible. Therefore, the enzyme cannot be released even though the reaction

conditions are changed. Chitosan-based materials have usually been employed as support because they are eco-friendly, low-cost, nontoxic and biodegradable. Furthermore, the presence of readily available amino groups in chitosan makes it readily reactive with the aldehyde group of glutaraldehyde. As a result, glutaraldehyde-activated chitosan beads can be prepared. Chitosan beads are generally prepared in a hydrogel form by a neutralization method [29]. This method is easy to use but the volumetric activity of the biocatalyst is quite low. Moreover, the structure of hydrogel beads is known to be jellylike and therefore can be easily distorted when the beads are facing a mechanical force or pressure. To achieve higher efficiency of supporting carriers, chitosan can be combined into a composite with various inorganic materials including silica [30-32], graphene oxide [33, 34], and various metal nanoparticles [35, 36]. Although the inorganic/chitosan composites have better properties than nonderivatized chitosan, the preparation of composite materials is usually complicated and incurs a high cost, which is not suitable when they are applied on an industrial scale.

In recent years, there have been many studies on the synthesis of fructooligosaccharides using immobilized bacterial levansucrase and fungal β -fructofuranosidase [37]. Nonetheless, to the best of our knowledge, there have been no reports on the immobilization of bacterial inulosucrase. Due to the structural difference between inulosucrase and β -fructofuranosidase, it is very interesting to study the production of IFOS by means of immobilized inulosucrase. In this work, various chitosan beads, namely porous core-shell chitosan beads (CSBs) and dried chitosan beads (DBs), were prepared to overcome some limitations of the jellylike form. Physical properties of the synthesized beads including surface morphology, porosity, and protein-binding capacity were studied and compared with those of normal hydrogel chitosan beads (HGBs). After that, the best chitosan beads were applied as a carrier for enzyme immobilization. Inulosucrase from *Lactobacillus reuteri* 121 (a single subunit enzyme with the MW of ~ 87 kDa) [2] was bound onto the chosen support through a covalent linkage via glutaraldehyde. The effects of immobilization conditions such as pH, glutaraldehyde, and enzyme concentration were

investigated. Biochemical properties of the immobilized enzyme were explored and compared to those of the free enzyme. Finally, the performance of the immobilized inulosucrase was further evaluated with regard to the production of IFOS in both batch and continuous processes.

2.3 Experimental

2.3.1 Materials

Chitosan polymer (MW > 600 000, degree of deacetylation > 80%) was obtained from Olizac Technologies Co., Ltd (Thailand). Standards of sugar 1-kestose and nystose were purchased from Sigma-Aldrich.

2.3.2 Enzyme expression and purification

The gene of inulosucrase from *Lactobacillus reuteri* 121 (inu; GenBank accession number AF459437) was synthesized by Genscript. The synthetic gene was subcloned into pET21-b via *Nde*I and *Xho*I sites. The recombinant vector (pETInS) was transformed into *Escherichia coli* BL21 (DE3). Plasmid-carrying *E. coli* strains were grown at 30 °C in the Luria-Bertani medium, supplemented with 100 µg/mL ampicillin, 10 mM CaCl₂, and 0.1 mM IPTG for enzyme induction. After 18 h, the cells were harvested using centrifugation (5000 × g) at 4 °C for 10 min. The cell pellet was resuspended in 50 mM sodium citrate buffer pH 5.0 and then sonicated. Cell debris were removed by centrifugation (10 000 × g, 4 °C, 15 min) to obtain the crude extract of the enzyme.

Inulosucrase was partially purified by anion exchange chromatography. The crude extract was loaded onto DEAE (Toyopearl DEAE-650M) resin that was pre-equilibrated with 25 mM potassium phosphate buffer pH 7.0 at 4 °C. The protein was eluted with the same buffer containing 50 mM NaCl. The obtained enzyme was further used for immobilization. The total protein concentration was measured by Bradford's assay [38].

2.3.3 Preparation of HGBs, DBs, and CSBs

The methodology for preparing three types of chitosan beads is summarized in Figure 5. For HGB preparation, 20 g of chitosan was dissolved in 1 L of a mixed acid

solution containing 2% (w/v) of acetic acid, 1% (w/v) of lactic acid, and 1% (w/v) of citric acid. The resulting chitosan solution was introduced dropwise into 0.8 N NaOH by a peristaltic pump. The resultant HGBs were washed with deionized water until pH became neutral. DBs were prepared by drying the HGBs obtained above at 60 °C for 24 h. For CSB preparation, DBs were soaked in a 0.5% (w/v) acetic acid solution for 60 s and then neutralized by the addition of an equal molar amount of NaOH.

2.3.4 Characterization of chitosan beads

To study the support capacity, an experiment on adsorption of a protein onto the chitosan beads was carried out. BSA served as a model protein. Approximately 0.1 g of DBs, HGBs or CSBs, which was preactivated with 1% (w/v) glutaraldehyde was incubated with a solution with a known concentration of BSA (C_0) at 4 °C for 24 h. The equilibrium concentration of BSA (C_e) was then determined on a spectrophotometer at 280 nm using 0–2 mg mL⁻¹ BSA as external standard. The adsorbed concentration (Q_e) can be calculated using the following equation: $Q_e = (C_0 - C_e)V/W$, where V is the volume of the BSA solution and W is the weight of chitosan beads (g). The Langmuir equation, $Q_e = K_L C_e / (1 + \alpha_L C_e)$, served for estimation of monolayer saturation capacity (K_L / α_L), where K_L and α_L are the isotherm parameters. Furthermore, the morphology of DBs and CSBs was also monitored under a light microscope (Leica M165 FC). All the beads were dried by critical point dryer (CPD) and were coated with gold particles prior to the scanning electron microscopy (SEM) analysis (Jeol JSM 6400).

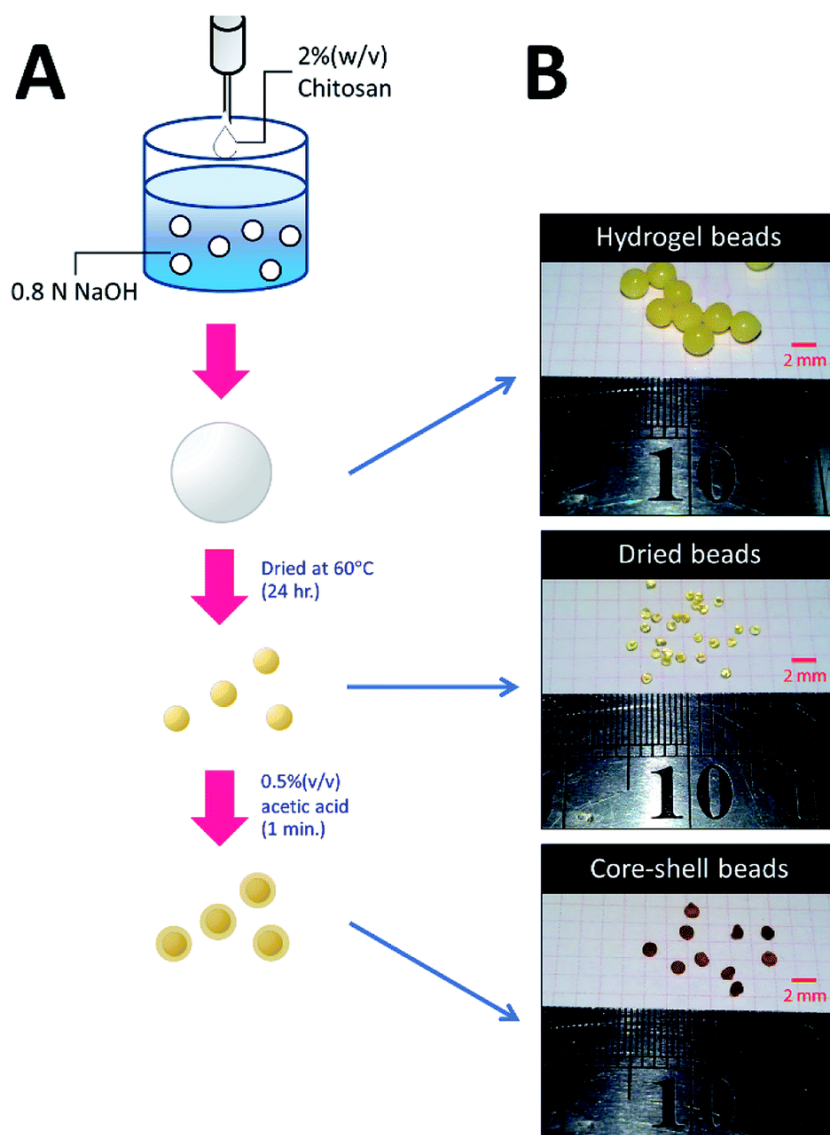


Figure 5. Preparation of HGBs, DBs, and CSBs. (A) A schematic diagram showing two-step processes for preparation of DBs and CSBs. (B) Photos of glutaraldehyde-cross-linked HGBs, DBs, and CSBs.

2.3.5 Immobilization of inulosucrase on HGBs and CSBs

To attain high efficiency of the biocatalyst, the immobilization conditions, such as pH and glutaraldehyde and enzyme concentrations, were optimized. HGBs and CSBs were activated with 0.05–8.0% (w/v) glutaraldehyde in a buffer with a pH range of 5.0–8.0 (acetate buffer pH 5.0–6.0; phosphate buffer pH 7.0–8.0) at 4 °C for 24 h. After that, the activated chitosan beads were incubated with an enzyme solution (25–800 U per g of beads; or 0.97–30.3 mg/g of beads) at 4 °C for 24 h with mild agitation. The immobilized enzymes were washed with 1 M NaCl to remove an electrostatically adsorbed enzyme and then were washed 3 times with 50 mM acetate buffer pH 5.5. The resultant immobilized enzyme was kept at 4 °C until further use. The immobilized activity and activity yield served as parameters to optimize immobilization conditions. The immobilized activity was calculated as immobilized activity (U) per gram of beads and the activity yield (%) was expressed as activity on beads (U)/[initial enzyme (U) – unbound enzyme (U)] × 100.

2.3.6 Enzymatic activity assay

Inulosucrase activity was determined by a DNS assay [39]. In brief, 10 μL of an appropriately diluted enzyme solution was added into 490 μL of a sucrose solution (250 mM of sucrose in 50 mM acetate buffer pH 5.5 with 1 mM CaCl_2) and incubated at 50 °C for 10 min. The reaction was stopped by the addition of an equal volume of the DNS reagent and then boiled for 10 min. The amount of reducing sugar was measured on a spectrophotometer at 540 nm. Glucose at concentrations 0–10 mM served as standard solutions. One unit of inulosucrase was defined as the amount of enzyme required to release 1 μmol of reducing sugar per minute under the described conditions.

2.3.7 Effects of pH and temperature on the activity of free and immobilized inulosucrase

The optimal pH for both free and immobilized inulosucrase on core–shell chitosan beads (INU-CSBs) was measured in a pH range of 3.0–8.0 at 50 °C in 50 mM citrate buffer (pH 3.0–4.5), acetate buffer (pH 4.5–6.0), or phosphate buffer (pH 6.0–

8.0). The optimum temperature for INU-CSBs and free enzyme was determined by assaying enzymatic activity in 50 mM acetate buffer pH 5.5 in a temperature range of 10–70 °C. For analysis of pH stability, the residual enzymatic activity was measured by preincubating the free and immobilized enzyme at 30 °C for 3 h at various pH levels in the Britton–Robinson universal buffer (pH 3–12). The thermostability of both enzyme samples was investigated by measuring residual activity of the enzyme after incubation in 50 mM acetate buffer pH 5.5 with 40 mM CaCl₂ at 50 °C from 0 to 12 h.

2.3.8 Sugar analysis

Identification of IFOS composition was conducted by high-performance anion exchange liquid chromatography with a pulsed amperometric detector (HPAEC-PAD ICS 5000 system, Dionex) and a CarboPack PA1 column. The column was equilibrated with 150 mM NaOH and then was eluted with a linear gradient of 0–250 mM sodium acetate in 150 mM NaOH for 30 min. Glucose, fructose, 1-kestose, and nystose served as external standards. Thin-layer chromatography (TLC) analysis was performed with a solvent system of acetonitrile : water (85 : 15, v/v). The TLC plate was dried and visualized by spraying with a solution containing 27 mL of ethanol, 10 mL of conc. H₂SO₄, 8 mL of water, and 0.1 g of orcinol.

Quantitative analysis of IFOS was performed on an HPLC system (Prominence UFLC, Shimadzu) with an amino column (Shodex Asahipak NH2P-50 4E) and a refractive index detector (SPD-M20A, Shimadzu). Samples were eluted with an isocratic solution, acetonitrile : water (65 : 35, v/v) at a flow rate of 1 mL min⁻¹. The trisaccharide 1-kestose and tetrasaccharide nystose were employed as external standards for peak quantification. Glucose was quantified with a Glucose Liquicolor Kit (Human), and total reducing sugar was quantified by the DNS assay. The molar amount of fructose was calculated from the difference between the molar amounts of reducing sugar and glucose.

2.3.9 Batch production of IFOS using immobilized inulosucrase

A preliminary experiment on IFOS synthesis was carried out at 40 °C. Ten units of free and immobilized inulosucrase (INU-CSBs) was incubated with 1 mL of 200 g/L

sucrose containing 50 mM acetate buffer pH 5.5 and 40 mM CaCl₂. After 24 h, IFOS syrup was sampled to analyze the composition by HPAEC-PAD. For the analysis of operational stability of the immobilized enzyme in a batch system, INU-CSBs were added into 200 g/L sucrose in 50 mM acetate buffer pH 5.5 with 40 mM CaCl₂ to achieve the final activity of 10 U mL⁻¹. The reaction was allowed to proceed in an orbital shaker at 40 °C for 2 h and then was stopped by removal of the biocatalyst. INU-CSBs were washed 3 times with cold 50 mM acetate buffer pH 5.5 for reutilization. The immobilized-enzyme activity of each production batch was measured by the method described above. The IFOS content was determined by HPLC. The IFOS yield was calculated as the percentage ratio of total IFOS (g/L) to initial sucrose content (g/L).

2.3.10 IFOS synthesis in a continuous fixed-bed bioreactor with immobilized inulosucrase

Five hundred units' worth of INU-CSBs was packed into a small double-jacket column with the total volume of 7 mL. The reaction was carried out at 40 °C for 30 h. The feeding solution (200 g/L sucrose in 50 mM acetate buffer pH 5.5 containing 40 mM CaCl₂) was loaded onto the column at a constant flow rate of 0.2 mL min⁻¹. The reaction mixture was sampled at certain intervals to analyze it for sugar composition by HPLC.



2.4 Results and discussion

2.4.1 Expression and purification of inulosucrase

The inulosucrase from *Lactobacillus reuteri* 121 was successfully cloned and expressed in *E. coli* BL21 (DE3) with specific activity of ~264 U per mg of protein. The recombinant inulosucrase was partially purified by anion exchange chromatography. The percent recovery of inulosucrase was 48% of the total activity with 3.9-fold purification (Figure 6 and Table 1).

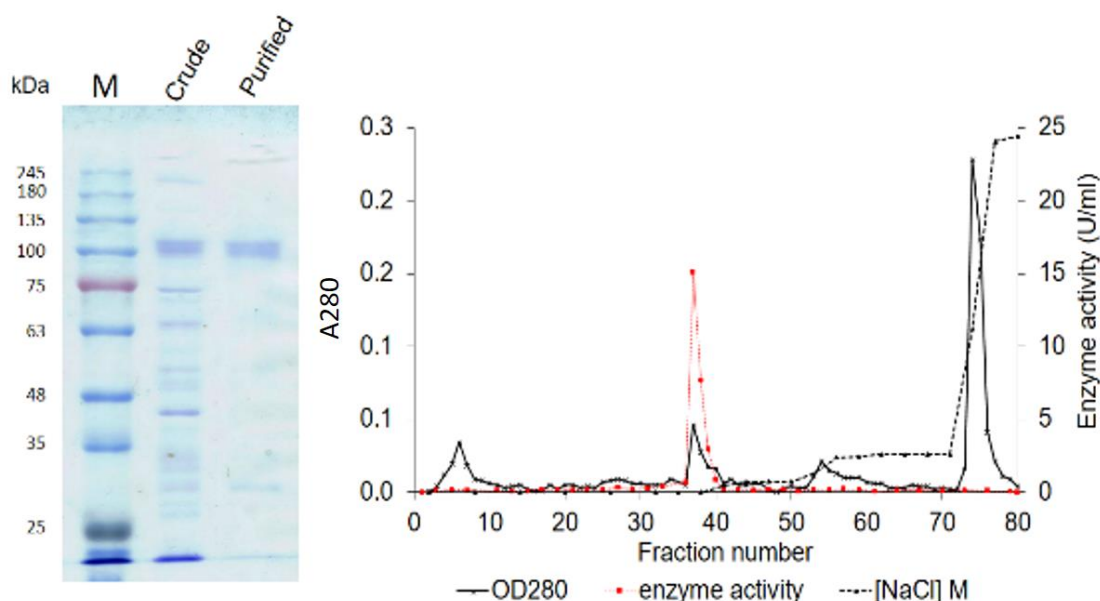


Figure 6. Inulosucrase purification profile by DEAE toyopearl chromatography.

Table 1. Inulosucrase purification data by DEAE toyopearl chromatography.

step	Volume (ml)	Protein (mg)	Activity (U)	Specific activity (U/mg)	Purification (fold)	Yield (%)
Crude	20	18.3	1.23×10^3	67.0	1	100
DEAE-toyopearl	23	2.22	587	264	3.94	49

2.4.2 Preparation and characterization of HGBs, DBs, and CSBs

To increase the surface area of chitosan beads, their volume was reduced by dehydrating the interior. In the present study, HGBs were dried at 60 °C for 24 h. Light microscopy showed that the shape of the resulting DBs was nearly spherical with a diameter of approximately ~ 1.3 mm (Figure 7A, Table 2). The reduction of bead diameter caused an increase of the surface area per volume ratio of the beads. As presented in Figure 5B, the size of DBs and CSBs was much smaller than that of HGBs. Furthermore, the resulting DBs were found to be more rigid than HGBs. Although this finding indicated that the compactness of the chitosan polymer after removal of adsorbed water improved the mechanical stability of the beads, the analysis of BSA

adsorption revealed that protein-binding capacity of DBs was much lower than that of HGBs (Table 3, Figure 8). The decrease in protein-binding capacity could be explained by the fact that the reactive surface of HGBs might have collapsed after drying. To recover the protein-binding capacity of DBs, the solid surface of DBs was next modified.

Reswelling of the solid beads in a dilute acetic acid solution for a while is a simple technique that can produce a highly reactive surface of solid chitosan beads. An adsorption assay using BSA as a model protein showed that the capacity of CSBs for protein binding was recovered up to $6.68 \text{ mg (mL}^{-1} \text{ beads)}$ (Table 3), which is approximately 2-fold higher than that of HGBs (3.24 mg/mL beads) and 43-fold higher than that of DBs ($0.157 \text{ mg/mL beads}$). The increase in protein-binding capacity of CSBs could have resulted from the increase of their surface area after the swelling. Light microscopy indicated that there was a thin layer of a chitosan gel around a solid core (Figure 7B). The thickness of this layer was found to be $\sim 0.1 \text{ mm}$ (Table 2). Thus, it did not significantly affect the whole size of the beads.

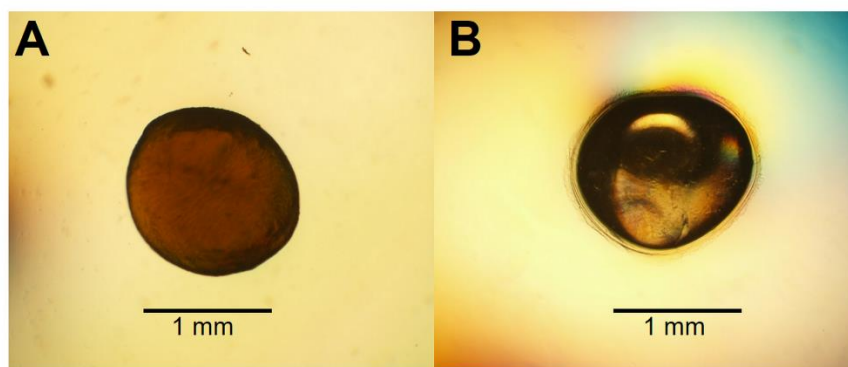


Figure 7. Light microscope magnification of (A) dried and (B) core-shell chitosan beads.

Table 2. Diameter of CSBs and DBs

CSBs diameter (mm)					DBs diameter (mm)	
No.	Total	Core	Shell	Shell/Core ratio	No.	Total
1	1.19	1.08	0.11	0.10	1	1.43
2	1.30	1.21	0.09	0.07	2	1.23
3	1.27	1.14	0.13	0.11	3	1.30
4	1.43	1.31	0.13	0.10	4	1.17
5	1.12	1.01	0.11	0.11	5	1.35
6	1.34	1.21	0.13	0.11	6	1.25
7	1.16	1.09	0.07	0.06	7	0.01
8	1.15	1.06	0.09	0.09	8	1.12
9	1.36	1.26	0.10	0.08	9	1.38
10	1.35	1.25	0.10	0.08	10	1.32
11	1.19	1.12	0.07	0.06	11	1.23
12	1.17	1.07	0.11	0.10	12	1.42
13	1.24	1.14	0.10	0.09	13	1.21
14	1.31	1.19	0.12	0.10	14	1.37
15	1.29	1.18	0.11	0.09	15	1.19
16	1.40	1.30	0.10	0.08	16	1.50
17	1.20	1.09	0.12	0.11	17	1.35
18	1.15	1.10	0.05	0.05	18	1.20
19	1.29	1.20	0.09	0.08	19	1.24
20	1.17	1.10	0.08	0.07	20	1.07
21	1.26	1.17	0.08	0.07	21	1.21
22	1.27	1.17	0.10	0.08	22	1.36
23	1.11	1.04	0.07	0.07	23	1.41
24	1.21	1.13	0.09	0.08	24	0.97
25	1.12	1.02	0.10	0.10	25	1.33
26	1.47	1.34	0.13	0.10	26	1.39
27	1.30	1.18	0.12	0.10	27	1.40
28	1.40	1.27	0.13	0.10	28	1.28
29	1.07	0.99	0.08	0.08	29	1.39
30	1.32	1.22	0.11	0.09	30	1.28
31	1.14	1.05	0.09	0.08	31	1.17
32	1.54	1.35	0.19	0.14	32	1.17
33	1.19	1.09	0.10	0.09	33	1.34
34	1.36	1.20	0.16	0.14	34	1.30
35	1.24	1.08	0.16	0.15	35	1.35
Mean	1.26	1.15	0.11	0.09	Mean	1.25
SD	0.11	0.10	0.03	0.02	SD	0.24

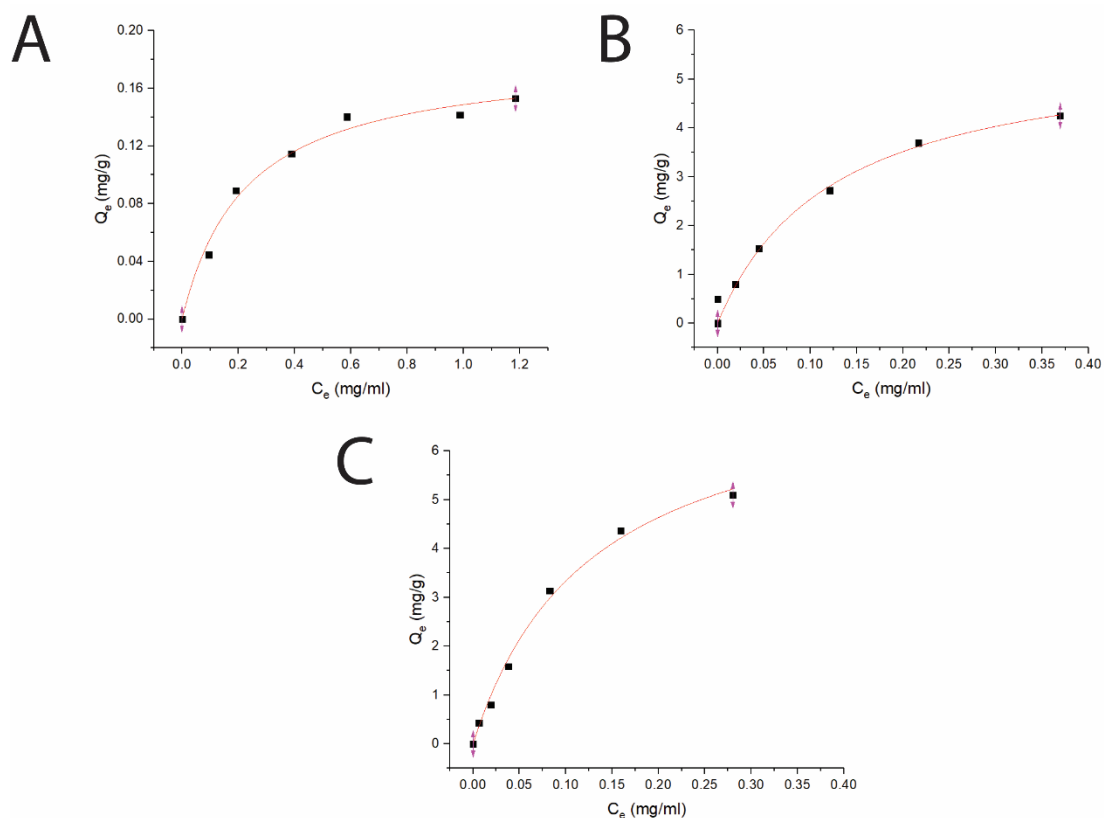


Figure 8. BSA isotherm on DBs (A), HGBs (B) and CSBs (C) of the Langmuir model.

Table 3. BSA adsorption analysis of HGBs, DBs, and CSBs

Beads	Bead density ^a (g/ml)	Protein binding capacity (mg/g)	Volumetric capacity ^b (mg/ml)
HGBs	0.568 ± 0.013	5.70 ± 0.18	3.24
DBs	0.862 ± 0.010	0.182 ± 0.011	0.157
CSBs	0.878 ± 0.032	7.61 ± 0.56	6.68

^a Gram of the bead packed in known volume of cylinder.

^b Volumetric capacity (mg/mL) = bead density (g/mL) × protein binding capacity (mg/g)

The morphology and porous structure of the beads were then further analyzed by SEM (Figure 9). The results showed that the external surface of HGBs and CSBs had high porosity whereas the DB surface was quite smooth. This observation indicated that reswelling process in the dilute acetic acid solution could regenerate the surface

porosity but did not affect rigidity of the core. Preparation of novel core–shell beads by this simple method can overcome the limitations of the traditionally synthesized hydrogel beads. CSBs did not only ensured higher stability of organic-based support but also enabled binding of the large amount of the enzyme, and thus, CSBs were selected for enzyme immobilization.

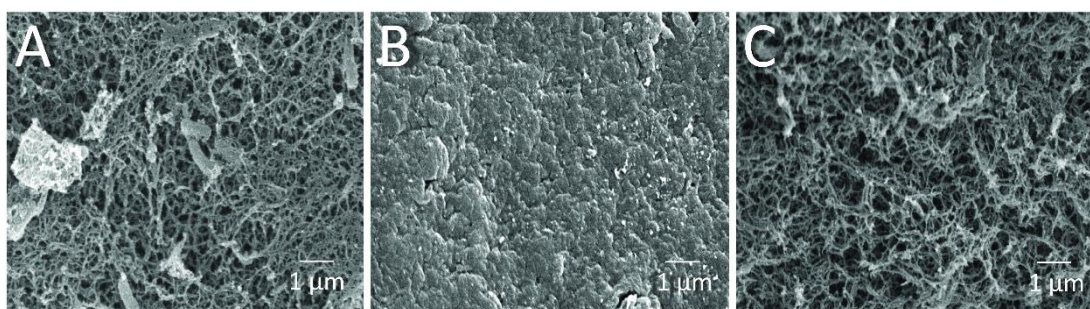


Figure 9. SEM micrographs of (A) HGBs, (B) DBs and (C) CSBs at magnification 10,000x.

2.4.3 Immobilization of inulosucrase on HGBs and CSBs

Due to the high protein-binding capacity of HGBs and CSBs, they were applied as supports for the immobilization of inulosucrase. The preparation of the immobilized enzyme via glutaraldehyde usually involves two steps: the first is activation of amino-functionalized beads using glutaraldehyde, and the second is covalent attachment of the enzyme to the activated beads [28, 40]. The immobilization conditions such as pH and glutaraldehyde and enzyme concentrations were optimized because the structure of glutaraldehyde and thus the immobilization efficiency are largely dependent on solution conditions [41, 42]. First, the effect of pH on immobilized activity and activity yield was investigated by fixing glutaraldehyde concentration and the initial enzyme amount in units at 1% (w/v) and 50 U per g of beads, respectively (Figure 10A). The activity assay revealed that the immobilized enzyme worked best at pH 7.0. Both INU-HGBs and INU-CSBs showed maximum immobilized activity of approximately 33.4 ± 1.5 and 33.2 ± 2.2 U/g with the activity yield of approximately $60.7\% \pm 5.7\%$ and $72.1\% \pm 4.6\%$, respectively. The highest activity of immobilized enzymes at this pH might have resulted from the irreversible formation of covalent bonds between glutaraldehyde and amino groups in the pH range of 7.0–9.0 [41, 42]. Moreover, higher

pH is conducive to the polymeric form of glutaraldehyde rather than monomeric form and reduces steric hindrance between the enzyme and support [41, 42].

Second, the effect of glutaraldehyde concentration (0.05–8.0%, w/v) on the immobilization procedure was then investigated at pH 7.0 (Figure 10B). The results showed that the immobilized activity and activity yield increased with an increase in glutaraldehyde concentration. Nevertheless, when glutaraldehyde concentration was higher than 1% (w/v), the immobilized activity did not increase. This finding indicated that the increase in glutaraldehyde concentration resulted in more covalent bonds per enzyme molecule and therefore may cause a conformational change of the enzyme. In addition, at a higher concentration of glutaraldehyde, there is good chance of a covalent modification close to the active site of the enzyme leading to enzyme inactivation.

Finally, the influence of enzyme concentration on enzyme immobilization was examined by incubating activated chitosan beads (1% (w/v) glutaraldehyde), with different concentrations of the enzyme (Figure 10C). Readers can see that when the amount of inulosucrase added per gram of beads increased from 0 to 400 U/g, the activity of INU-HGBs and INU-CSBs rapidly increased. After that, the activity of both immobilized-enzyme samples reached a plateau. This result might be explained as follows: the reactive groups on the support were saturated with the enzyme. In addition, INU-CSBs showed approximately 1.5- to 2.5-fold higher volumetric activity of the packed biocatalyst as compared with INU-HGBs when the same concentration of the enzyme was added (Figure 11). This result is consistent with the above finding that CSBs have higher protein-binding capacity than HGBs. Although the immobilized activity of both immobilized enzymes increased with enzyme concentration, their activity yield was found to decrease. The substantial enzyme loading on the support generally leads to a reduction in the activity yield owing to steric hindrance. Consequently, substrates were prevented from accessing the active site of the enzyme. This could also result from the diffusional effect of substrate and product to and from the immobilized enzyme molecules. For further analysis, an enzyme concentration of 50 U/g was chosen because it provided the highest activity yield of approximately $63.7\% \pm 6.5\%$ and $68.2\% \pm 7.8\%$ for INU-HGBs and INU-CSBs, respectively.

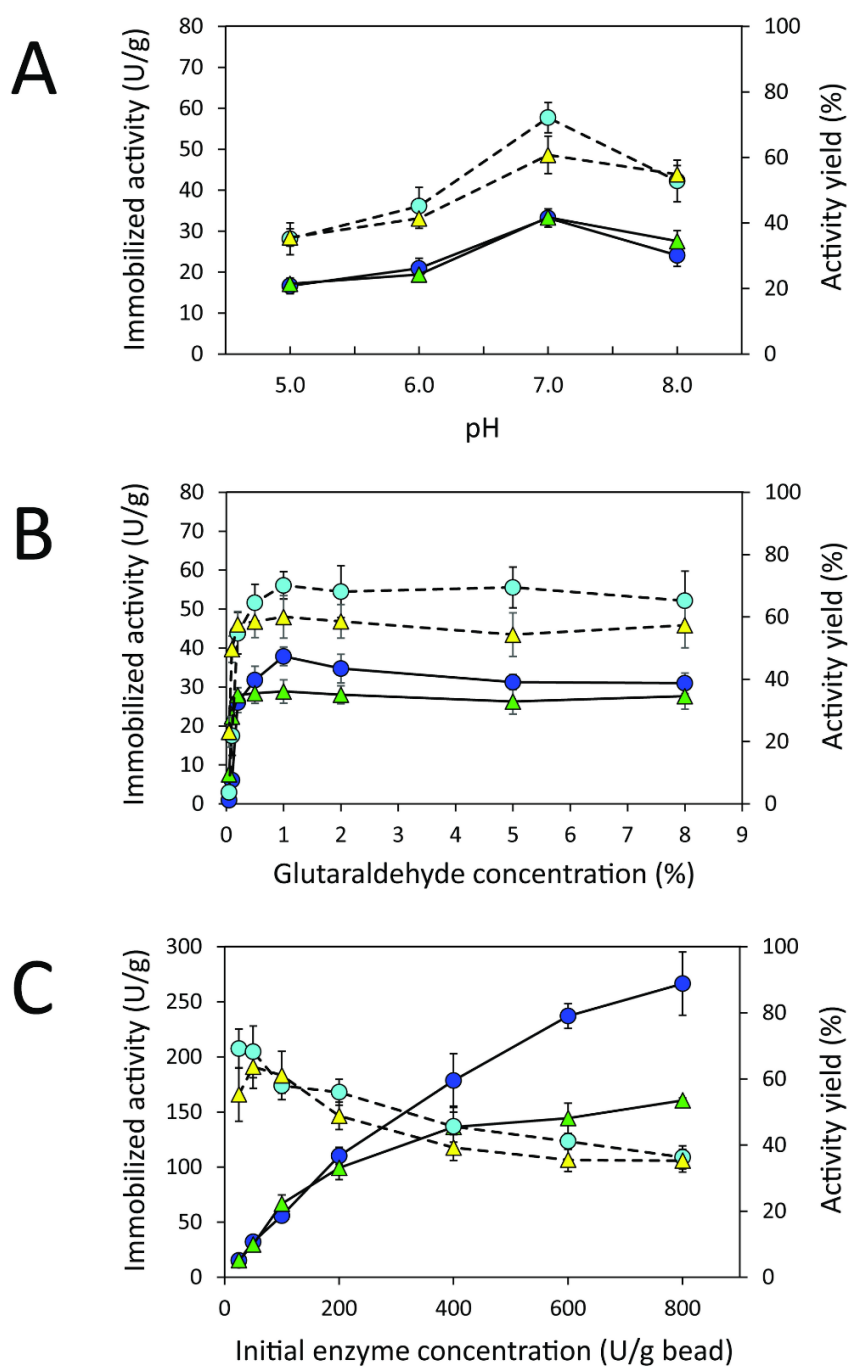


Figure 10. Effects of (A) pH and (B) glutaraldehyde and (C) enzyme concentrations on the immobilized activity (▲, INU-HGB; ●, INU-CSB) and activity yield (▲, INU-HGB; ●, INU-CSB) of immobilized inulosucrase. The data represent means of five assays and error bars represent the standard deviation of five experiments.

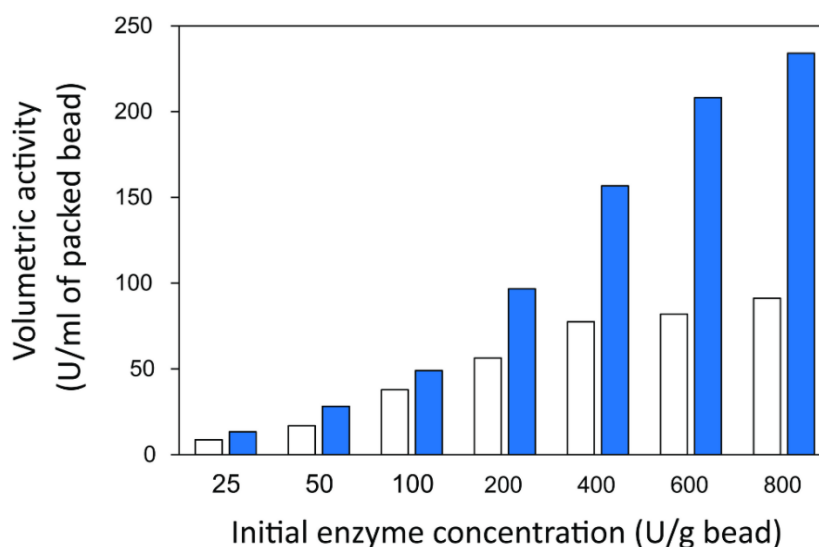


Figure 11. Volumetric activity of inulosucrase on immobilized HGBs (white bars) and CSBs (blue bars).

The homology modeling of the three-dimensional (3D) structure of inulosucrase revealed that the immobilization via a glutaraldehyde linkage is appropriate because lysine residues, which can readily react with the aldehyde group of glutaraldehyde, are located on the enzyme surface, not in the active site (Figure 12). This finding has been reported in the case of levansucrase from *Z. mobilis* immobilized on vinyl-sulfone activated silica [43]. Because INU-CSBs had higher stability and activity of the immobilized enzyme than INU-HGBs did, INU-CSBs were further characterized and chosen as a biocatalyst for the synthesis of IFOS.

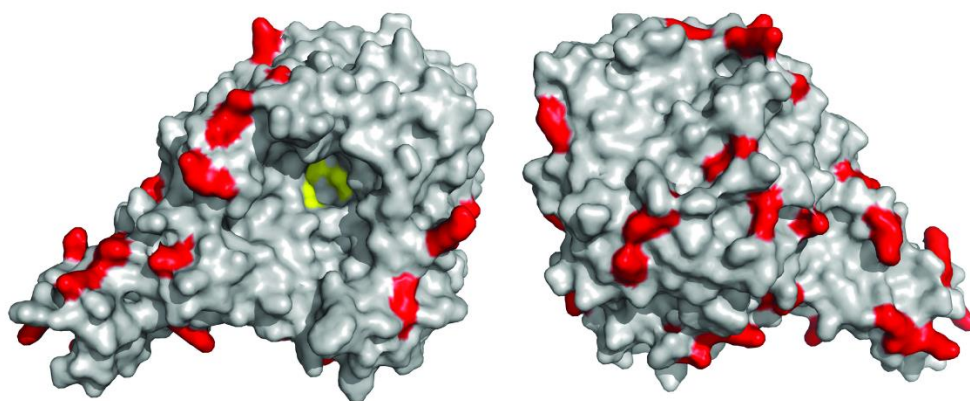


Figure 12. Homology modeling of inulosucrase of *Lactobacillus reuteri* 121 by means of Swissmodel, using the 3D structure of inulosucrase from *Lactobacillus johnsonii* NCC 533 (Protein Data Bank [PDB] ID: 2YFR, 73% identity) as a template. On the left is a frontal view, and on the right is the posterior view of protein; Lys residues are red, and three catalytic residues are yellow.

2.4.4 Effects of pH and temperature on the activity of free and immobilized inulosucrase

An immobilization process may change the kinetics and other properties of an enzyme [44]. Enzymes are sensitive to changes in pH and can work best within their limited optimal pH range. After immobilization, the biochemical properties of INU-CSBs were studied and compared with those of the free enzyme. The free and immobilized enzymes had the same optimal pH, 5.5 (Figure 13A), whereas the reaction temperature optima of inulosucrase were found to shift from 50 °C to 60 °C after immobilization (Figure 13B). In addition, immobilization of inulosucrase showed a protective effect even at 70 °C, whereas the free enzyme lost all activity at the same temperature. This finding indicated that our immobilization technique gave greater stability to the enzyme, which was still able to function at a high temperature. The increase of optimal temperature of enzymes after immobilization had been reported in the case of *Aspergillus* β -glucosidase immobilized on chitosan [45]. For analysis of pH stability, the retention of activity of both biocatalyst samples was measured after incubation at various pH levels at room temperature (30 °C) for 3 h. The results revealed that both free and immobilized enzymes were stable in a broad pH range: 2.0–10.0. Nonetheless,

the enzyme of INU-CSBs was more stable than the free enzyme because it retained approximately 100% of its initial activity, whereas the free enzyme retained only 80% at pH 4.0–8.0 (Figure 14A). The high stability of INU-CSB activity suggested that CSBs provided a microenvironment for enzyme molecules that prevented their conformational change during a pH change in the bulk solution. This phenomenon is known for immobilized α -amylase [46] and tannase [47].



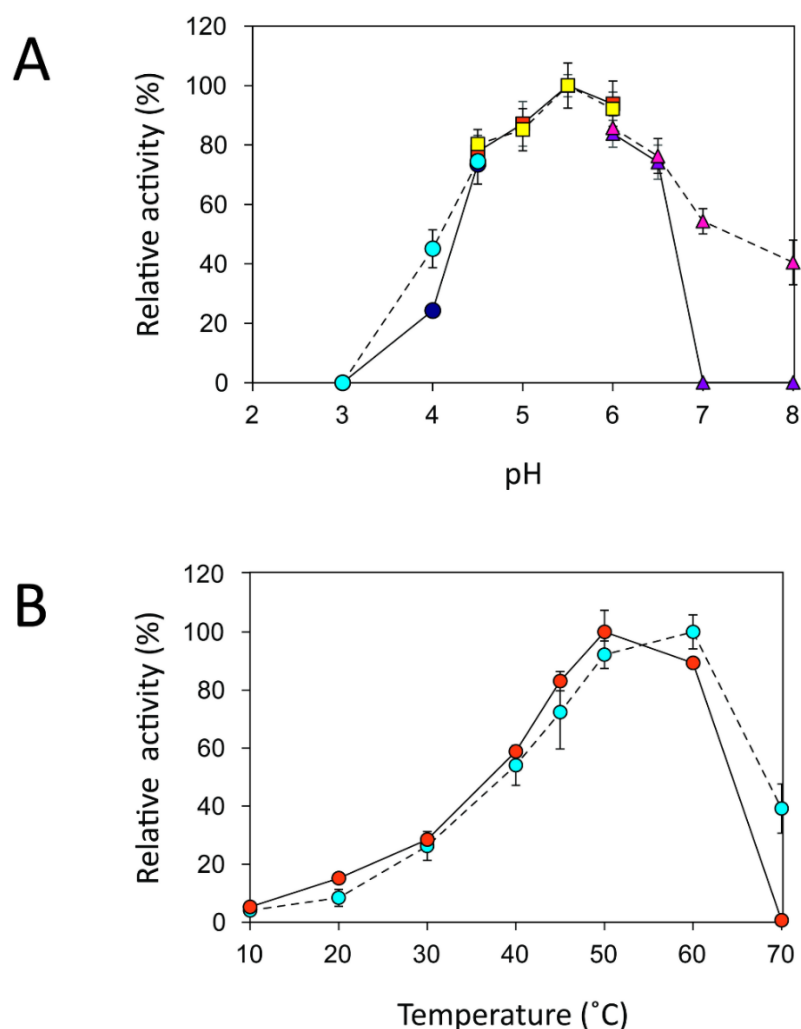


Figure 13. Biochemical characterization of free and immobilized inulosucrase. (A) Effects of pH on activity of free (●, citrate buffer; ■, acetate buffer; ▲, potassium phosphate buffer) and immobilized (●, citrate buffer; ■, acetate buffer; ▲, potassium phosphate buffer) inulosucrase when the reaction was carried out at 50°C. (B) Effects of temperature on the activity of free (●) and immobilized (●) inulosucrase when the reaction was carried out at pH 5.5. Approximately 15 U of INU-CSBs or free inulosucrase were used for these experiments.

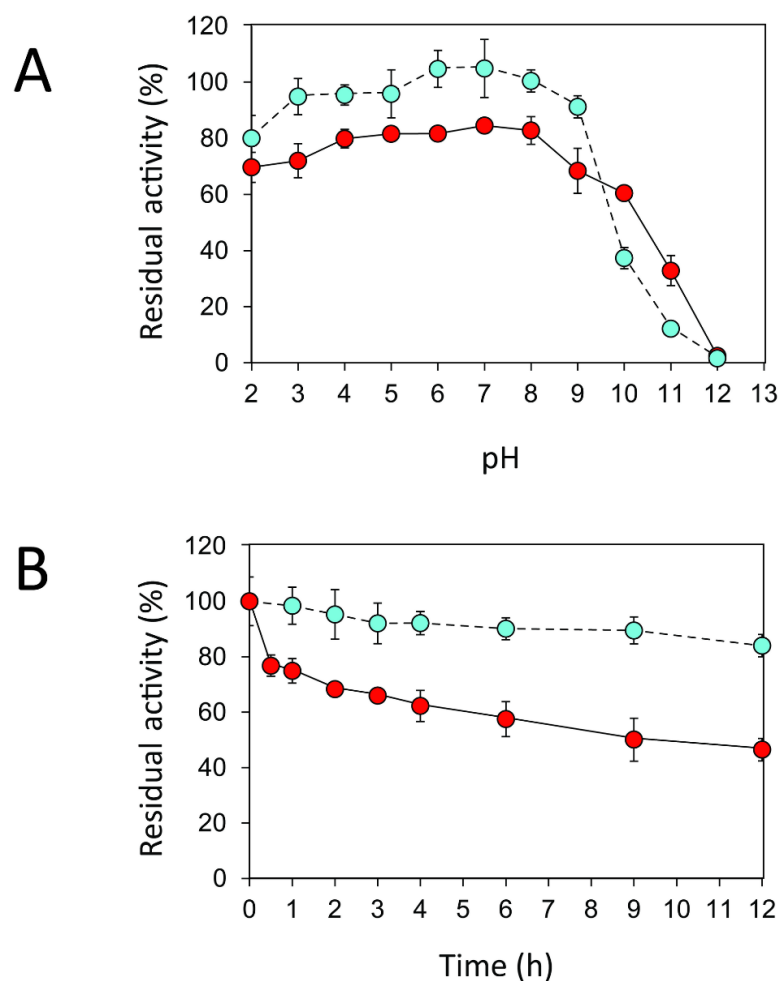


Figure 14. Effects of (A) pH and (B) temperature on stability of free (●) and immobilized (●) inulosucrase. Approximately 15 U of INU-CSBs or free inulosucrase were used for these experiments.

Because activity and stability of inulosucrase are largely dependent on Ca^{2+} concentration, thermostability of the biocatalyst was studied in a buffer containing 40 mM CaCl_2 (see APPENDIX). As shown in Figure 14B, the thermostability of INU-CSBs was higher than that of the free enzyme. INU-CSBs retained $\sim 84\%$ of activity after incubation at 50 °C for 12 h, whereas the residual activity of the free enzyme was lower than 50% under the same conditions. This phenomenon has been observed in many studies. For example, *Aspergillus aculeatus* β -fructofuranosidase that was immobilized on chitosan beads retains $\sim 100\%$ of activity after incubation at 50 °C for 50 h, while the free β -fructofuranosidase retains only 50% of activity at the same

temperature [25]. β -Fructofuranosidase from *Aspergillus japonicus* loses almost all the activity after incubation at 37 °C for 7 days, whereas the immobilized enzyme retains approximately 60% [14]. The enhanced thermostability of INU-CSB may result from the increase of enzyme rigidity after covalent linking onto the support. This approach has provided many advantages for industrial applications. For example, inulosucrase needs to use sucrose as a substrate, but at a high concentration of a sucrose, the solution is viscous. The reaction then needs to be conducted at a higher temperature to lower the viscosity. In addition, at the temperature higher than 50 °C, the growth of some pathogenic microorganisms will be stopped [48].

2.4.5 IFOS synthesis in batch mode on INU-CSBs

Although immobilization of an enzyme through multiple covalent bonds provides a stable biocatalyst, it may cause a conformational change of the enzyme [49]. Because 3D structure of an enzyme determines the specificity for substrates or products that they catalyze or synthesize, it is possible that the product patterns of a free and immobilized enzyme may be different. To investigate the effect of immobilization on the IFOS profile, a qualitative analysis of IFOS derived from both free and immobilized enzymes was performed by HPAEC-PAD. In this work, IFOS was synthesized by incubating 10 U/mL INU-CSB or free enzyme with 200 g/L sucrose at pH 5.5 and 40 °C for 24 h. HPAEC analysis showed that the pattern of products synthesized by INU-CSBs and free enzyme were comparable (Figure 15). The IFOS products contained at least eight different oligosaccharides. In comparison with 1-kestose and nystose standards, the resulting oligosaccharides were IFOSs in which fructose is covalently linked *via* the $\beta(2\rightarrow1)$ linkage. The results indicated that immobilization did not affect the product pattern of the enzyme.

One of the advantages of the immobilized enzyme in industrial applications is its reusability. The operational stability of INU-CSB was evaluated in a series of batch reactions. The IFOS synthesis by INU-CSB was performed at 200 g/L sucrose as a substrate. After 2 h of incubation of each batch, the retained activity of INU-CSBs was measured, and IFOS content was then analyzed.

As shown in Figure 16, the IFOS amount synthesized by the first batch was the highest, 70.9 ± 8.7 g/L, with the yield of $35.4\% \pm 4.4\%$. After that, it gradually decreased and seemed to be constant at ~ 30 g/L IFOS (16% yield) after six cycles of reuse. The reduction of the IFOS amount in the early cycles correlated with the retained activity of the biocatalyst. INU-CSBs retained $\sim 60\%$ of activity after the first 4 cycles and remained quite stable at approximately 45% even though it was reused for 12 cycles. This loss of activity in early cycles is characteristic of covalent immobilization because enzyme molecules that are noncovalently attached to the carrier may be desorbed by polarity of a sugar solution [43].

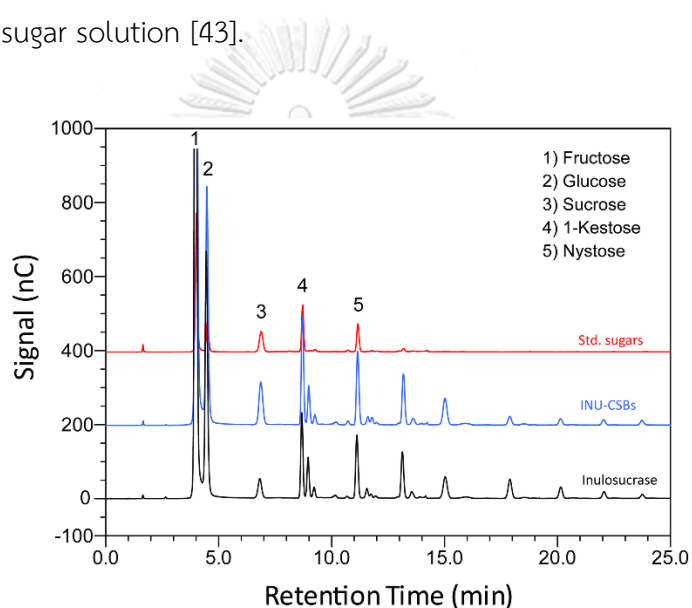


Figure 15. An HPAEC chromatogram of standard sugars, IFOS synthesized by INU-CSBs and free inulosucrase. IFOS was synthesized by incubating 10 U/mL biocatalysts with 200 g/L sucrose at 40°C for 24 h.

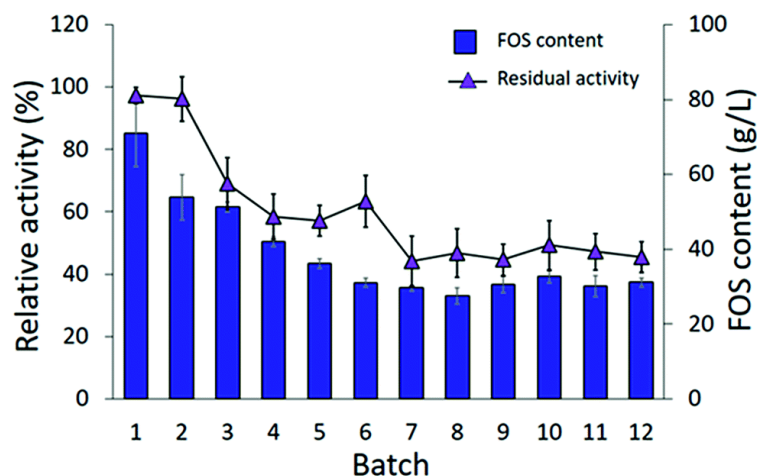


Figure 16. Batch reusability of INU-CSBs for IFOS synthesis. Reaction condition: 10 U/mL of biocatalysts were incubated with 200 g/L sucrose in acetate buffer pH 5.5, 40°C and 2 h per batch.

Moreover, it is possible that the population of enzyme molecules that was differently attached to the support may be less stable than the others. These molecules may be denatured or degraded after early cycles of reuse, whereas some enzyme molecules still retain their activity even after many cycles of reuse. In comparison, in other studies, the operational stability of levansucrase immobilized on chitosan beads was studied at only 5 min per cycle; the immobilized enzyme lost ~40% of its initial activity after working for 85 min (17 cycles) [50]. According to Santos-Moriano's report, after only 3 cycles of reuse of levansucrase immobilized on vinyl sulfone-activated silica, approximately 60% of activity was retained, and the reaction was allowed to proceed for only 20 min per cycle [43]. In our study, each batch reaction time was 2 h. The immobilized enzyme was found to retain as much as 45% of its activity after 12 repeated uses for 24 h in total.

2.4.6 IFOS synthesis in a continuous fixed-bed bioreactor on INU-CSBs

The operational stability of the immobilized inulosucrase system was also investigated in a continuous fixed-bed reactor. A double-jacket column was packed with INU-CSBs. The continuous synthesis of IFOS was operated by feeding 200 g/L sucrose at a flow rate of 0.2 mL/min and 40 °C for 30 h. IFOS syrup was sampled and analyzed at certain intervals by HPLC. As shown in Figure 17, the INU-CSB fixed-

bed reactor synthesized various types of IFOSs, mainly 1-kestose, at least for 30 h with the average final total IFOS concentration of 53.0 g/L. Although total IFOS content gradually decreased during initial operating time (14 h), it was nearly constant when the operating time was up to 30 h. Moreover, readers can clearly see that 1-kestose was constantly synthesized, with the average amount of approximately 37 g/L. These results indicated that INU-CSBs have potential applications to the production of IFOSs from sucrose in both batch and continuous processes.

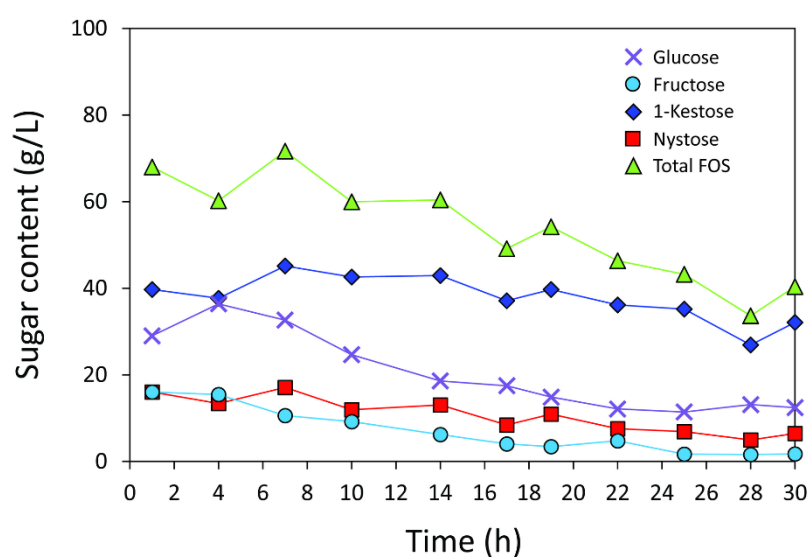


Figure 17. Continuous production of IFOS by immobilized inulosucrase in the fixed-bed reactor in which INU-CSBs (~200 U in total) were packed into small double-jacket column. Sucrose at a concentration of 200 g/L was fed at a flow rate of 0.2 mL/min. This process was conducted at 40°C for 30 h.

2.5 Conclusion

This is the first study to show immobilization of a bacterial inulosucrase and the use of this immobilized enzyme in IFOS synthesis. It is evident that chitosan beads in core-shell format can overcome some limitations of traditional hydrogel beads and thus may be useful for the development immobilization methods for other enzymes. Inulosucrase immobilized on CSBs manifested resistance to thermal denaturation and has promising operational stability for batch and continuous production of IFOSs. These properties make INU-CSBs highly attractive as an alternative biocatalyst for the synthesis of IFOSs and for future biotechnological applications.



CHAPTER III
IDENTIFICATION OF OLIGOSACCHARIDE BINDING SITE OF INULOSUCRASE
BY SITE-DIRECTED MUTAGENESIS

Modulation of fructooligosaccharide chain length and insight into the product binding motif of *Lactobacillus reuteri* 121 inulosucrase

Thanapon Charoenwongpaiboon^a, Thassanai Sitthiyotha^{a, b}, Pratchaya Pramroj Na Ayutthaya^c, Karan Wangpaiboon^a, Surasak Chunsrivirota^{a, b}, Manchumas Prousoontorn^a and Rath Pichyangkura^a

^a Department of Biochemistry, Faculty of Science, Chulalongkorn University, Payathai Road, Bangkok 10330, Thailand.

^b Structural and Computational Biology Research Group, Department of Biochemistry, Faculty of Science, Chulalongkorn University, Payathai Road, Bangkok 10330, Thailand.

^c Interfaculty Institute of Biochemistry, University of Tübingen, Hoppe-Seyler-Strasse 4, Tuebingen 72076, Germany

CHULALONGKORN UNIVERSITY
Published in Carbohydrate polymer (2019), 209, 111-121

3.1 Abstract

Inulosucrase (E.C. 2.4.1.9) is a bacterial fructosyltransferase that synthesizes inulin-type fructooligosaccharide, using sucrose as a substrate. We modulated the size of fructooligosaccharide synthesized by *Lactobacillus reuteri* 121 inulosucrase using rational designed mutagenesis. Nine residues; D478, D479, S482, R483, N543, W551, N555, N561 and D689, were changed based on the active site architecture and amino acids potentially interacting with saccharides. The selected residues were substituted with alanine to investigate the contribution of these residues to FOS chain length. Enzymatic activity assays demonstrated that the transglycosylation/hydrolysis ratios of D479A, R483A, N543A, W551A and N555A mutants were significantly different from that of the wild type. Almost all mutants, except D478A, synthesized oligosaccharides with different size distribution compared to that of wild type. Molecular docking further provides insights into the product binding motif of *Lactobacillus reuteri* 121 inulosucrase and strengthens an important role of amino acid residues at remote locations from the active site on the enzymatic activity and product specificity.

3.2 Introduction

Fructooligosaccharides (FOS) are carbohydrate molecules, which consist of fructosyl moieties covalently linked by glycosidic linkages. FOS are well-known as a commercial prebiotic and a dietary supplement for low-carbohydrate consumers because they are digested in human's gastrointestinal tract [3]. FOS can be synthesized by enzymatic transglycosylation reaction using fructosyltransferase (FTFs) and fructosyl-moieties donor. Inulosucrase (E.C. 2.4.1.9) and Levansucrase (E.C. 2.4.1.10) are FTFs that catalyze transfructosylation reaction using sucrose as a donor substrate (Figure 18). These FTFs were classified into glycoside hydrolase family 68 (GH68) (<http://www.cazy.org>) [51]. Although these FTFs display highly amino acid sequence similarities, they relatively differ in their derived product spectrum. Ozimek and colleague observed that *L. reuteri* 121 Inulosucrase produced inulin-type oligosaccharide (β (2-1) linkage) via a non-processive transglycosylation, while *L. reuteri* 121 levansucrase mainly synthesized levan polymer (β (2-6) linkage) via a processive transglycosylation [52].

Biological activities of oligosaccharides are largely dependent on their size distribution, commonly referred as the degree of polymerization (DP), therefore, it is crucial to improve the production process by increasing the yield of desired oligosaccharide species. For example, FOS with DP 2 – 8 provides high prebiotic activity compared to the long chain FOS [53]. Screening of new enzyme sources is a traditional approach that provides new biocatalysts with new catalytic properties. Enzymes from different origins have been reported that they produced different product patterns. For instance, levansucrase of Gram-positive bacteria, such as *Bacillus subtilis* [54], *Bacillus megaterium* [55], *Bacillus licheniformis* [56] and *Lactobacillus reuteri* [52], mainly produced levan polymer, while Gram-negative bacteria Levansucrase, such as *Erwinia amylovora* [57] and *Zymomonas mobilis* [58], mainly synthesized tri- and tetrasaccharides of FOSs with relatively low levan polymer.

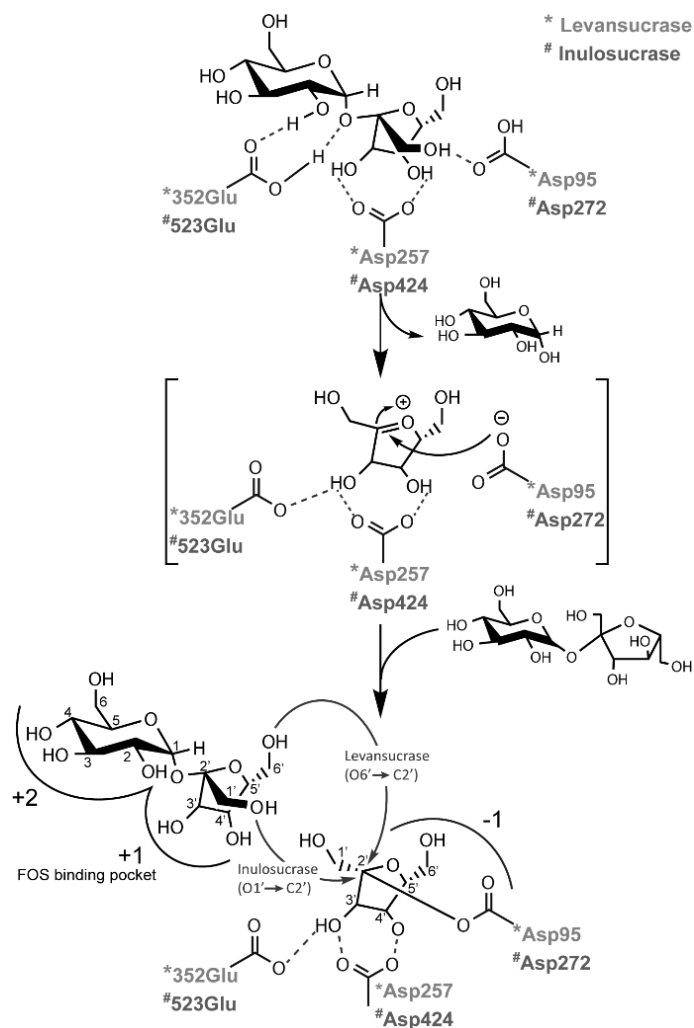


Figure 18. Proposed molecular mechanism of levansucrase and inulosucrase. The residue number of levansucrase (*) and inulosucrase (#) were from *Bacillus megaterium* [55, 59] and *Lactobacillus reuteri* 121 [60], respectively.

Nevertheless, screening techniques require high-throughput methods, or usually takes considerable experimental procedures. On the other hand, novel enzymes can be directly created *in vitro* from existing ones using enzyme engineering. Particular amino acid residues can be changed by site-directed mutagenesis approach. However, to select the target mutation sites, the information concerning structure-function relationship of the target enzymes should be available. Thus, molecular insight into the mechanism of FTFs is crucial.

Structure-function relationship of FTFs has been elucidated using crystallographic and mutagenesis studies. High-resolution 3D structure of levansucrase and its sucrose and raffinose complexes were initially reported for *B. subtilis* (Bs_SacB) [54, 61]. In addition, the structures of levansucrase from other bacterial species, such as *B. megaterium* (Bm_SacB) [59], *G. diazotrophicus* (Gd_LdsA) [62] and *E. amylovora* (Eam_LsC) [63] were also studied. In the case of inulosucrase, 3D structures of *InuI* from *L. johnsonii* was published in its apo form as well as in complex with sucrose and 1-kestose [64]. Crystallographic data provide insights into the mechanism of FTF synthesis and roles of some amino acid residues surrounding the catalytic site. Besides crystal structure information, the functions of several amino acid residues involving enzyme specificity and activity have been identified by mutagenesis studies. For instance, mutants K373A, N252A and Y247A of *B. megaterium* levansucrase synthesized unique oligosaccharide patterns with distinguishable chain length. The size of oligosaccharides produced by these mutants correlated well with the location of the mutated residues, the further away of the mutated residues were from the catalytic nucleophile subsite -1, the longer the synthesized oligosaccharides patterns were observed, showing specific terminations of the polymerization progression [59]. This finding indicated that this path may be the oligosaccharide binding track of levansucrase. Although the role of these residues in levansucrase were identified in many studies, the amino acid residues in inulosucrase involving in product size determination have been poorly studied. Anwar *et al.* revealed that the product specificity of *L. reuteri* 121 inulosucrase could be altered by mutations of residues distal to the active site [60]. Nonetheless, due to the structural differences between levan ($\beta(2-6)$) and inulin ($\beta(2-1)$), it is possible that the key residues in inulosucrase might not be equivalent to those recently reported in levansucrase. Here, we attempted to engineer *L. reuteri* 121 inulosucrase (Lrlnu) by using rational designed mutagenesis. Nine positions, D478, D479, S482, R483, N543, W551, N555, N561 and D689, were rationally selected based on 3D structure of homology modeling and saccharide-amino acid interaction information. The target residues were substituted with alanine, and the enzymatic activity, kinetic parameters as well as product pattern of each variants were determined and compared to those of the wild type. Finally,

molecular docking of inulosucrase with fructooligosaccharide (1,1,1-Kestopentaose; GF4) was employed to further elucidate the product binding motif and possible interactions between the enzyme and oligosaccharides.

3.3 Materials and methods

3.3.1 Molecular techniques

The C-terminus truncated Lrlnu from *L. reuteri* 121, Inu Δ 699His [60], synthesized by Genescript, was used as a parental gene (wild-type) in this study. Mutations were introduced by PCR overlapping extension method [65], using the primers described in APPENDIX. PrimeStar™ (Takara) DNA polymerase was used for DNA amplification. The mutant genes were ligated into pET-21b at *Xho*I and *Nde*I sites. The recombinant plasmids were then transformed into *E. coli* strain Top10 for cloning purposes. All introduced mutations of the Lrlnu gene were confirmed by DNA sequencing (1stBASE).

3.3.2 Enzyme expression and purification

To express wild-type and mutant inulosucrase, sequence-verified plasmids were transformed into *E. coli* BL21 (DE3). The cells carrying recombinant plasmid were cultured in LB broth supplement with 100 μ g/ml ampicillin, 10mM CaCl₂ and 0.5% glucose at 37 °C, shaking at 250 rpm. After OD600 reached 0.4-0.6, IPTG was added to the final concentration of 0.1 mM and cells were further incubated at 37 °C, 200 rpm for 18 hr. The cells were harvested by centrifugation at 5000xg for 20 min then lysed by sonication. Finally, crude enzyme was separated from cell debris by centrifugation at 12000xg for 20 min.

Crude enzyme was further loaded onto TOYOPEARL™ AF-Chelate-650M column pre-equilibrated with 25 mM potassium phosphate buffer (pH 7.4). The column was washed with the same buffer containing 20 mM imidazole and 500 mM NaCl. Finally, the enzyme was eluted with 500 mM imidazole in previous buffer. The purity was checked by SDS-PAGE (Figure 19). Protein concentrations were determined by Bradford's assay using BSA as a standard [38].

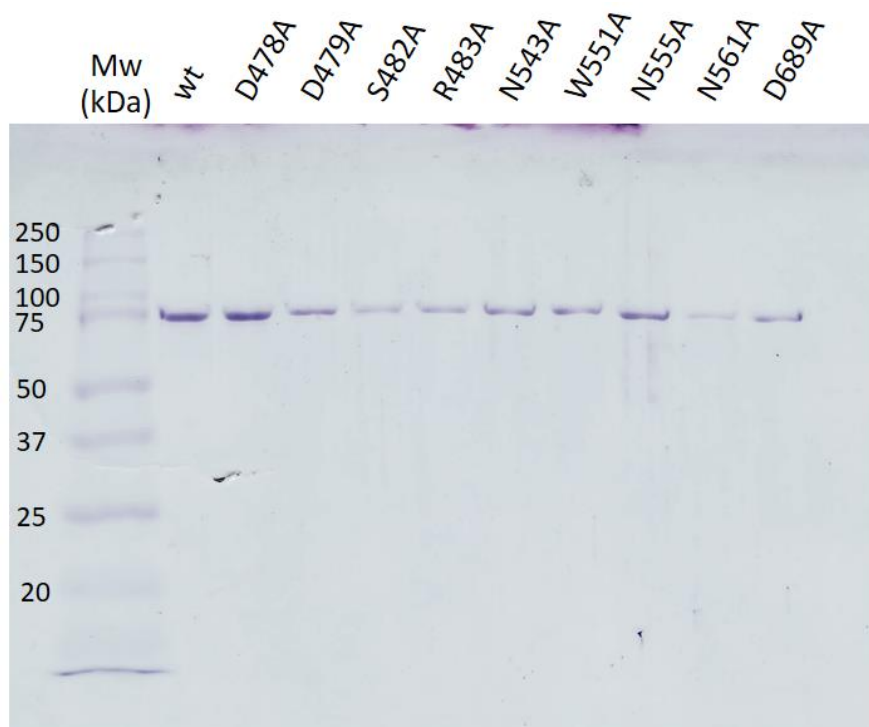


Figure 19. SDS PAGE of purified wild-type and mutant inulosucrase

3.3.3 Enzyme activity assay and biochemical characterization

The enzyme was incubated with 500 μ l of 250 mM sucrose in 50 mM sodium acetate buffer (pH 5.5) with 1 mM CaCl_2 at 50 $^\circ\text{C}$ for 10 min. The reaction was immediately terminated by adding 15 μ l of 1 N NaOH. The amount of glucose released by enzymes was measured by glucose liquicolor kit (HUMANTM), while the total reducing sugar released by enzymes was determined by DNS assay [39]. The mole of fructose was calculated from the difference between the mole of reducing sugar and glucose. One unit of total inulosucrase was defined by the amount of enzyme required for releasing 1 μ mol of glucose per min, while hydrolysis activity was defined by the amount of enzyme required for releasing 1 μ mol of fructose per min. For transglycosylation activity, enzyme units were calculated by the difference between total activity and hydrolysis activity.

3.3.4 FOS production and sugar analysis

Fructooligosaccharides and polymers were synthesized by incubating equal units of each mutant enzyme, 5 U/ml of glucose releasing activity, with 0.5 M sucrose in 50 mM acetate buffer pH 5.5 containing 1 mM CaCl_2 . The reactions were incubated at 30 and 50 °C for 24 hrs. After that, the reactions were terminated by boiling for 10 mins. The obtained reaction mixtures were further analyzed by TLC, HPAEC-PAD and HPLC.

TLC analysis was performed by using TLC silica gel 60 F254 (Merck). Eighty-six micrograms of sugar were spotted into TLC plate. Then, sugar mixture was separated by using 3:3:2 (v/v/v) of 1-butanol: glacial acetic acid: water. The TLC plate was dried and visualized by staining with solution containing 27 mL of ethanol, 10 mL of conc. H_2SO_4 , 8 mL of water and 0.1 g of orcinol.

HPAEC-PAD was performed on Dionex™ ICS 5000 system with CarboPac™ PA-1 column. The column was initiated with 150 mM NaOH and then eluted by the gradient of 0 – 250 mM sodium acetate in 150 mM NaOH for 30 min. FOS compositions were identified by retention time in comparison with standards.

HPLC was performed on Shimadzu™ (Prominence UFLC) equipped with refractive index detector. Oligosaccharide products were separated by Asahipak NH2P-50 4E column (Shodex™) using 70:30 (v/v) acetonitrile:water as a mobile phase at flow rate of 1.0 mL/min. Quantitative analysis was performed by an external standard using calibration curves of fructose (UNIVAR™), glucose (UNIVAR™), sucrose (UNIVAR™), 1-kestose (Sigma–Aldrich™) to determine mono-, di- and tri-saccharide, and nystose (Sigma–Aldrich™) to determine tetra-saccharides and longer oligosacchrides. The experiments were performed in triplicated and error bar represented the standard error of means (S.E.M).

The mass of oligosaccharide products were determined by MALDI-TOF mass spectroscopy (JEOL™ SpiralTOF MALDI Imaging-TOF/TOF Mass Spectrometer (JMS-S3000)). 2,5-dihydroxybenzoic acid (DHB) was used as matrix.

3.3.5 Kinetic study

The kinetic study of the wide type and mutants were performed in 50 mM acetate buffer pH 5.5 containing 1 mM CaCl_2 at 50°C. The final concentration of enzyme

used was 3.6 µg/mL and sucrose concentrations were between 0.5 – 750 mM. The release of glucose and fructose were determined using the method described above. The kinetic parameters were determined based on activity versus sucrose concentration curve, using either the Michaelis-Menten or the Hill equation.

3.3.6 Investigation of enzyme-saccharide interaction

Eighty four protein-saccharide complexes from RCSB protein data bank (www.rcsb.org) were used in this investigation (see APPENDIX). The selected protein-saccharide complexes were glycosyl hydrolases or transferases containing their natural substrates or products in the active site. The interactions between enzymes and saccharides were revealed by PoseView 2D interaction diagrams (<https://proteins.plus>).

3.3.7 Identification of catalytically competent binding conformations

The structure of GF4 was obtained from the crystal structure of *S. pneumoniae* transporter protein (PDB ID: 5G62). It was immersed in an isomeric truncated TIP3P water box and minimized using AMBER14 [66]. To construct the homology model of *Lactobacillus reuteri* 121 inulosucrase, SWISS-MODEL server [67] was employed, using *Lactobacillus johnsonii* inulosucrase structure (PDB ID: 2YFS with 74.17% identity) as a template. This structure was protonated at the experimental pH of 5.5 using H++ server [68]. To construct the fructosyl-D272 (fru-D272) intermediate, the structure of the fructosyl residue and N272 were taken from the crystal structure of *Lactobacillus johnsonii* inulosucrase in complex with sucrose (PDB ID: 2YFS), where N272 was mutated to D272 using SWISS-PDB viewer program [69]. Gaussian09 program [70] and Antechamber module of AMBER14 were employed to generate charges and parameters of fru-D272. LEaP module was used to build the inulosucrase structure with fru-D272 intermediate. It was immersed in a TIP3P water box and minimized using AMBER14.

Autodock Vina [71] was employed to determine catalytically competent binding conformations of GF4 in the binding site of *L. reuteri* 121 inulosucrase (see APPENDIX). In order for inulosucrase to be able to extend an inulin chain, GF4 should bind in catalytically competent orientations, where O1 atom of the non-reducing end of GF4

turns toward C2 atom of the fructosyl residue of fru-Asp272 with reasonable distance between these two atoms (O1-C2 atom distance). Employing this assumption, only a binding conformation, where O1 atom of the non-reducing end of GF4 turns toward C2 atom of the fructosyl residue of fru-Asp272 with the O1-C2 distance less than 5 Å was selected. One binding conformation passed these criteria and was chosen to be a predicted catalytically competent binding conformation. This binding conformation was immersed in a TIP3P water box and minimized using AMBER14. In this study, a hydrogen bond was considered to occur if the following criteria were met: (i) a proton donor-acceptor distance ≤ 3.50 Å and (ii) a donor-H-acceptor bond angle $\geq 120^\circ$.

3.4 Results

3.4.1 Structural analysis of Lrlnu and selection of mutation sites

To identify the amino acid residues in Lrlnu that are potentially important in saccharide-enzyme interaction, 60 non-homologous, glycosylhydrolases and glycosyltransferases, were investigated. Crystal structures from 84 carbohydrate-enzyme complexes revealed amino acid residues, which were frequently found to interact with carbohydrate molecules in the binding site of the enzymes. The frequency, in percentage, of these amino acid residues found in the carbohydrate binding site was shown in Figure 20A. Eighty percent of residues frequently found to interact with sugars in the binding site of these enzymes were charge and polar amino acids, aspartic acid (15%), glutamic acid (14%), asparagine (11%), glutamine (8%), lysine (3%) and arginine (9%), while interactions between non-polar amino acids and sugars were rarely observed. Results from this analysis indicated that the enzyme tended to interact with saccharides via hydrogen bonding or polar interaction. Thus, these amino acids on the Lrlnu surface were considered for further analysis.

These frequently observed residues on Lrlnu surface were then colored with shades of blue according to the frequencies of these residues being found in the carbohydrate binding site, where light color indicates low frequency and dark color indicates high frequency (the color set was described in Figure 20A). Together with the topology of the enzyme surface, two tracks of amino acids that might be relevant to carbohydrate binding can be perceived. These tracks have a reasonable topology

(groove/channel) and contain high density of amino acid residues frequently found to interact with saccharides: track A (N543, W551, R483, D479, S482, and D478) and track B (N543, N561, N555, and D689) (Figure 20B).

Co-crystal structures of InuJ with sucrose and 1-kestose provided insights into the catalytic and substrate binding site of inulosucrase in detail [64]. Structural superimposition between the modeled Lrlnu (this work) and InuJ (PDB ID: 2YFT with 75.93% identity) suggested the position of sugar residue in the binding site and amino acid residues that may be involved in sugar binding of Lrlnu. The three catalytic residues found in InuJ were D272, D425 and E524, corresponding to residues D272, D424 and E523 in Lrlnu, and they were located at the central pocket of the enzyme. Subsites responsible for saccharide binding are commonly termed by molecular enzymologists from +n to -n (where n is an integer), +n represents the saccharide binding site preceding the catalytic site and -n represents saccharide binding site following the catalytic site, with cleavage taking place between the +1 and -1 subsites [72]. Residues that interact with sugar (sucrose and 1-kestose) at sub-site -1 in InuJ were W271 and R424, corresponding to residues W271 and R423 in Inu. Residues interacting with the sugar at sub-site +1 of InuJ were E522, E524 and R542, corresponding to residues E521, E523 and R541 in Inu, while residues interacting with 1-kestose at sub-site +2 were R542 and R545 in InuJ, corresponding to residue R541 and R544 in Inu. The residues in these sub-sites were sequentially located from -1 to +2 spanning the active site of the enzyme as shown in Figure 20C.

For this reason, the two amino acid tracks predicted above may plausibly contain subsequent sub-sites (+3, +4, +5, etc.) and might play a role in product size determination. The selected amino acid residues for mutagenesis in these 2 tracks were shown in Figure 20D.

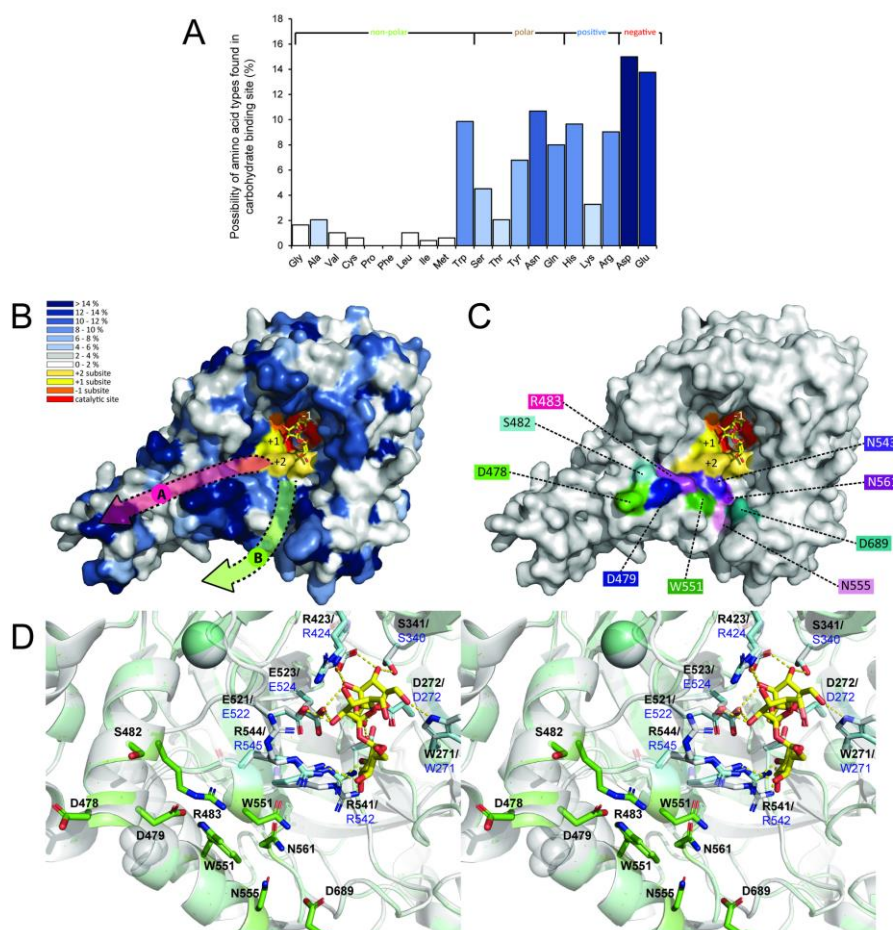


Figure 20. Rational design of target residues for mutagenesis. (A) Amino acid residues that are frequently observed in carbohydrate binding pockets were displayed as a bar graph colored by shades of blue corresponding to their observed frequency. (B) These shades of blue were also colored on the surface structure of *LrInu* from homology modeling. The predicted carbohydrate binding tracks, “A” and “B”, were displayed by magenta and green arrows, respectively. In (B) and (C), the catalytic triad of *LrInu* was shown in red, residue D272, D424, and E523, whereas sub-site -1, +1 and +2 were shown in orange, yellow and gold, respectively. (C) The selected mutation sites were predicted to locate near sub-site +2. The homology model of *LrInu* were superimposed with the crystal structure of *InuJ* (2YFT) with 1-kestose. (D) Close-up cross-eye stereo view of two superimposed *Lactobacillus inulosucrase* catalytic sites; *LrInu* (from 3D modelling, white) and *InuJ* (2YFT, pale blue). Residues of *InuJ* interacting with 1-kestose were labeled in blue, and the residues in *LrInu* were labeled in black. The selected residues of *LrInu* for mutagenesis were shown in green.

Interestingly, multiple amino acid sequence alignment of fructosyltransferases revealed that selected residues for mutagenesis within the proposed tracks (Figure 21) were conserved in inulosucrases (D479, R483, N543, W551, N555, N561 and D689, except for inulosucrase from *Le. Citreum*). Moreover, D479 was also conserved in some levansucrases. These findings suggested that these amino acid residues might play an important role in oligosaccharide product binding of inulosucrase, and modification of residues at these positions might influence the enzymatic activity and product specificity. However, residues D478 and S482 that were not conserved among inulosucrase and levansucrase were also selected for mutagenesis in this study since their position were aligned with the proposed saccharide binding track.

Mutated residues of Lrlnu		478	479	482	483	543	551	555	561	689
Inulosucrase										
<i>L. reuteri</i> 121 (this work)	AAN05575	D	D	S	R	N	W	N	N	D
<i>L. gasseri</i> DSM 20243	BK006921	S	D	D	R	N	W	N	N	D
<i>L. gasseri</i> DSM 20604	ACZ67286	S	D	D	R	N	W	N	N	D
<i>L. johnsonii</i> NCC 533	AAS08734	S	D	D	R	N	W	N	N	D
<i>L. reuteri</i> TMW1.106	CAL25302	D	D	S	R	N	W	N	N	D
<i>Le. citreum</i> CW28	AAO25086	S	N	L	Y	N	P	-	G	D
Levansucrase										
<i>L. reuteri</i> 121	AAO14618	K	K	E	L	S	T	N	N	D
<i>L. gasseri</i> DSM 2077	ACZ67287	N	D	A	L	S	T	N	N	D
<i>S. salivarius</i>	AAA71925	K	H	N	L	N	T	R	D	D
<i>L. sanfranciscensis</i>	CAD48195	K	N	E	L	S	N	I	N	D
<i>Le. mesenteroides</i> LevS	AAY19523	P	D	K	L	S	D	-	N	F
<i>Le. mesenteroides</i> LEUM_1409	ABJ62502	A	D	K	F	S	D	-	N	F
<i>Le. mesenteroides</i> LEUM_1411	ABJ62504	A	H	D	V	D	N	-	T	F
<i>B. subtilis</i>	CAA26513	D	K	R	T	S	T	-	D	-
<i>B. megaterium</i>	ADF38395	S	N	E	K	S	G	-	D	-
<i>B. velezensis</i>	RAP13023	A	K	R	D	S	N	-	D	-
<i>Z. mobilis</i>	AAA27702	T	E	D	G	S	G	-	P	-
<i>W. confusa</i>	RAU01220	D	D	V	R	N	W	N	N	D
<i>L. gasseri</i>	BBD48912	N	D	A	L	S	T	N	N	D

Figure 21. Amino acid sequence alignment of Lrlnu from *L. reuteri* 121 and other FTFs in GH68. The alignment was performed using Clustal Omega. Identical residues found among these enzymes were highlighted in grey.

3.4.2 Enzyme activity and biochemical characterization of inulosucrase with single mutations

Activity assay showed that the mutations affected significantly the transglycosylation activity of LrInu, while hydrolysis activity was not significantly altered (Figure 22). The reduction of transglycosylation activity was slightly observed in mutants D479A, R483A, N543A, W551A and N555A, which exhibited only 80%, 73%, 67%, 58% and 75% of the total wild-type activity, respectively. The decrease in transglycosylation activity might be a result from the enzyme losing its processivity. However, the overall activity of mutants was sufficient for FOS production.

The effects of pH and temperature on the initial catalytic rate of mutated LrInu were also analyzed using DNS assay. The results demonstrated that optimum pH and temperature of the mutated enzymes were similar to those of the wild type (pH 5.0 - 6.0 and 50 °C) and not altered by alanine substitution at these positions (Figure 23).

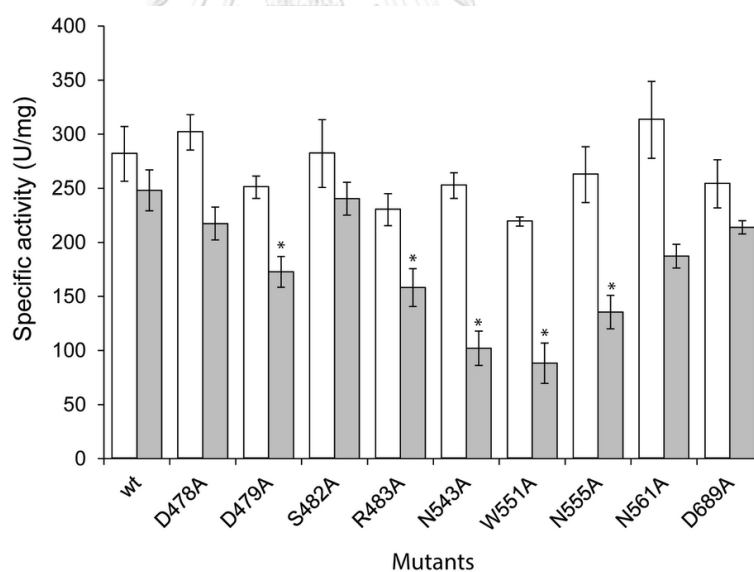


Figure 22. Specific activities of wild-type and mutant LrInu at 50°C. The white columns represent the hydrolysis activity and the gray columns represent the transglycosylation activity. Error bars represent \pm standard error (S.E.). Asterisks (*) indicate significant difference between wild-type and each mutant LrInu ($p \leq 0.05$).

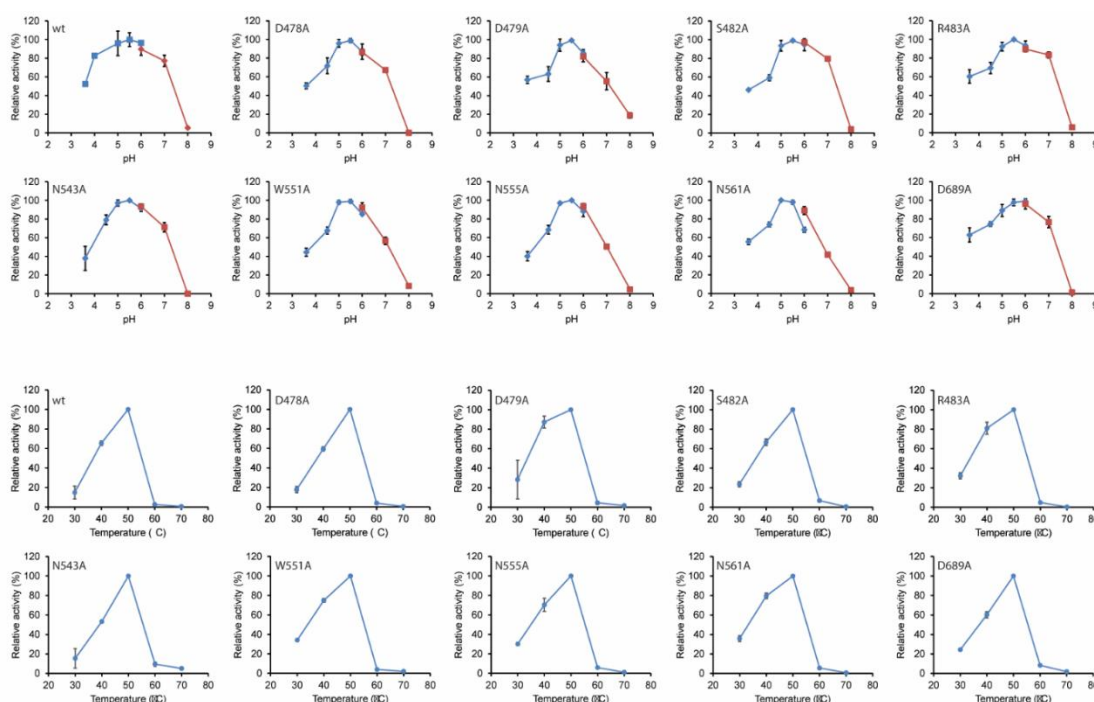


Figure 23. Optimum pH and temperature of wild-type and mutant inulosucrase. The optimal pH of wild type and mutant inulosucrases was determined by measuring the initial catalytic rate of enzyme in the pH range of 3.6 – 8.0 at 50 °C using DNS assay. The buffer systems, namely 50 mM sodium acetate buffer (3.6 – 6.0) and 50 mM Bis-tris buffer (6.0-8.0), were used in this study. The optimal temperature of the enzymes was determined in the temperature range of 30 – 70 °C in 50 mM acetate buffer pH 5.5

จุฬาลงกรณ์มหาวิทยาลัย
CHULALONGKORN UNIVERSITY

3.4.3 Kinetic parameters of wild-type and mutant Lrlnu

Kinetic constants of the wild type and mutants of Lrlnu were determined based on enzyme activity (V^G , V^F and V^{G-F}) versus sucrose concentration curve (Figure 24). Curve fitting was employed for these three graphs using Michaelis-Menten, Hill and substrate inhibition models. The results showed that even when the highest concentration of sucrose was used, the total and transglycosylation activity of Lrlnu had not been saturated, resulting in the high standard errors [73]. The total activity (V^G) of all variants were suitably fitted with Hill equation, while transglycosylation activity (V^{G-F}) were suitably fitted with Michaelis-Menten kinetic. In the case of hydrolysis activity (V^F), the fructose-releasing rate was declined, when higher sucrose

concentration was used. This result suggested that hydrolysis activity of all mutants Lrlnu were optimally fit to substrate inhibition model. Of all mutants, N543A and W551A mutants displayed the lowest turnover rates for total (k_{cat}^G) and transglycosylation (k_{cat}^{G-F}) reactions, which were approximately 2-3 folds lower than those of the wild type. For hydrolytic activity, catalytic turnover rates (k_{cat}^F) of D479A, R483A, N543A, W551A, N555A and D689A were slightly lower than that of the wild type. The $K_{50/m}$ values of all Lrlnu reactions were not significantly different among all mutant enzymes as shown in Table 4.

Table 4. Apparent kinetic constants of WT and mutant Lrlnu.

Kinetic parameter		wt	D478A	D479A	S482A	R483A
k_{cat}^G	s-1	2056 ± 530	1721 ± 463	2020 ± 538	2148 ± 784	1830 ± 835
$K_{50/m}^G$	mM	-a	-a	-a	-a	-a
$k_{cat}^G \times (K_{50/m}^G)^{-1}$	mM-1 s-1	-a	-a	-a	-a	-a
Hill factor		0.44 ± 0.04	0.46 ± 0.06	0.41 ± 0.03	0.42 ± 0.06	0.40 ± 0.05
k_{cat}^F	s-1	523.2 ± 62.0	519.2 ± 43.2	413.1 ± 23.8	532.6 ± 60.1	361.4 ± 28.4
$K_{50/m}^F$	mM	25.25 ± 7.26	24.25 ± 4.97	22.07 ± 3.36	23.59 ± 6.24	18.62 ± 4.19
$k_{cat}^F \times (K_{50/m}^F)^{-1}$	mM-1 s-1	20.72	21.41	18.72	22.58	19.41
K_i	mM	549.9 ± 174	572.6 ± 131	782.6 ± 144	416.9 ± 115	986.2 ± 287
k_{cat}^{G-F}	s-1	1829 ± 297	2138 ± 358	1974 ± 513	2175 ± 280	1396 ± 363
$K_{50/m}^{G-F}$	mM	1202 ± 282	1656 ± 371	2024 ± 674	1490 ± 263	1513 ± 536
$k_{cat}^{G-F} \times (K_{50/m}^{G-F})^{-1}$	mM-1 s-1	1.52	1.29	0.98	1.46	0.92
Kinetic parameter		N543A	W551A	N555A	N561A	D689A
k_{cat}^G	s-1	863.8 ± 141	765.7 ± 179	1623 ± 645.4	1742 ± 640	1849 ± 782
$K_{50/m}^G$	mM	224.29 ± 157	-a	-a	-a	-a
$k_{cat}^G \times (K_{50/m}^G)^{-1}$	mM-1 s-1	3.85	-a	-a	-a	-a
Hill factor		0.49 ± 0.06	0.48 ± 0.08	0.43 ± 0.06	0.49 ± 0.09	0.42 ± 0.07
k_{cat}^F	s-1	375.1 ± 23.2	329.0 ± 13.3	402.9 ± 28.9	518.2 ± 51.4	409.4 ± 36.7
$K_{50/m}^F$	mM	20.32 ± 3.60	23.07 ± 2.62	22.11 ± 4.54	24.14 ± 6.86	19.83 ± 4.90
$k_{cat}^F \times (K_{50/m}^F)^{-1}$	mM-1 s-1	18.46	14.26	18.22	21.46	20.65
K_i	mM	1196 ± 298	1341 ± 228	1493 ± 484	2033 ± 1095	845.1 ± 211
k_{cat}^{G-F}	s-1	1132 ± 375	966.7 ± 574	1619 ± 476	1977 ± 407	1325 ± 196
$K_{50/m}^{G-F}$	mM	1676 ± 741	1832 ± 1422	2064 ± 774	2003 ± 530	985.9 ± 222
$k_{cat}^{G-F} \times (K_{50/m}^{G-F})^{-1}$	mM-1 s-1	0.68	0.53	0.78	0.99	1.34

^a These kinetic parameters could not be determined since the enzymes were unsaturated with sucrose, and resulted in high standard errors.

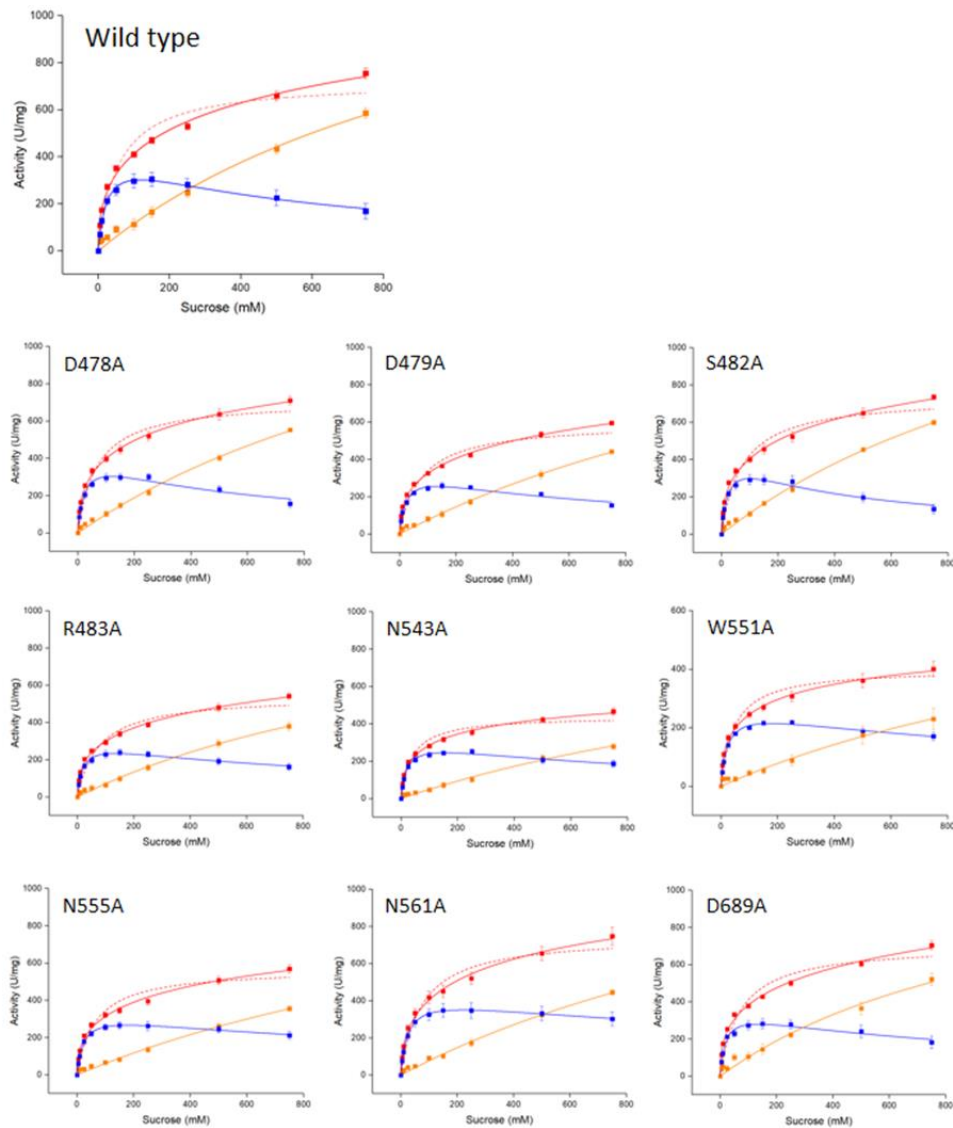


Figure 24. Graphs of relationship between initial velocity (V) and sucrose concentration for wild-type and mutant inulosucrase. The kinetic parameters were determined based on activity versus sucrose concentration curve, using 'OriginPro' as curve fitting software. Either The Michaelis-Menten formula: $V = V_{max} \cdot x / (K_m + x)$, The Michaelis-Menten formula with a substrate inhibition constant: $V = V_{max} \cdot x / (K_m + x \cdot (1 + x/K_i))$, or the Hill formula: $V = V_{max} \cdot x^n / (K_{50}^n + x^n)$, were used. In these formula, V is the specific activity (U/mg), x is the sucrose concentration (mM), n is the Hill coefficient, K_m is the Michaelis-Menten constant (mM), K_{50} is the Hill constant (mM) and K_i is the substrate inhibition constant (mM). Each data point is mean of six replicates obtained from two independent experiments \pm standard error (S.E.).

3.4.4 Effect of mutation on FOS profiles

TLC analysis showed that all mutants, except D478A, produced different product patterns, as compared to that of the wild type (Figure 25A and B). At 30°C, all mutant enzymes produced longer chain length FOS, as compared to that at 50°C. Temperature was found to influence the hydrolysis/transglycosylation activity of inulosucrase [73]. Hijum and co-worker studied the kinetic behavior of WT *L. reuteri* 121 inulosucrase at 50°C and 22°C, and found that LrInu have higher transglycosylation activity at lower temperature, which was also observed in our studies. This result suggested that lower temperatures might help reduce the disassociation of the oligosaccharide product from the enzyme, increasing its processivity. Furthermore, it was found that W551A and N561A incompletely hydrolyzed their sucrose at 50°C though equivalent initial enzymatic activity was used. This result suggested that the mutations at position W551 and N561 may affect inulosucrase stability (Figure 25B).

Quantitative analysis of FOSs produced by these mutants were also performed by HPLC (Figure 25C, D). The synthesized oligosaccharide products were categorized into 3 groups: short FOS (DP3-6), medium FOS (DP7-10) and long FOS (DP \geq 10). At 30 °C, D479A, S482A and R483A mutants showed higher accumulations of medium FOS, whereas the amount of long FOS was decreased. Mutants of W551A, N555A, N561A and D689A mainly synthesized short FOS in the range of DP3–5, whereas N543A synthesized the shortest range of oligosaccharides of DP3–4 (Figure 25C). At 50°C, All mutants produced more short FOS products, while the amount of medium and long FOS products was reduced. Moreover, fructose was the main product of these reactions, approximately 50% by D478A, D479A, S482A and R483A, and over 60% by N543A, N555A and D689A (Figure 25D).

Furthermore, double mutations at N543/R483 and R483/D479 to alanine were performed. These double mutants gave FOS product patterns similar to that of the single mutation at the residues closer to the active site, N543A and R483A, respectively (Figure 26). This result demonstrated that mutations at the more distal positions in these double mutants did not have additional effect on the DP of FOS produced.

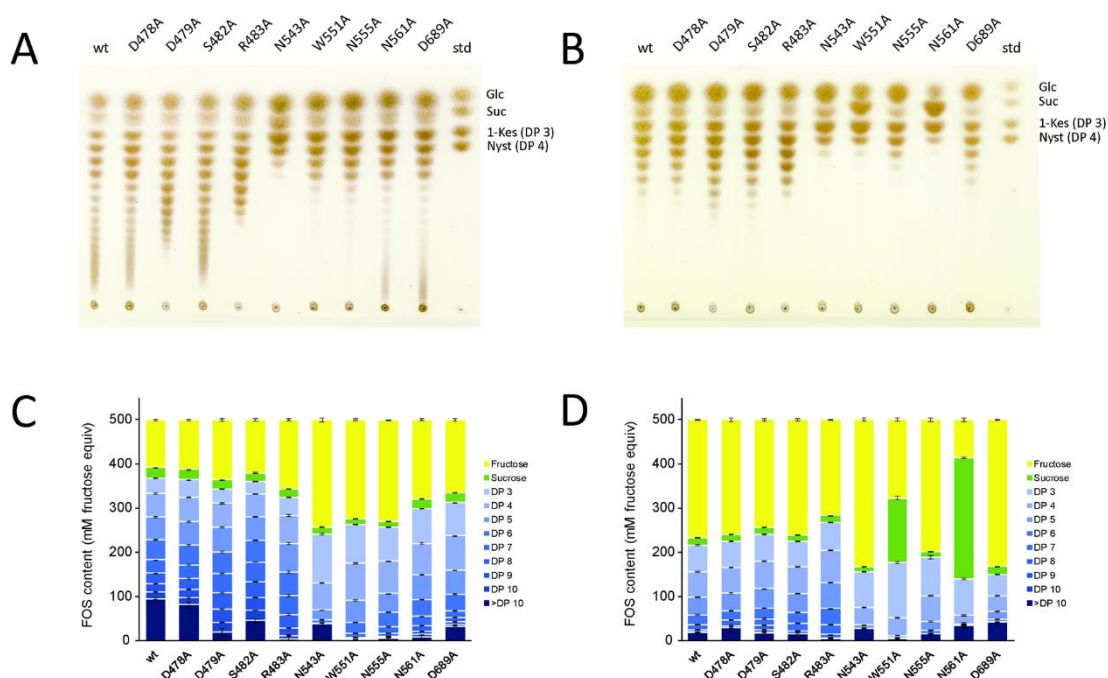


Figure 25. Analysis of mutants FOS profiles by TLC (A and B) and HPLC (C and D). FOS was synthesized by incubating 5 U/ml of each mutant enzyme with 0.5 M sucrose at 30°C (A and C) and 50°C (B and D) for 24 h.

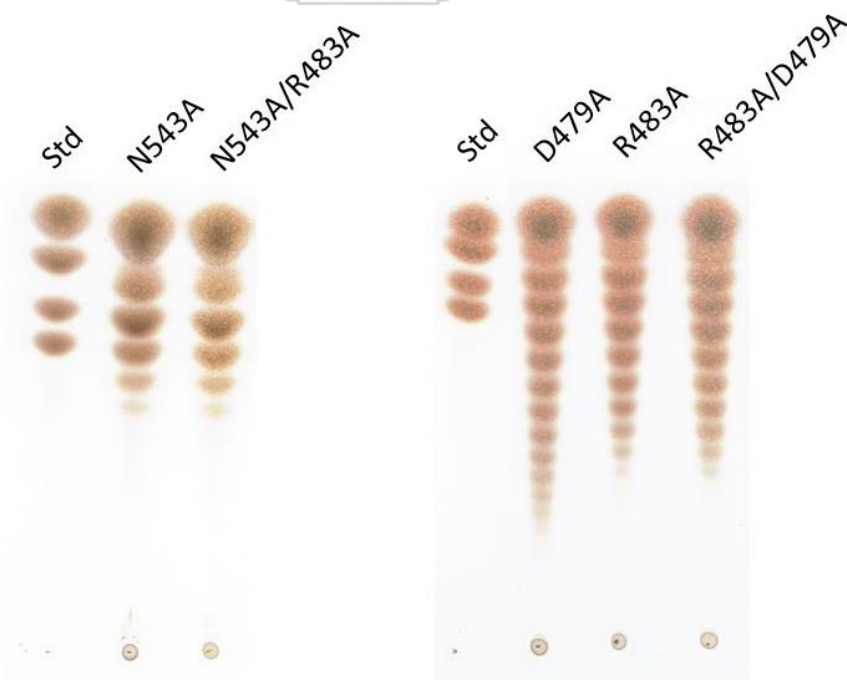


Figure 26. TLC of FOS products synthesized from double mutant inulosucrase.

MALDI-TOF MS and high resolution HPAEC-PAD analysis were subsequently performed to support the product size distribution, previously found by TLC and HPLC. HPAEC-PAD results demonstrated that the mutations influenced only the size, but not the linkage type of oligosaccharide (Figure 27). The product peaks observed in each mutant were also present in the wild type, and only reduction in the DP was observed. MALDI-TOF MS showed that variants R483A, D479A and S482A synthesized FOS up to DP 12 ($m/z=1985.65$), 16 ($m/z=2634.83$) and 21 ($m/z=3444.11$), respectively, whereas wild type and D478A synthesized up to DP 23 ($m/z=3769.17$) at 30°C (see APPENDIX, Figure S4-S13). Interestingly, N561A and D689A variants synthesized the whole range of FOS similar to that of the wild type; however, the amount of the products with DP>7 was lower than that of the wild type.

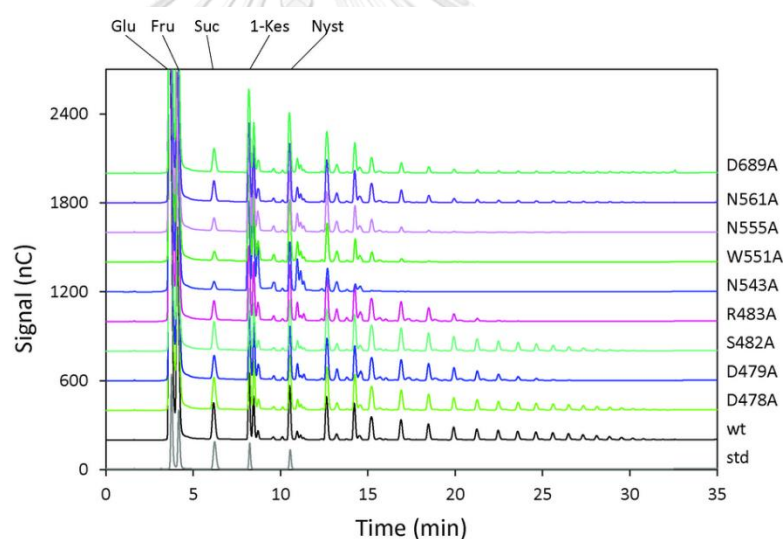


Figure 27. HPAEC-PAD chromatograms of wild-type and mutant FOS.

3.4.5 Identification of catalytically competent binding conformation

With the assumption that the system that allows transfructosylation to occur should be the one that has O1 atom of the non-reducing end of GF4 turning toward C2 atom of the fructosyl residue of fru-D272, and these two atoms should not be too far from each other, the predicted catalytically competent binding conformation was determined using Autodock Vina and selected based on these assumptions. The predicted catalytically competent binding conformation after minimization was

illustrated in Figure 28A. This result showed that O1 atom of the non-reducing end of GF4 turns toward C2 atom of the fructosyl residue of fru-D272, and the O1-C2 distance is reasonable (4.6 Å), based on the previous molecular dynamics study by Sitthiyotha et al. that employed the distance cutoff of 5 Å [74]. Within this distance, O1 atom of the non-reducing end of GF4 should be able to move and attack C2 atom of the fructosyl residue of fru-D272 and extend GF4 by one fructosyl residue, completing the transfructosylation reaction. (Figure 28B). Moreover, important interactions between GF4 and the binding residues of inulosucrase were analyzed. GF4 was predicted to form hydrogen bonds with Fru-D272, N367, A417, N419, R423, R483, E521, E523, N543 and R544 (Figure 28C). Therefore, transfructosylation should be able to occur in this system, and the predicted catalytically competent binding conformation is on the expected binding “track A”.



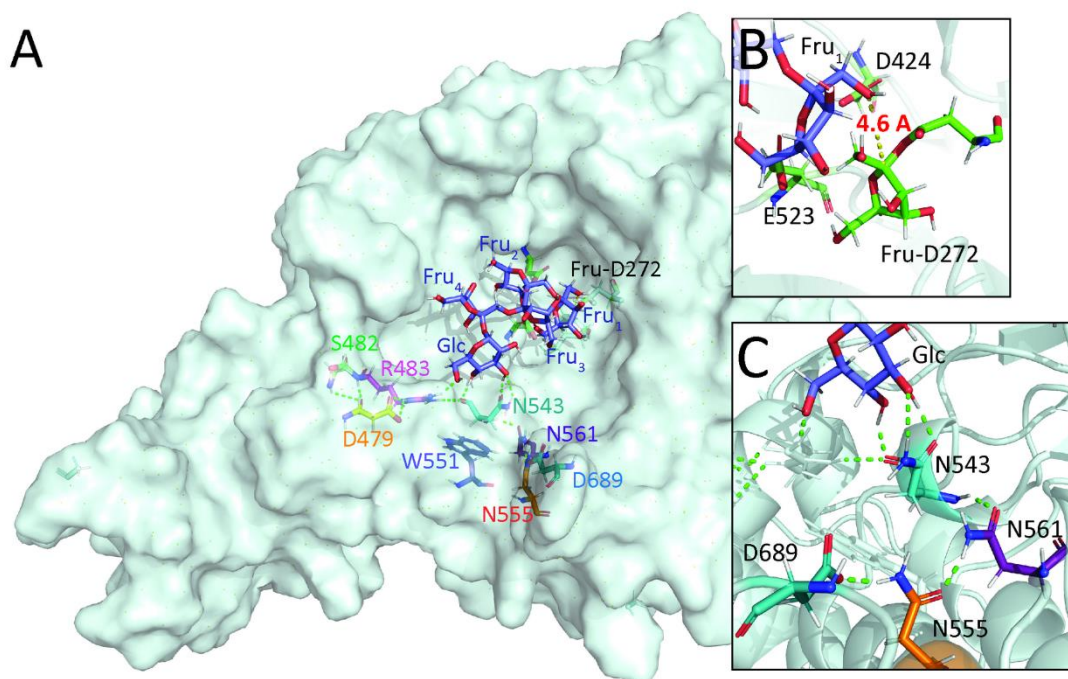


Figure 28. Prediction of a catalytically competent binding conformation of fructosyl nystose (GF4) by molecular docking. (A) Terminal glucose of GF4 was predicted to interact with R483 and N543 residues of LrInu, indicating that binding conformation is on the expected binding “track A”. (B) The proximity between atoms necessary for transfructosylation: the distance between O1 atom of the non-reducing end of GF4 and C2 atom of the fructosyl residue. (C) N555, N561 and D689 residues of LrInu were predicted to form a hydrogen bond network with N543, which was also predicted to form hydrogen bonds with the terminal glucose of GF4, suggesting that remote residues could determine the product specificity.

3.5 Discussion

Although structure and function relationship of GH68 FTFs has been explored in various levansucrases, the knowledge on the structural features of inulosucrase that regulate the type and size of oligosaccharide products are still limited. Most mutagenesis studies of GH68 FTFs usually focused on conserved residues based on amino acid sequence alignment, or residues located close to the activity site (sub site -1 to +2). Mutations in these sites usually resulted in the loss of overall activity, and the enzyme synthesizes only short chain FOS. Recently, mutagenesis study of inulosucrase from *L. reuteri* 121 [60] and levansucrase from *B. licheniformis* 8-37-0-1 [75] revealed that residues located far away from the activity site might contribute to the product specificity. Therefore, in this study, we attempted to identify the remote residues surrounding the active site of Lrlnu, which can modulate the size of synthesized FOS, and the ratio of oligosaccharide versus polymer produced. Based on the homology model of Lrlnu and structural analysis of numerous carbohydrate binding proteins, nine possible residues were reasonably relevant to fructan acceptor binding.

Substitution of N543 by alanine caused accumulation of short FOS (DP3-6) at 30°C, while the formation of long FOS was drastically reduced. Homology model of Lrlnu showed that N543 located near the +2 sub-site (N544), suggesting that N543 was probably in the higher order sub-sites. Mutation at this residue was previously reported by Anwar *et al.*, where N543 was mutated to serine [60]. FOS patterns derived from the N543A and N543S mutants were dramatically different. The N543S mutant produced long chain oligosaccharides and some polymer, while the N543A mutant produced only short chain FOSs. These results further emphasized the importance of N543 on oligosaccharide product binding and its involvement in the oligosaccharide binding track. Mutation of this residue to serine can still provide interaction(s) with the oligosaccharide acceptors, yielding longer oligosaccharide products. However, the S372A mutant of *B. megaterium* levansucrase (equivalent to N543A of Lrlnu) did not show any effects on the product size distribution [59], indicating that N543 is a crucial residue that determines the size of oligosaccharides produced by inulosucrase, but not levansucrase.

Likewise, W551A mutant of Lrlnu also altered FOS chain lengths, it synthesized mainly short FOS. Mutation at W551 of Lrlnu has been earlier reported as threonine substitution, in which W551T exhibited higher transglycosylation activity over wild type [60]; however, W551A (this work) showed lower transglycosylation activity. This finding suggested that the bulkiness and rigidity of aromatic side-chain may provide the structural requirement needed for the appropriate position between oligosaccharide acceptor and enzyme [59, 60, 64]. Molecular docking studies suggested that N543 of Lrlnu formed hydrogen bond interactions with GF₄. It supported the experimental results that N543A mutation abolished the synthesis of an inulin polymer. N543A mutant produced mainly fructooligosaccharides, which may be due to the loss of its ability to bind with GF₄ tightly enough to extend GF₄ with more fructosyl residues and subsequently cannot produce a long inulin polymer.

R483A, D479A and S482A of Lrlnu formed a unique pattern of FOS with distinguishable chain lengths, correlating well with distance of the mutated sites on Lrlnu surface from the catalytic site, as shown by the three dimensional structure model. The further away the mutated residues were from the catalytic site, the longer the synthesized oligosaccharides were produced. The side-chains of R483, D479 and S482 were capable of forming hydrogen bonds with the incoming sugar residues. These results suggested the proper orientations of S482, D479 and R483 side chains and their involvement in substrate binding. The lack of these side chains might reduce the binding affinity between sugars and enzyme, leading to the reduction in the processivity. In comparison with previous studies, mutant K312A and K315A of *B. megaterium* levansucrase, equivalent to D479 and R483 of Lrlnu, respectively, did not showed any effect on the chain length of FOS produced [59].

Three other mutations, N555A, N561A and D689A, also formed FOS patterns that were different from that of wild type. However, the size of FOS produced from mutant Lrlnu at these three residues did not correlate with the distances of these mutations from the catalytic sites. N561A and D689A synthesized the whole range of oligosaccharide similar to the range of FOS produced by the wild type. These residues are not likely involved in oligofructosyl acceptor binding, but possibly contribute in FOS chain length regulation. N561A and D689A continued to synthesize polymer,

interestingly, with slightly lower amount of FOS with DP>7, while the accumulation of FOS with DP3-6 was observed. Computational analysis predicted that D689, N555, and N561 of Lrlnu probably formed a hydrogen bond network with the backbone carbonyl group of N543 (Figure 28C). These residues did not directly bind GF₄ but they probably helped strengthen the binding between N543 and GF₄. When these residues were mutated to alanine, this hydrogen bond network was also disrupted, reducing the interactions between N543 and GF₄. It has recently been shown in other fructansucrase that hydrogen bond networks can indirectly facilitate the binding of the acceptor oligosaccharide in its active site [74]. In the case of the crystal structure of *L. johnsonii* inulosucrase, there is also a hydrogen bond network forming among N544, N562 and N556 (equivalent to N543, N561 and N555 of Lrlnu). This hydrogen bond network is slightly different from that of the predicted catalytically competent binding conformation of GF₄ in the active site of *L. reuteri* 121 inulosucrase, probably because the crystal structure does not contain GF₄, while our predicted structure contains GF₄. Moreover, the predicted catalytically competent binding conformation was also minimized to improve favorable interactions such as hydrogen bonds, as well as to eliminate unfavorable interactions.

These results suggested that fructooligosaccharide binding path were positioned along “track A” (N543 → R483 → D479). Accordingly, the role of amino acid residues in inulosucrase could be proposed; N543, R483, D479 and S482 probably located in the high order sub-sites (+3, +4, +5, etc), which could provide favorable binding interactions and stabilize acceptors in the proper orientation for long oligosaccharide elongation, while N555, N561 and D689 possibly functioned by providing the hydrogen bond network and positioning N543 in the proper orientation (Figure 28A).

To further confirm the authenticity of the proposed track A derived from the single mutation results, double mutation analysis was also employed. FOS product patterns of N543A/R483A and R483A/D479A were similar to that of the single mutation at the residues closer to the active site, N543A and R483A, respectively, demonstrating that the FOS product pattern was determined by the residues positioned closer to the active site. These results further emphasized the importance of these residues on DP

of FOS based on their distances from the catalytic site, and their involvement in the higher order sub-sites.

We found that the position of oligosaccharides binding track of inulosucrase and levansucrase, were different, though they shared high amino sequence similarity. As shown in Figure 29B, the potential FOS binding track of *B. megaterium* levansucrase (SacB), proposed by Strube *et al.* [59], located along Y247, N252 and K373 track since alanine substitution by these residues resulted in the decrease of oligosaccharide chain length. In this work, N414 (equivalent to Y247 of SacB) and N419 (equivalent to N252; conserved in many levansucrase and inulosucrase) of Lrlnu were also substituted by alanine (Figure 30). The N414A mutation did not affect FOS production as expected. However, N419 was found to interact with the docked GF4; therefore, the N419A mutation caused the production of shorter oligosaccharides. The different position of oligosaccharides binding track among FTFs may result from the difference of the conformation of their product, levan or inulin. However, the precise position of oligosaccharide binding track cannot be fully elucidated by using only mutagenesis studies, supplementary co-crystal structure data is required [60].

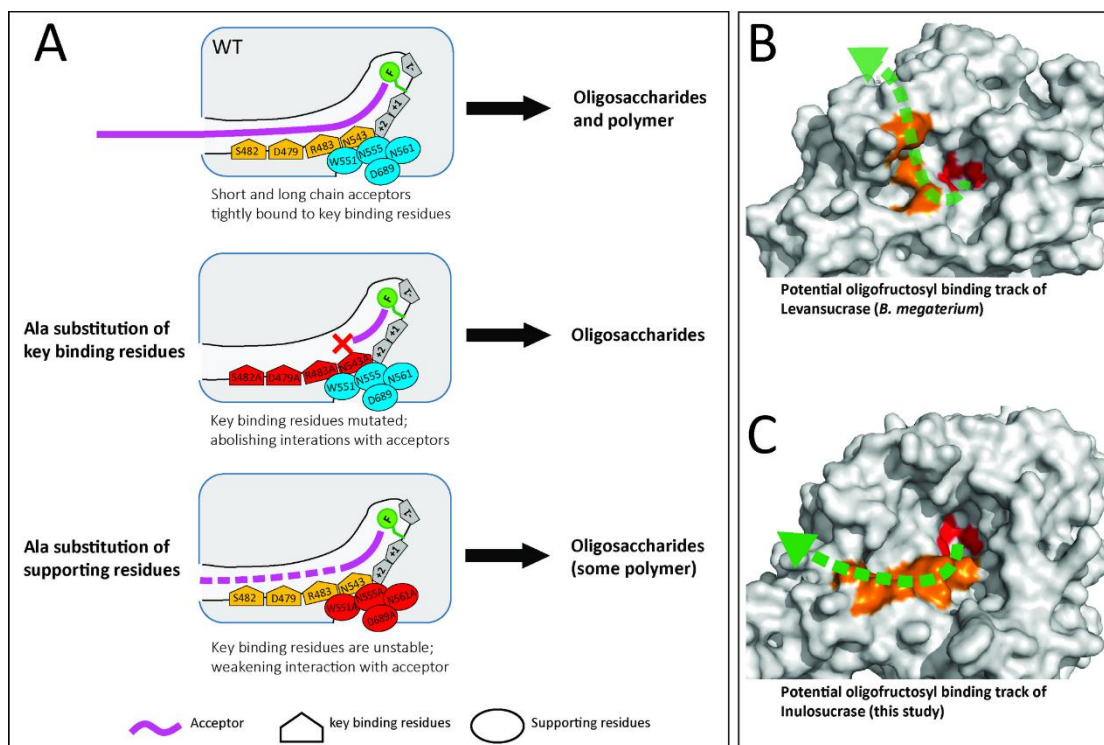


Figure 29. (A) Schematic representation of proposed inulosucrase mechanism. Wild-type inulosucrase synthesize a wide range of oligosaccharide, since the enzyme contains amino acid residues that provide sufficient binding affinity for FOS stabilization. Shorter FOS was obtained for variants, since the interaction of the enzyme with FOS was abolished or reduced. (B) The proposed oligosaccharide binding track of *B. megaterium* levansucrase and (C) the proposed oligosaccharide binding track of *L. reuteri* 121 inulosucrase. These two 3D structures were positioned in similar orientation. The catalytic triad is colored in red, while the proposed binding residues in the binding tract were colored in orange.

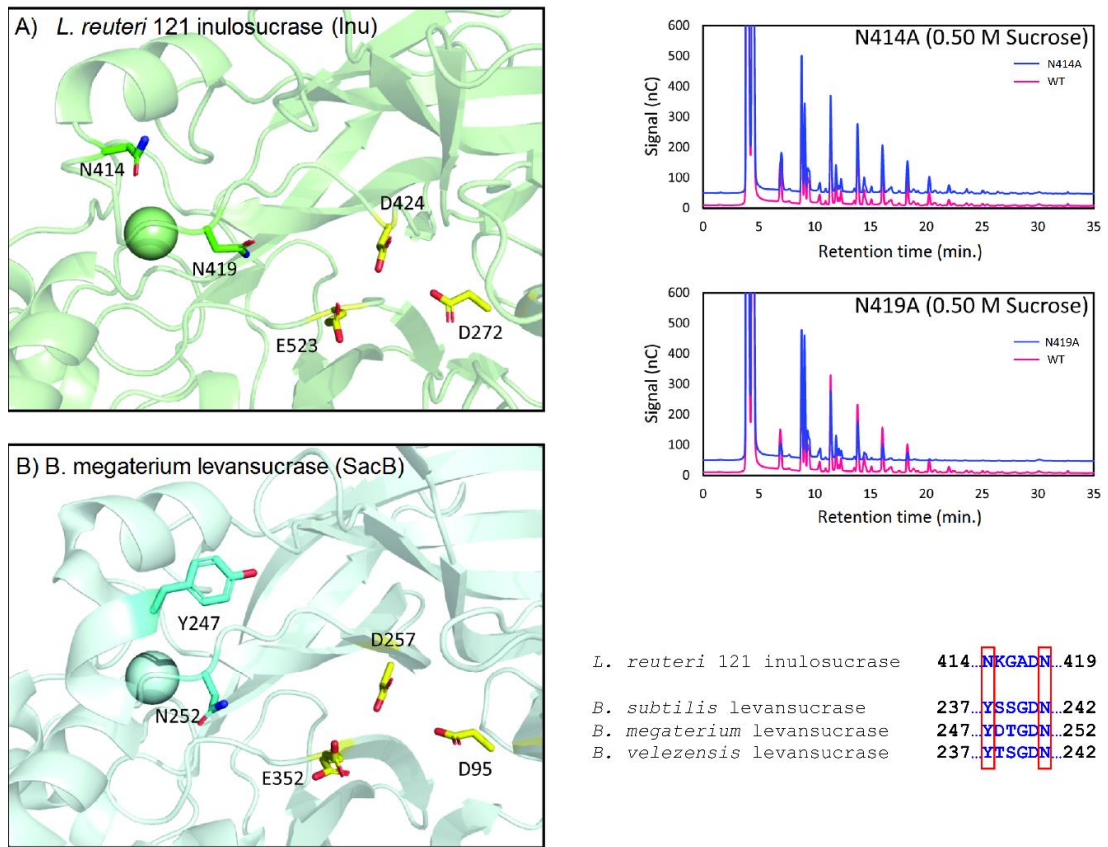


Figure 30. the FOS profile of N414A and N419A of Inu (equivalent to Y247 and N252 of SacB) analyzed by HPAEC. The alignment was performed using Clustal Omega.

3.6 Conclusion

Rational designed mutagenesis of the inulosucrase was employed to modulate the chain length of FOS. Mutations of single amino acid residues at remote locations from the active site can change the produced FOS species. The product ratio of each oligo-FOS species as well as oligo-FOS versus polysaccharide were also changed. Alanine substitution at these residues may disrupt the interaction(s) between acceptor oligosaccharide and enzyme, causing the release of short chain oligosaccharides from its binding surface. Moreover, these mutants retained most of their sucrose activity, though their processivity decreased. This study not only offers novel mutations that can modulate the chain length of FOS, but also provides insight into the product binding motif of *Lactobacillus reuteri* inulosucrase.



CHAPTER IV
IMPROVEMENT OF PRODUCT PATTERN OF INULOSUCRASE BY RATIONAL
SITE-DIRECTED MUTAGENESIS

Rational re-design of *Lactobacillus reuteri* 121 inulosucrase for product
chain length control

Thanapon Charoenwongpaiboon^a, Methus Klaewkla^{a,b}, Surasak Chunsriviro^{a,b},
Karan Wangpaiboon^a, Rath Pichyangkura^a, Robert A. Field^c and Manchumas Hengsakul
Prousoontorn^a

^a Department of Biochemistry, Faculty of Science, Chulalongkorn University,
Payathai Road, Bangkok 10330, Thailand.

^b Structural and Computational Biology Research Group, Department of
Biochemistry, Faculty of Science, Chulalongkorn University, Payathai Road, Bangkok
10330, Thailand.

^c Department of Biological Chemistry, John Innes Centre, Norwich Research
Park, Norwich, NR4 7UH, UK.

จุฬาลงกรณ์มหาวิทยาลัย
CHULALONGKORN UNIVERSITY

Published in RSC Advances 9(26), 14957-14965

4.1 Abstract

Fructooligosaccharides (FOSs) are well-known prebiotics that are widely used in the food, beverage and pharmaceutical industries. Inulosucrase (E.C. 2.4.1.9) can potentially be used to synthesise FOSs from sucrose. In this study, inulosucrase from *Lactobacillus reuteri* 121 was engineered by site-directed mutagenesis to change the FOS chain length. Three variants (R483F, R483Y and R483W) were designed, and their binding free energies with 1,1,1-kestopentaose (GF4) were calculated with the Rosetta software. R483F and R483Y were predicted to bind with GF4 better than the wild type, suggesting that these engineered enzymes should be able to effectively extend GF4 by one residue and produce a greater quantity of GF5 than the wild type. MALDI-TOF MS analysis showed that R483F, R483Y and R483W variants could synthesise shorter chain of FOSs with a degree of polymerization (DP) up to 11, 10, and 10, respectively, while wild type produced longer FOSs and in polymeric form. Although the decrease in catalytic activity and the increase of hydrolysis/transglycosylation activity ratio was observed, the variants could effectively synthesise FOSs with the yield up to 73% of substrate. Quantitative analysis demonstrated that these variants produced a larger quantity of GF5 than wild type, which was in good agreement with the predicted binding free energy results. Our findings demonstrate the success of using aromatic amino acids residues, at position D418, to block the oligosaccharide binding track of inulosucrase in controlling product chain length.

4.3 Materials and methods

4.3.1 Model construction and binding free energy calculation

The structure of the catalytically competent binding conformation of GF4 in the active site of *Lactobacillus reuteri* 121 inulosucrase containing a fructosyl-D272 intermediate (fru-D272) was constructed from crystal structure of *Lactobacillus johnsonii* inulosucrase (PDB ID: 2YFS with 74.17% identity) [64], according to method described in previous study [76], and was used as a template for mutations. The coordinates of this model are in APPENDIX. This catalytically competent binding conformation (GF4/Fru-WT) was defined as a binding conformation of GF4 in the active site of *Lactobacillus reuteri* 121 inulosucrase containing fru-D272, where the enzyme could potentially extend GF4 by one fructosyl residue via transfructosylation. This binding conformation has the O1 atom of the non-reducing end of GF4 turning towards the C2 atom of the fructosyl residue of fru-D272, where the distance between these two atoms (O1-C2) is reasonable [76]. The FastDesign protocol [77] of Rosetta 3.6 [78] with the talaris2013 energy function [79, 80] was employed to predict and optimize the binding conformations of GF4 in the active site of the wild type, R483A, R483F, R483Y and R483W variants to create GF4/Fru-WT, GF4/Fru-R483A, GF4/Fru-R483F, GF4/Fru-R483Y and GF4/Fru-R483W complexes, respectively. This protocol also employs the fast relax protocol to allow the movement of sidechains and backbones to resolve energetically unfavorable features such as steric clashes, and subsequently find low energy conformations. Fifty independent runs of this protocol [81] were employed to produce 50 binding conformations for the wild type, R483A, R483F, R483Y and R483W variants. Four separate sets of calculations were performed for the R483A, R483F, R483Y and R483W mutations. In each set, R483 was allowed to change to A, F, Y or W, respectively, and the residues within 10 Å of residue 483 were repacked and minimized. The free energy of each binding conformation (ΔG) was calculated in Rosetta Energy Units (REU). $\Delta G_{\text{binding}}$ of each binding conformation was calculated by subtracting the free energy of protein ($\Delta G_{\text{protein}}$) and ligand (ΔG_{ligand}) from the free energy of the complex ($\Delta G_{\text{complex}}$): $\Delta G_{\text{binding}} = \Delta G_{\text{complex}} - \Delta G_{\text{protein}} - \Delta G_{\text{ligand}}$. The details of binding free energy calculation by Rosetta are in Supplementary Data. The outlier

data of each enzyme were detected using SPSS software and eliminated. The average values of $\Delta G_{\text{binding}}$ were then calculated.

4.3.2 Construction, expression and purification of inulosucrase

The construct Inu Δ 699His [60] synthesised by Genescript, was used as a parental gene (wild-type) in this study. Site-directed mutagenesis was performed by the PCR overlapping extension method [65] using PrimeStar™ DNA polymerase (Takara). The primers used for mutagenesis are described in APPENDIX. The variant genes were ligated into pET-21b (Novagen™) at *Xho*I and *Nde*I sites and were further transformed into *E. coli* strain Top10 (Invitrogen™) for cloning purposes.

The recombinant plasmids were transformed into *E. coli* BL21 (DE3). The *E. coli* carrying plasmid were cultured in LB broth supplemented with 100 $\mu\text{g}/\text{mL}$ ampicillin, 10mM CaCl_2 and 0.5% glucose, at 37 °C, shaking at 250 rpm. After the cell density reach (OD₆₀₀) 0.4-0.6, IPTG was added to the final concentration of 0.1 mM. The cells were further cultured at 37 °C, shaking at 200 rpm for 18-20 h. The cells were then separated from media by centrifugation at 5000 $\times g$ for 20 min and lysed by ultrasonication. The cell debris was removed from crude enzyme by centrifugation at 12000 $\times g$ for 20 min.

Crude enzymes were purified on a TOYOPEARL™ AF-Chelate-650M column pre-equilibrated with 25 mM potassium phosphate buffer (pH 7.4). The column was washed with the same buffer containing 20 mM imidazole and 500 mM NaCl. Finally, the enzyme was eluted with 500 mM imidazole in the previous buffer. Protein concentrations were determined by Bradford assay using a BSA as standard [38].

4.3.3 Enzyme activity assay and biochemical characterisation

Inulosucrase activity was measured by incubating the enzymes (3.6 $\mu\text{g}/\text{mL}$) in 250 mM sucrose, containing 50 mM sodium acetate buffer (pH 5.5) and 1 mM CaCl_2 , to reach the final volume of 500 μL , at 50 °C. Then, the reaction was terminated by an adding 15 μL of 1 M NaOH. The total reducing sugar released by enzymes was determined by DNS assay [39], while the total glucose was determined by a glucose liquicolor kit (human™). The molar concentration of fructose produced from enzyme

was calculated from the difference between the quantity of reducing sugar and glucose. One unit of total inulosucrase activity was defined as the amount of enzyme required to release 1 μmol of glucose per min, while hydrolysis activity was defined as the amount of enzyme required to release 1 μmol of fructose per min. Transglycosylation activity was calculated as the difference between total activity and hydrolysis activity.

The optimal pH of wild-type and variant Lrlnu was measured in the pH range of 3.6 – 8.0 at 50 °C using the DNS assay. The buffer systems used were 50 mM sodium acetate buffer (3.6 – 6.0) and 50 mM Bis-tris buffer (6.0-8.0). The optimal temperature of enzymes was determined in the temperature range of 30 – 70 °C in 50 mM acetate buffer pH 5.5.

4.3.4 Enzyme kinetic

Kinetic parameters of wild-type and variant inulosucrase were determined according to the method described previously [76]. In brief, the variant and wild-type inulosucrase (3.6 $\mu\text{g}/\text{mL}$) were incubated with 500 μL of substrate solutions containing 0.5 - 500 mM sucrose, 50 mM acetate buffer (pH 5.5) and 1 mM CaCl_2 at 50 °C. The reactions were terminated by adding 15 μL of 1 M NaOH, and the amount of glucose and fructose released was determined by the method described above. Activity versus sucrose concentration curves were plotted and fitted to either Hill or Michaelis-Menten equation using OriginPro software in order to determine kinetic parameters of the enzymes.

4.3.5 FOSs synthesis and characterisation

FOSs were synthesised using 5 U/ml (glucose releasing activity) wild-type or variant inulosucrase, 500 mM sucrose, 50 mM acetate buffer (pH 5.5) and 1 mM CaCl_2 . The reactions were incubated at 50 °C for 24 h, then terminated by boiling for 10 min. The resulting reaction mixtures were then analyzed by TLC, HPLC and MALDI-TOF MS.

The TLC system used in this study consists of 1-butanol: glacial acetic acid: water, 3:3:2 (v/v/v). The separation was performed by using TLC silica gel 60 F254 (Merck). The TLC plates were dried and stained with a solution comprising 8 mL of water, 10 mL of conc. H_2SO_4 , 27 mL of ethanol and 0.1 g of orcinol. The TLC were visualized by heating.

HPLC was performed on a Shimadzu™ (Prominence UFLC) instrument equipped with a refractive index detector. FOSs were separated with an Asahipak NH2P-50 4E column (Shodex™) using isocratic elution with 70% acetonitrile at a flow rate of 1 mL/min. As described in our previous study, the amount of identified FOSs was determined using the standard curve of glucose and fructose to determine monosaccharide, sucrose to determine disaccharide, 1-kestose to determine trisaccharide, and nystose to determine longer oligosaccharides.[76, 82]

The mass of FOSs products was evaluated by MALDI-TOF mass spectrometry (JEOL™ SpiralTOF MALDI Imaging-TOF/TOF Mass Spectrometer (JMS-S3000)). 2,5-Dihydroxybenzoic acid (DHB) was used as the matrix.

4.4 Results and discussion

4.4.1 Rational protein design

Many studies have shown that specificity of carbohydrate-modifying enzymes can be improved by enzyme engineering. The size of glycan produced may be regulated by using two different strategies: removing the interactions between substrates and the enzymes' binding sites or blocking the substrate binding track with some amino acids, for instance aromatic amino acids (Figure 31). Previously, many researches demonstrated that a single mutation at some specific amino acid residues of LrInu affected the size of inulin oligosaccharide that could be produced [60, 76, 83]. The yield of short-chain oligosaccharides was significantly improved when some amino acid residues of LrInu were mutated to be alanine, which may reduce the interactions between the enzyme and substrates with medium or long chain lengths. This finding has also been reported on other fructosyltransferases, such as *Bacillus megaterium* levansucrase [59] and *Bacillus licheniformis* levansucrase [75]. However, those variants usually produced either very short range of FOSs (DP 3-6) or long range of FOSs (DP \geq 12). To control the size of medium range of FOSs at DP \leq 10 is still challenging for the field of enzyme engineering and food industry. Therefore, in this study, inulosucrase was redesigned by computational assisting method in order to increase the specificity of FOS produced in medium range.

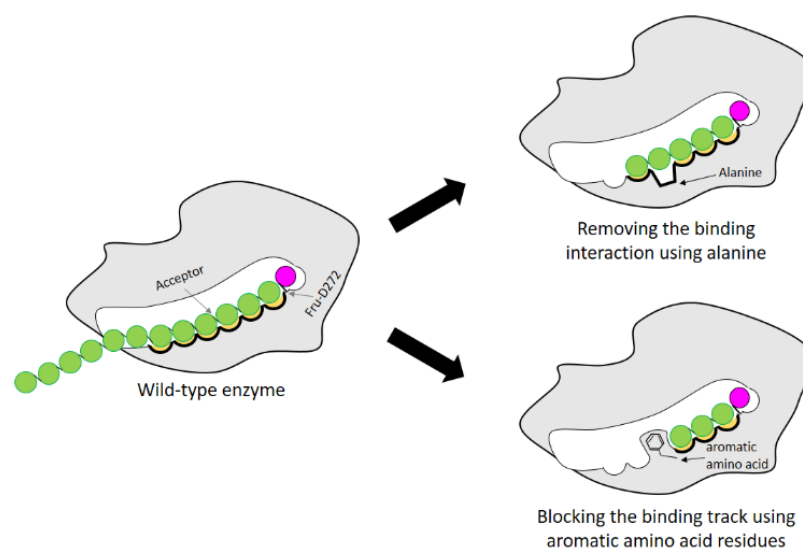


Figure 31. Schematic display of enzyme engineering for modulation of the size of oligosaccharide produced by glycosyltransferase.

From previous study, D479, S482, R483 and N543 residues were predicted to be the carbohydrate binding residues of *Lactobacillus reuteri* 121 inulosucrase [76]. Nevertheless, we noticed that the size of oligosaccharides synthesised by the variants did not correlate well with the distance between the mutated sites and catalytic sites. In the case of LrInu, for example, the N543A variant mainly produced FOSs with DP3-6, while the R483A variant, whose R483 was located close to N543, produced the FOSs up to DP12. Although these two residues were close, the sizes of their FOSs products were dramatically different. This finding suggested that there was more than one amino acid residue located in the same binding site that played an important role in substrate binding. Although one of the binding residues was mutated, other residues still could hold the substrate, allowing transglycosylation to occur.

Previous study found that blocking the oligosaccharide binding track of levansucrase with aromatic residues (F, Y and W) was an effective strategy to block elongation of polysaccharide and increase the yields of oligosaccharides [84]. Therefore, we employed this approach in redesigning LrInu so that it could produce high yields of short to medium chain length oligosaccharides. Because R483 of LrInu is located next to N543, we hypothesized that blocking at this position might increase

the yield of short FOSs like that obtained from the N543A variant. To test this hypothesis, R483 residue of the catalytically competent binding conformation (GF4/Fru-WT) was changed *in silico* to A, F, Y and W to create GF4/Fru-R483A, GF4/Fru-R483F, GF4/Fru-R483Y and GF4/Fru-R483W complexes, respectively, using the Rosetta program. This catalytically competent binding conformation (GF4/Fru-WT) was defined as a binding conformation of 1,1,1-Kestopentaose (GF4) in the active site of *Lactobacillus reuteri* 121 inulosucrase containing fru-D272. Since our previous study found that the R483A variant synthesized more GF5 (DP6) than the wild type, the GF4/Fru-R483A complex was used as positive control in this study. Fifty independent runs of the FastDesign protocol were employed to resolve unfavorable interactions and find low energy binding conformations of all complexes (Figure 32). $\Delta G_{\text{binding}}$ of each binding conformation was computed, and the average values are shown in Table 5. We hypothesized that there might be a possible correlation between the quantity of GF5 (DP6) product and the recognition of GF4 (DP5). If an enzyme binds well with GF4, it should be able to effectively extend GF4 by one fructosyl residue to form GF5 via transfructosylation. As shown in Table 5, the Fru-R483A was predicted to bind GF4 better than the Fru-WT, suggesting a possible correlation between the quantity of GF5 products and $\Delta G_{\text{binding}}$ of GF4 in the active site of Fru-R483A LrInu. Furthermore, our results show that the average values of $\Delta G_{\text{binding}}$ of other variants are better than or about the same as that of the wild type, suggesting that they may be able to synthesize more quantity of GF5 products than the wild type as well. Therefore, the R483F, R483Y and R483W variants were selected for further kinetic study and product characterizations.

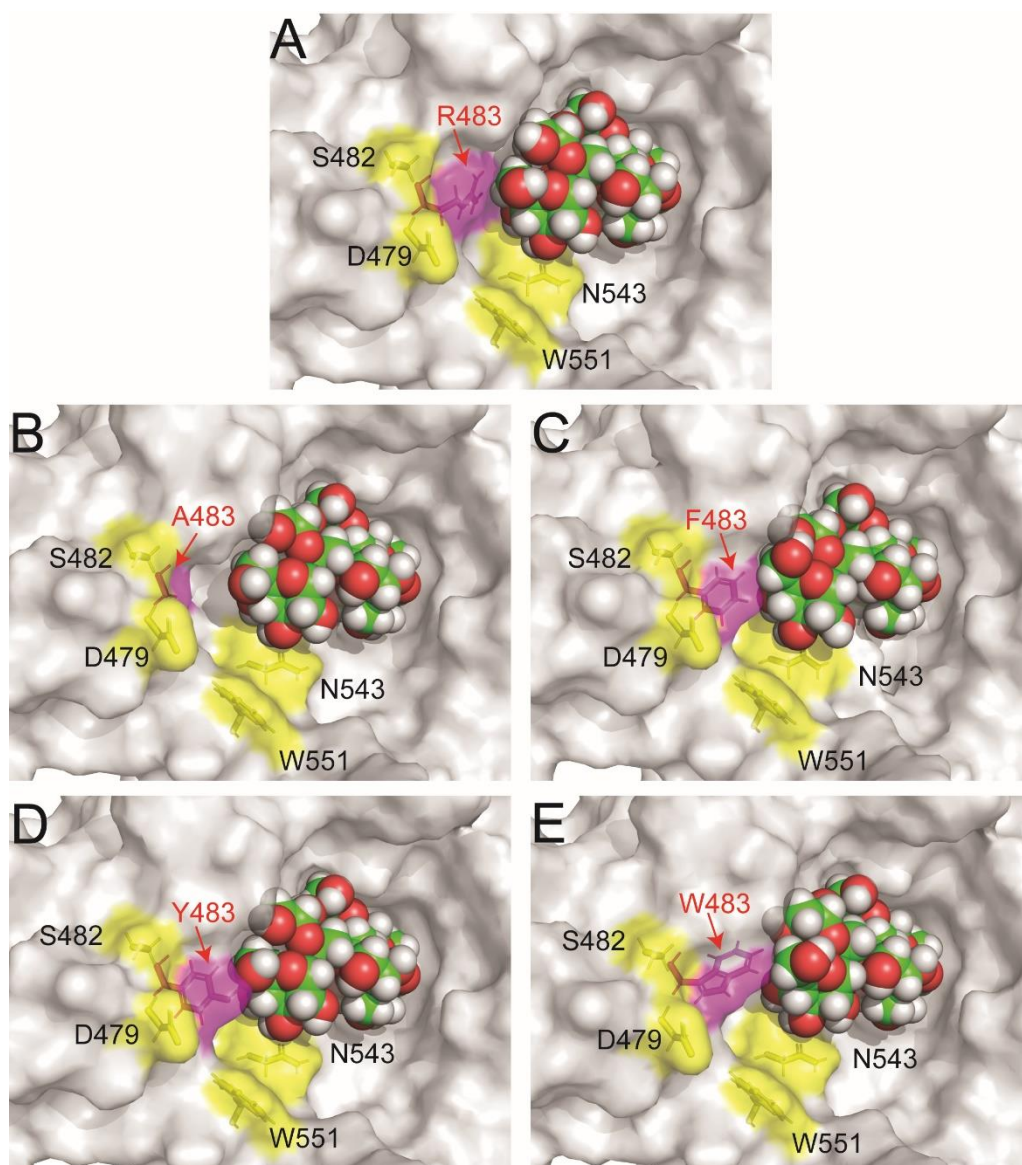


Figure 32. The predicted catalytically competent binding conformations of (A) wild type (B) R483A (C) R483F (D) R483Y and (E) R483W variants by Rosetta.

Table 5. The average values of predicted binding free energy ($\Delta G_{\text{binding}}$) of GF4 in the active sites of the wild-type and variant *LrInu* containing a fructosyl-D272 intermediate (Fru-WT, Fru-R483A, Fru-R483F, Fru-R483Y and Fru-R483W) calculated by Rosetta.

System	$\Delta G_{\text{binding}}$ (REU)	
	Average	s.e.m.
GF4/Fru-WT	-6.3	0.1
GF4/Fru-R483A	-7.1	0.1
GF4/Fru-R483F	-7.0	0.1
GF4/Fru-R483Y	-7.0	0.2
GF4/Fru-R483W	-6.3	0.2

When this study was conducted, the crystal structure of *Lactobacillus reuteri* 121 inulosucrase was not available. Therefore, its homology model was created in the previous study [76] based on the crystal structure of *Lactobacillus johnsonii* inulosucrase (PDB ID: 2YFS) [64] and also used in this study. The sequence identity of these two enzymes are reasonable with the value of 74.17%. Moreover, the quality of this homology model was evaluated by Ramachandran plots. The results show that this homology model has promising quality because the majority of amino acid residues are in favored region (93.7%) and allowed region (5.6%). Additionally, the catalytic residues (D272, D424, and E523) of the homology model of inulosucrase from *Lactobacillus reuteri* 121 are in similar positions to those of inulosucrase from *Lactobacillus johnsonii*, and they should be in appropriate positions for the catalysis of transfructosylation. Moreover, other studies also employed homology models in creating structures of variant proteins using the Rosetta program [81, 85, 86]. In any case, if a crystal structure of *Lactobacillus reuteri* 121 inulosucrase is available in the future and used as an input for the Rosetta program, more accurate results might be obtained.

4.2 Introduction

Fructooligosaccharides (FOSs) are well-known prebiotics that are widely used in food, beverage and pharmaceutical applications. FOSs are generally synthesised from sucrose using β -fructofuranosidase (E.C. 3.2.1.26) derived from fungi, such as *Aspergillus niger* [10, 11], *Aspergillus japonicas* [12-14], *Aspergillus aculeatus* [25, 26] and *Aspergillus oryzae* [16]. Bacterial enzymes, such as levansucrase (E.C. 2.4.1.10) and inulosucrase (E.C. 2.4.1.9), have also been used to synthesise FOSs starting from sucrose producing β -2,6 linked levan and β -2,1 linked inulin, respectively [21, 52]. The biological activity of FOSs is largely dependent on their degree of polymerization (DP). Many studies have attempted to engineer these enzymes to increase the yield of FOSs at the expense of macromolecular polymer formation. In the case of levansucrase, for example, the size of levan, as well as the polymer/oligosaccharide ratio, synthesised by *Bacillus megaterium* levansucrase could be controlled by site-directed mutagenesis [55, 59]. Furthermore, rationally designed variants of *Bacillus licheniformis* levansucrase can increase the yield of oligosaccharides (DP4-25) up to 60% of the total products, and also alter the ratio of isomeric trisaccharide products [75].

Previously, we reported the amino acid residues of *Lactobacillus reuteri* 121 inulosucrase (Lrlnu) that play an essential role in FOSs chain length determination [76]. Some variants of this enzyme, such as D479A, S482A, and R483A, can produce a broad range of oligosaccharides with a small amount of accumulating polymer, while N543A mainly produces the short chain FOSs (DP3-6, with traces of DP \geq 7). Since FOSs show optimal prebiotic activity in the DP 2-8 range [53], it is interesting to use the N543A variant of Lrlnu as a biocatalyst for the synthesis of such oligosaccharides. However, this variant produced low amounts of transglycosylated product, but liberates high amounts of fructose from sucrose hydrolysis. Therefore, in this study, we engineered inulosucrase to change its product chain length using computer-aided rational design. The position of Lrlnu selected for mutagenesis was based on the oligosaccharide binding track of Lrlnu reported in previous study [76]. The Rosetta program was employed using the homology model of Lrlnu, built from crystal structure of *Lactobacillus johnsonii* inulosucrase (PDB ID: 2YFS) [64], to assess variants of Lrlnu to

F, Y or W, to predict the substrate binding conformations and to compute the binding free energies ($\Delta G_{\text{binding}}$) of the substrate/enzyme complexes. The enzyme activities, biochemical properties and kinetic parameters of Lrlnu variants were determined and compared to that of the wild type. Finally, the FOSs produced by variant enzymes were analysed by TLC, HPLC and MALDI-TOF MS. As predicted by Rosetta program, this study demonstrated the effectiveness of using aromatic amino acids to block the oligosaccharide binding track and to control the size of oligosaccharides synthesised by inulosucrase.

4.4.2 Activity and kinetic study of inulosucrase variants

The designed Lrlnu variants above were expressed and purified by the method described previously [76]. Activity assays revealed that the engineered proteins had lower hydrolysis and transglycosylation activity than that of wild type (Table 6). In addition, the hydrolysis/transglycosylation ratio was changed. The percentage of hydrolysis activity of the variant proteins was significantly increased, up to 75% of total activity (Figure 33).

Table 6. Specific activity and kinetic parameters of WT and variant inulosucrase.

			WT ¹	R483F	R483Y	R483W
Specific activity	Total	U mg ⁻¹	530 ± 14	123 ± 3	157 ± 6	125 ± 7
	Hydrolysis	U mg ⁻¹	282 ± 25	90.2 ± 2.4	117 ± 5	88.4 ± 2.4
	Transglycosylation	U mg ⁻¹	248 ± 19	32.7 ± 3.5	40.0 ± 3.9	36.3 ± 5.5
Kinetic parameter	k_{cat}^G	s ⁻¹	2060 ± 530	876 ± 460	691 ± 389	608 ± 373
	$K_{50/m}^G$	mM	nd	nd	nd	Nd
	$k_{cat}^G \times (K_{50/m}^G)^{-1}$	mM ⁻¹ s ⁻¹	nd	nd	nd	Nd
	Hill factor		0.44 ± 0.04	0.36 ± 0.03	0.41 ± 0.07	0.41 ± 0.07
	k_{cat}^F	s ⁻¹	523 ± 62	120 ± 3	153 ± 5	119 ± 3
	$K_{50/m}^F$	mM	25.3 ± 7.3	26.5 ± 3.0	24.7 ± 3.9	27.6 ± 2.8
	$k_{cat}^F \times (K_{50/m}^F)^{-1}$	mM ⁻¹ s ⁻¹	20.7	4.52	6.18	4.31
	k_{cat}^{G-F}	s ⁻¹	1830 ± 300	154 ± 35	269 ± 76	176 ± 35
	$K_{50/m}^{G-F}$	mM	1200 ± 280	638 ± 250	1110 ± 470	733 ± 241
$k_{cat}^{G-F} \times (K_{50/m}^{G-F})^{-1}$	mM ⁻¹ s ⁻¹	1.52	0.241	0.242	0.240	

nd = the result cannot be determined

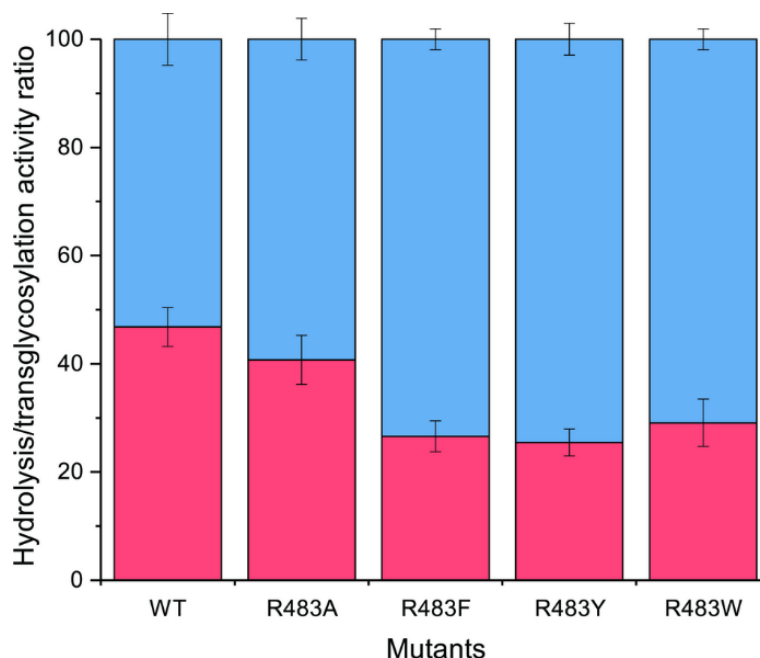


Figure 33. Analysis of the H/T activity. The activity of wild-type and variant inulosucrase was measured using 3.6 $\mu\text{g/ml}$ enzyme and 250 mM sucrose, in 50 mM acetate buffer (pH 5.5) and 1 mM CaCl_2 at 50°C. The blue columns represented the hydrolysis activity (H), while the red columns represented the transfructosylation activity (T).

In comparison to the previous studies, the variants of fructosyltransferase that produced the higher yield of oligosaccharides usually have a higher hydrolysis activity, such as, Y246A, N251A, K372A, R369A, R369S and R369K variants of levansucrase from *Bacillus licheniformis* 8-37-0-1 [75], N252A and K373R variant of levansucrase from *Bacillus megaterium* [59], and N543S variant of inulosucrase from *Lactobacillus reuteri* 121 [60].

The kinetic parameters of the wild-type and variant Lrlnu were determined based on activity versus sucrose concentration curves, fitted with Hill and Michaelis-Menten equations (see APPENDIX) [73, 76]. In previous study, we reported the kinetic parameters of wild-type Lrlnu. The total activity (V^G) of wild-type Lrlnu was fitted with Hill equation, while the transglycosylation activity (V^{G-F}) was fitted with a Michaelis-

Menten equation, and hydrolysis activity (V^F) was fitted with a substrate inhibition model [76]. In this study, the kinetic behavior of R483F, R483Y and R483W was also determined. The results demonstrated that the total activity (V^G), transglycosylation activity (V^{G-F}) and hydrolysis activity (V^F) of all variants were best fitted with Hill equation, Michaelis-Menten equation, and substrate inhibition model, respectively, indicating that the variant Lrlnu exhibited the same kinetic behavior as the wild type. As shown in Table 6, the turnover rate of all activities (k_{cat}^G , k_{cat}^F and k_{cat}^{G-F}) of R483F, R483Y and R483W inulosucrases were significantly decreased compared to that of wild type, while the $K_{50/m}$ values of these inulosucrase variants were increased. Thus, the reduction of catalytic efficiency ($k_{cat}/K_{50/m}$) of R483F, R483Y and R483W variants were observed. The reduction of catalytic activity of variants might be result from the conformational change of the enzyme cavity, which possibly influence the proximity between C2' atom of fructosyl intermediate and O1' atom of acceptors.

After that, the effect of pH and temperature on enzyme activities was also employed in the pH and temperature range of 3.6-8.0 and 10-70 °C, respectively. The results showed that the optimum pH of all of the variant enzymes was not significantly changed, while the optimum temperature of R483F, R483Y and R483W was significantly shifted from 50-60°C to 40-50°C (Figure 34). The change in optimal temperature of inulosucrase might be resulted from the change of enzyme kinetics or stability after mutation. However, in practice, we usually synthesized the FOSs at sub-optimal temperature because of a higher transglycosylation activity and stability. At high temperature, inulosucrase usually synthesized high amount of fructose due to the increase in hydrolysis activity.

4.4.3 Synthesis of FOSs by engineered inulosucrase

To synthesis FOSs, the engineered inulosucrase were incubated with 0.5 M sucrose in 50 mM acetate buffer (pH 5.5) at 30°C for 24 h. The reactions were performed at this sub-optimum temperature since it provides the enzyme higher transglycosylation activity and stability [76]. TLC result demonstrated that the product patterns of all variant enzymes were different (Figure 35A). The variant enzymes synthesized a wide range of oligosaccharides, while the polymeric form was not

observed. MALDI-TOF MS showed that wild type, R483A, R483F, R483Y and R483W produced the FOSs with the degree of polymerization (DP) up to 22 ($m/z = 3606.78$), 12 ($m/z = 1985.48$), 11 ($m/z = 1823.46$), 10 ($m/z = 1661.47$) and 10 ($m/z = 1661.47$), respectively (Figure 35B). The size of FOSs was decreased with the increase of molecular weight of aromatic side chains, suggesting that the bigger aromatic residue may block the enzyme's binding track better.

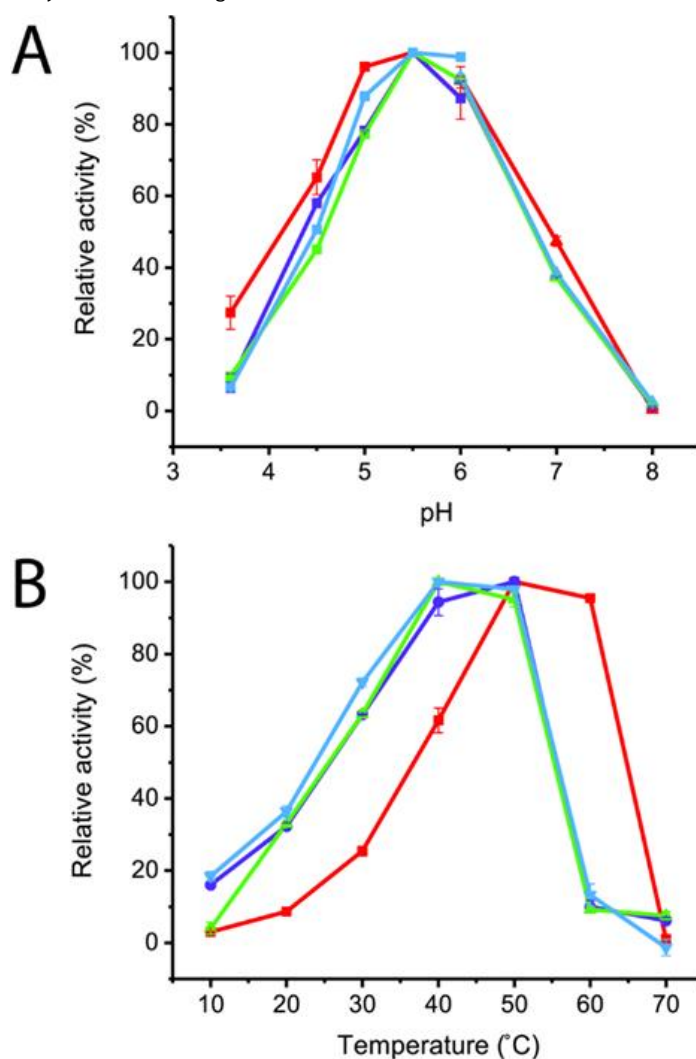


Figure 34. (A) Effect of pH on initial velocity of wild-type and variant inulosucrase. The reactions were performed using 3.6 $\mu\text{g/ml}$ enzymes and 250 mM sucrose in acetate buffer (pH 3.5 – 6.0) and Bis-tris buffer (pH 6.0 – 8.0) at 50°C. (B) Effect of temperature on initial velocity of wild-type and variant inulosucrase. The reactions were performed using 3.6 $\mu\text{g/ml}$ enzymes and 250 mM sucrose in acetate buffer (pH 5.5) at the temperature range of 10 - 70°C.

Quantitative analysis of FOSs was performed by HPLC. The result showed that the total transglycosylation products (total FOSs) of variant Lrlnu were slightly decreased when compared to that of wild type (Figure 36A). The transglycosylation products of R483A, R483F, R483Y and R483W were approximate of 73%, 73%, 68% and 71% of total carbohydrate, respectively, while that of wild type was 76%. This finding indicated that the increase in hydrolysis activity of variant enzymes slightly affected the yield of total FOSs. Furthermore, although the catalytic activity of variant enzymes decreased, it can be compensated by adding more biocatalyst to reach sufficient enzyme activity. Despite the fact that this strategy might increase the cost of FOS synthesis, these variant Lrlnu are still useful since they produce higher valued product (bioactive FOSs). In addition, the FOS products are easier to purify, hence, the cost of purification can be reduced.

The amounts of some identified FOSs of variant and wild-type Lrlnu were also determined. It was found that R483F, R483Y and R483W produced a higher amount of some FOS species when compared to that of wild type (Figure 36B). R483F produced a higher amount of DP5-8, whereas R483Y synthesized higher yield of DP4-8. Moreover, R483W also increased the yield of FOSs with DP3-7 when compared to that of the wild type. These findings supported our conclusions from computational studies which suggested that substitution by aromatic side chain would alter the product chain length specificity of Lrlnu.

According to the predicted $\Delta G_{\text{binding}}$ in Table 5, Fru-R483F and Fru-R483Y have better binding affinity to substrate GF4 (DP5) than the wild type, which may promote transfructosylation between the fru-D272 intermediate and acceptor GF4 (DP5). This would result in the accumulation of product GF5 (DP6) and support the synthesis of longer oligosaccharides. However, although the average value of $\Delta G_{\text{binding}}$ of the R483W variant is about the same as that of the wild type, its ability to produce DP6 was unexpectedly higher than that of the wild type. This might be the limitation of the computational protein design since no protein design software guarantees 100%

successful results. Therefore, it should be confirmed by the in vitro studies. However, in the author's opinion, this methodology is still useful for protein engineering and might have a potential application for improving product specificity of other enzymes.

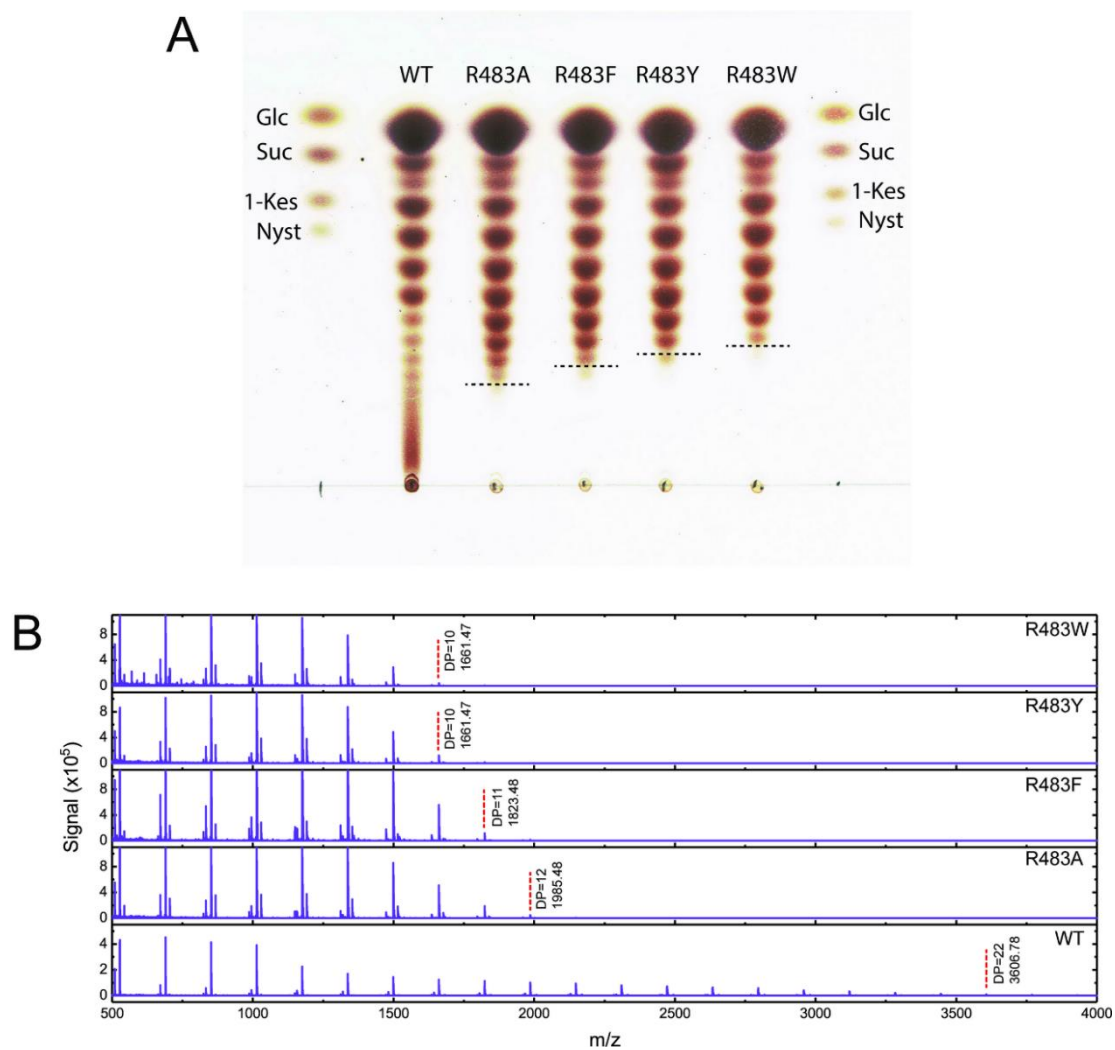


Figure 35. TLC analysis and (B) MALDI-TOF MS spectra of FOS products synthesised by the wild-type and variant *Lrlnu*. The reactions contained 0.5 M sucrose and 5U/mL of the enzymes in 50 mM acetate buffer (pH 5.5) at 30 °C for 24 h.

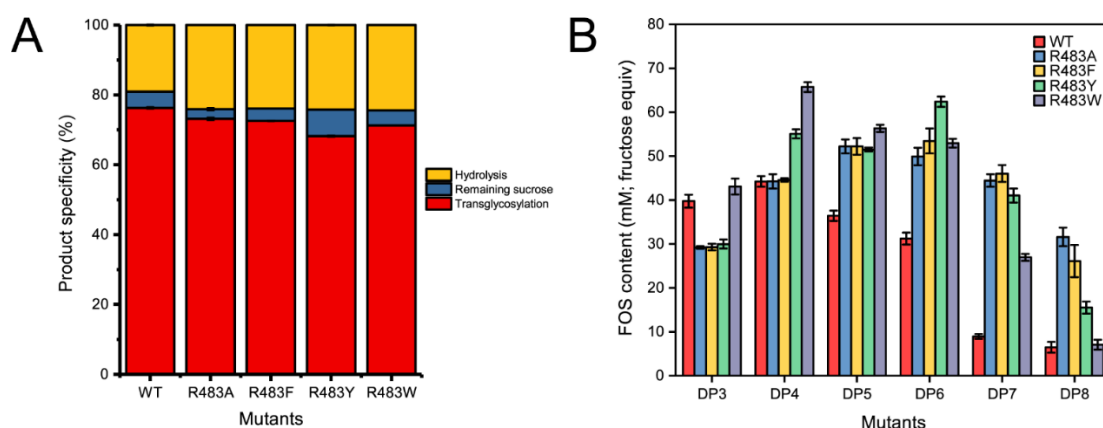


Figure 36. (A) The product specificity of wild-type and variant inulosucrase. (B) The amount of each FOS species produced by wild-type and variant inulosucrase. The reactions contained 0.5 M sucrose and 5U/mL of the enzymes in 50 mM acetate buffer (pH 5.5) at 30 °C for 24 h.

4.5 Conclusion

Employing computer-aided rational protein mutagenesis, we successfully engineered Lrlnu variants (R483F, R483Y and R483W variants) that can produce significantly higher yield of DP 4-8 oligosaccharides than the wild type. Our results indicate that the yields of some FOS synthesized by inulosucrase variants correlate, to some extent, with the relative binding free energies predicted by the Rosetta program. Overall, this study showed the success of using aromatic amino acids, as predicted by Rosetta program, to block the oligosaccharide binding track in inulosucrase controlling the size of oligosaccharides synthesized and demonstrating the effectiveness of the designed enzymes in producing high yields of useful FOSs.

CHAPTER V
IMMOBILIZATION OF MUTANT INULOSUCRASE

Preparation of cross-linked enzyme aggregates (CLEAs) of an inulosucrase mutant for the enzymatic synthesis of inulin-type fructooligosaccharides

Thanapon Charoenwongpaiboon^a, Rath Pichyangkura^a, Robert A. Field^b and
Manchumas Hengsakul Prousoontorn^a

^a *Department of Biochemistry, Faculty of Science, Chulalongkorn University,
Payathai Road, Bangkok 10330, Thailand.*

^b *Department of Biological Chemistry, John Innes Centre, Norwich Research
Park, Norwich, NR4 7UH, UK.*

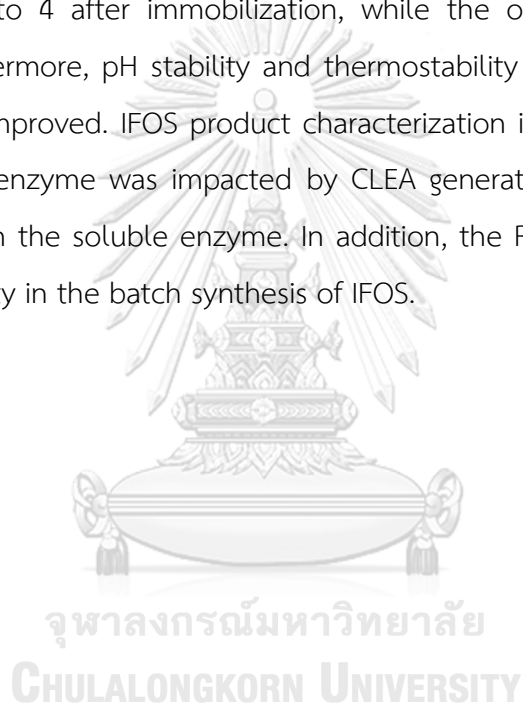
Published in *Catalysts*, 9(8), 641.



จุฬาลงกรณ์มหาวิทยาลัย
CHULALONGKORN UNIVERSITY

5.1 Abstract

Fructooligosaccharides are well-known carbohydrate molecules that exhibit good prebiotic activity and are widely used as sweeteners. Inulin-type fructooligosaccharides (IFOS) can be synthesized from sucrose using inulosucrase. In this study, cross-linked enzyme aggregates (CLEAs) of *Lactobacillus reuteri* 121 inulosucrase (R483A-LrInu) were prepared and used as a biocatalyst for IFOS production. Under optimum conditions, R483A-LrInu CLEAs retained 42% of original inulosucrase activity. Biochemical characterization demonstrated that the optimum pH of inulosucrase changed from 5 to 4 after immobilization, while the optimum temperature was unchanged. Furthermore, pH stability and thermostability of the R483A-LrInu CLEAs was significantly improved. IFOS product characterization indicated that the product specificity of the enzyme was impacted by CLEA generation, producing a narrower range of IFOS than the soluble enzyme. In addition, the R483A-LrInu CLEAs showed operational stability in the batch synthesis of IFOS.



5.2 Introduction

Inulin-type fructooligosaccharides (IFOS) are well known as excellent prebiotics since they promote the growth of beneficial bacteria in the colon [3]. Additionally, IFOS have also been used as a low-calorie sweetener [4]. They can be synthesized enzymatically from sucrose using a β -fructofuranosidase (E.C. 3.2.1.26) derived from fungal species such as *Aspergillus niger* [10, 11], *Aspergillus japonicas* [12-14], *Aspergillus kawachii* [15], and *Aspergillus oryzae* [16]. In addition, IFOS have been synthesized by hydrolysis of inulin using endo-inulinase [87, 88].

Inulosucrase (E.C. 2.4.1.9) is a fructosyltransferase found in many bacterial species such as *Leuconostoc citreum* [17], *Lactobacillus reuteri* [2], *Lactobacillus johnsonii* [18], *Lactobacillus gasseri* [19-21], and *Streptomyces viridochromogenes* [22]. In comparison with fungal β -fructofuranosidase, inulosucrase has a higher transglycosylation activity [89]; it synthesizes both inulin and IFOS from sucrose, while β -fructofuranosidase produces mainly hydrolysis products and short chain oligosaccharides. Production of inulin and IFOS using inulosucrase has been reported with both soluble and immobilized enzymes, the latter being frequently used to increase the stability and reusability of enzymes [90-92]. The efficiency of immobilized biocatalysts is dependent on the supporting material and the linker used. The enzyme can be immobilized on either inorganic or organic materials via bifunctional cross-linkers, or without the supporting carriers. A well-known carrier-free immobilization technique which has attracted extensive attention involves the generation of cross-linked enzyme aggregates (CLEAs). CLEAs are prepared by precipitating the target enzyme using precipitating agents (salts, organic solvents, and non-ionic polymers), followed by cross-linking using bifunctional cross-linkers [93, 94]. This technique provides insoluble, highly concentrated enzyme with enhanced operational and storage stability, which can be freely separated from the reaction by filtration or centrifugation. Many studies have revealed that this method can be applied to a broad range of carbohydrate-modifying enzymes, for instance α -amylase [95], β -galactosidase [30] and levansucrase [96]. Nevertheless, to the best of author's knowledge, only our work has been reported on IFOS synthesis using an immobilized

inulosucrase [82], and no reports have been made on the preparation of CLEAs of inulosucrase. To fully understand the potential application of the different forms of immobilized inulosucrase for IFOS synthesis, further studies are required.

Recently, we reported a series of mutations of *L. reuteri* 121 inulosucrase, with the mutant R483A (R483A-Lrlnu) showing potential application for the production of IFOS [76]. In the present study, R483A-Lrlnu was prepared as a CLEAs format, with optimization of reactions conditions. The activity of the resulting CLEAs was improved by Triton-X treatment. The biochemical properties of R483A-Lrlnu CLEAs were assessed and compared to those of the corresponding soluble enzyme. Finally, the resulting CLEAs of the inulosucrase mutant were used as a biocatalyst for IFOS production.

5.3 Materials and Methods

5.3.1 Expression and purification of inulosucrase mutant

The R483A mutant inulosucrase from *L. reuteri* 121 was expressed and purified according to the method described previously [76]. In brief, the constructed inulosucrase gene was ligated into pET-21b vector (Novagen™) via *Xho*I and *Nde*I site. The cloning of a gene into pET-21b introduced a His6 tag on the C terminus of the recombinant protein. The sequence-verified plasmid was transformed into *Escherichia coli* BL21 (DE3) by electroporation. The recombinant *E. coli* was cultured in LB broth medium supplemented with 100 µg/mL ampicillin, 0.5 % (w/v) glucose and 10 mM CaCl₂, shaking at 250 rpm, at 37°C. Once an OD₆₀₀ reached 0.4–0.6, Isopropyl β-D-1-thiogalactopyranoside (IPTG) was added to a final concentration of 0.1 mM. The cells were further grown by shaking at 200 rpm, at 37 °C for 20 h, and then were harvested by centrifugation at 5000 xg for 20 min.

Cells were disrupted by ultra-sonication and the cell debris was separated from the crude extract enzyme by centrifugation at 12,000 xg for 20 min. The resulting cleared lysate was loaded into TOYOPEARL™ AF-Chelate-650M column pre-equilibrated with 25 mM potassium phosphate buffer (pH 7.4). The column was washed with 25 mM KH₂PO₄ buffer containing 500 mM NaCl and 20 mM imidazole (pH 7.4). The enzyme was eluted from the column with 25 mM KH₂PO₄ buffer containing

500 mM NaCl and 500 mM imidazole (pH 7.4). The fraction containing inulosucrase activity was collected. Bradford assay [38] was used to determine the protein concentration.

5.3.2 Enzyme activity assay

Inulosucrase activity was determined using a DNS assay [39]. The enzyme was incubated in a substrate solution containing 250 mM sucrose, 50 mM acetate buffer (pH 5.5) and 1 mM CaCl₂ at 50°C for 10 min. Then, the reactions were terminated by adding an equal volume of DNS reagent, boiled for 10 min, and the concentration of reducing sugar produced by the enzyme was determined at 540 nm, using a dilution series of glucose concentrations for calibration. A unit of inulosucrase activity was defined as the amount of enzyme required for release of 1 μmol of reducing sugar per minute.

5.3.3 Preparation of cross-linked inulosucrase aggregates

For preparing CLEAs, the enzyme is commonly precipitated, followed by cross-linking using bifunctional agents. In this study, precipitating agents, namely methanol, ethanol, 2-propanol, acetone, acetonitrile, and saturated ammonium sulfate, were investigated. Each precipitation agent (800 μL) was added to 200 μL of inulosucrase solution (to final concentration of 0.2 mg protein/mL). After keeping the mixture with mild agitation at 4°C for 3 h, the precipitated protein was harvested by centrifugation at 10,000 xg for 10 min. The enzyme was re-dissolved in 50 mM acetate buffer (pH 5.5) before measuring enzyme activity by the method described above. The precipitating agent that provided the highest recovered activity of inulosucrase was selected for further studies.

Subsequently, the effects of cross-linking conditions, such as glutaraldehyde concentration, pH and time, were also explored using a suitable precipitating agent. After the enzyme was precipitated, glutaraldehyde was added at different concentration [0, 0.1, 0.2, 0.5, 1.0, 1.5 and 2.0% (v/v)]. The effects of pH and time for cross-linking efficiency were also determined in the pH range of 4-8 and 1- 24 h, respectively. The reaction was terminated by adding 0.1 mL of 1 M Tris-HCl (pH 7.0),

CLEAs were collected by centrifugation at 3,000 $\times g$ for 20 min and then re-suspended in 50 mM acetate buffer (pH 5.5). The CLEAs were washed 3 times with ice-cold acetate buffer (pH 5.5) and kept in this buffer until further characterization. The percentage of recovered activity of the aggregated enzyme was determined by the total inulosucrase activity of CLEAs/total inulosucrase activity of free enzyme $\times 100$.

5.3.4 Biochemical characterization of free and CLEAs R483A-LrInu

The optimal pH for both CLEAs and free R483A-LrInu was determined by assaying enzymatic activity in the pH range of 2.0–10.0 using Britton–Robinson universal buffer [97]. The optimum temperature for both free and immobilized enzymes was also determined, by assaying enzymatic activity in 50 mM acetate buffer (pH 5.5) at a temperature range of 20–70 °C. For analysis of pH stability, the enzymes were pre-incubated at various pH levels (pH 3.0–8.0) using the Britton–Robinson universal buffer. After that, the residual enzymatic activity was measured by the method described above. The thermostability of both enzyme samples was explored by measuring the enzyme activity after incubation in 50 mM acetate buffer (pH 5.5) with 40 mM CaCl_2 at 50 °C from 0 to 9 h.

5.3.5 Oligosaccharide synthesis and analysis

Five units of CLEAs (~0.09 mg CLEAs) or free inulosucrase mutant were incubated with 1 mL of 5 % (w/v) sucrose containing 50 mM acetate buffer pH 5.5 and 40 mM CaCl_2 . The amount of glucose, fructose, and sucrose was analyzed at time points using HPLC with a standard external method. HPLC system was performed with a Prominence UFLC (Shimadzu) fitted with a Sugar-Pak™ column (Water) and a refractive index detector. The samples were separated by 50 mg/L CaEDTA at a flow rate of 0.5 mL/min at 70 °C. The amount of total IFOS was calculated according to the following formula: Total IFOS [% (w/v)] = $\text{Suc}_{\text{initial}}$ [% (w/v)] – $\text{Suc}_{\text{remaining}}$ [% (w/v)] – Glc [% (w/v)] – Fru [% (w/v)], where Suc, Glc and Fru are referred to as sucrose, glucose and fructose, respectively.

The compositions of IFOS were quantitated by HPLC with Asahipak NH2P-50 4E column (Shodex™) using 70% (v/v) acetonitrile as a mobile phase at flow rate of

1.0 mL/min. Quantitative analysis was performed in triplicated using calibration curves of 1-kestose (Sigma–Aldrich) to determine trisaccharide, and nystose (Sigma–Aldrich) to determine tetrasaccharides and longer oligosacchrides. The error bar represented the standard deviation (SD).

HPAEC-PAD was performed by ICS 5000 system (Dionex) and a CarboPack PA1 column at a flow rate of 1.0 mL/min. The IFOS were separated using a linear gradient of 0–250 mM sodium acetate in 150 mM NaOH for 30 min.

Mass of IFOS products was evaluated by MALDI-TOF mass spectrometry (Autoflex speed, BRUKER) using 2,5-Dihydroxybenzoic acid (DHB) as the matrix.

5.3.6 Operational stability

The operational stability of R483A-Lrlnu CLEAs was evaluated by assessing IFOS synthesis in 10 consecutive experimental cycles. The reaction conditions were 5 U/ml CLEAs, 5% (w/v) sucrose, 50 mM acetate buffer (pH 5.5), 30 °C for 20 min. After each cycle of operation, the CLEAs were collected by centrifugation at 3000 xg for 10 min. The pellets were washed twice with ice-cold acetate buffer (50 mM, pH 5.5). The remaining activity of CLEAs was measured by the method as described above.

5.4 Results and discussion

5.4.1. Preparation of immobilized inulosucrase mutant

CLEAs are usually prepared by two steps: precipitation of the enzyme from an aqueous solution and cross-linking of this aggregated enzyme with a bifunctional cross-linking agent. In this study, six different protein precipitating agents were investigated, analyzed and compared. Activity assays showed that, of the tested precipitants, ammonium sulfate provided the highest recovered activity of R483A-Lrlnu ($79.0 \pm 6.1\%$) (Figure 37A). The optimum amount of ammonium sulfate required for activity recovery was then investigated, using a concentration range of 2-40% (w/v) ammonium sulfate. It can be seen that the precipitated enzyme can retain $85.5 \pm 9.4\%$ of its initial enzyme activity using 40% (w/v) of ammonium sulfate (Figure 37B). This results are consistent with earlier reports that ammonium sulfate has been used to prepare high enzyme activity of various CLEAs, such as α -amylase [95], β -galactosidase [30], lipase [98],

tyrosinase [99, 100], subtilisin [101], phytase [102], feruloyl esterase [103], invertase [104] and levansucrase [96].

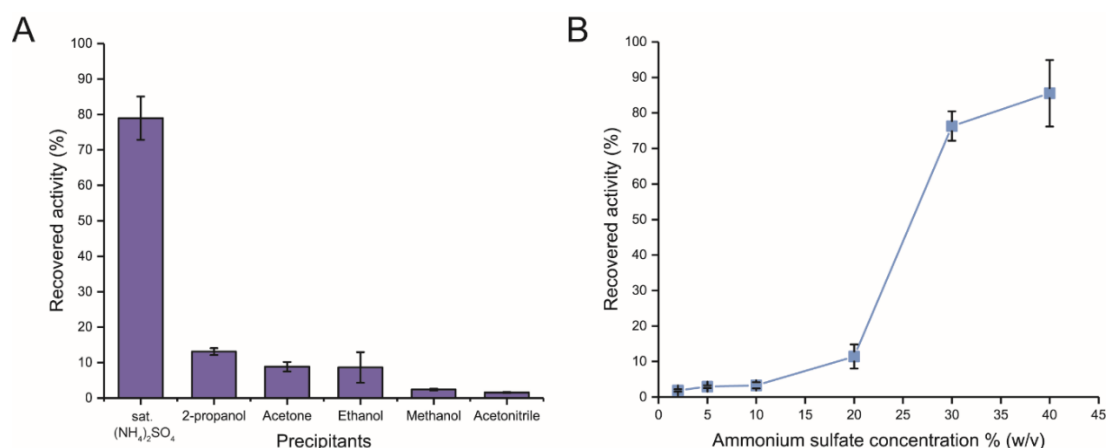


Figure 37. (A) Precipitation of R483A-LrInu with different precipitating agents. (B) The effect of ammonium sulfate concentration on the recovered activity of precipitated R483A-LrInu. The data represent the mean of three assays, and error bars represent the standard deviation of three experiments.

The effect of cross-linker concentration on CLEA activity was further explored using different final glutaraldehyde concentration of 0 – 2% (v/v). It was found that the highest recovered activity was achieved when the enzyme was cross linked with 0.5%(w/v) glutaraldehyde (Figure 38A). The effect of cross-linking pH was also investigated in the pH range of 4–8. At pH 5–7, the enzyme retained the highest activity (Figure 38B). The pH may affect the stability of the enzyme during the cross-linking process. Moreover, pH also affects the cross-linking mechanism of glutaraldehyde, influencing the rigidity or flexibility of CLEAs [41, 42, 94]. Subsequently, the effect of cross-linking time was explored, and it was found that cross-linking at 4°C for 3 h was optimal, and the recovered activity of CLEAs gradually decreased when the cross-linking time increased beyond that (Figure 38C). The R483A-LrInu CLEAs prepared under these conditions showed a retention of 35.4±4.1% of initial LrInu activity. The reduction in enzyme activity on CLEA formation may result from conformational changes of enzyme after the cross-linking process or the shielding of the catalyst active site by other aggregated proteins after precipitation. To reduce the effect of enzyme

aggregation on LrInu activity, the CLEAs were incubated with 0.1% Triton-X100, a nonionic surfactant, for 1 h. From the results in Figure 38D, it can be seen that the precipitated enzyme activity was improved ($42.0 \pm 6.0\%$) when compared to that of the untreated CLEAs. This suggested that Triton-X might remove non-specific hydrophobic interaction between the aggregated enzymes molecules, thereby increasing the rate of substrate/product diffusion to/from the active site. Under this condition, the CLEAs have immobilization yield about 94% with specific activity of 53 U/mg.

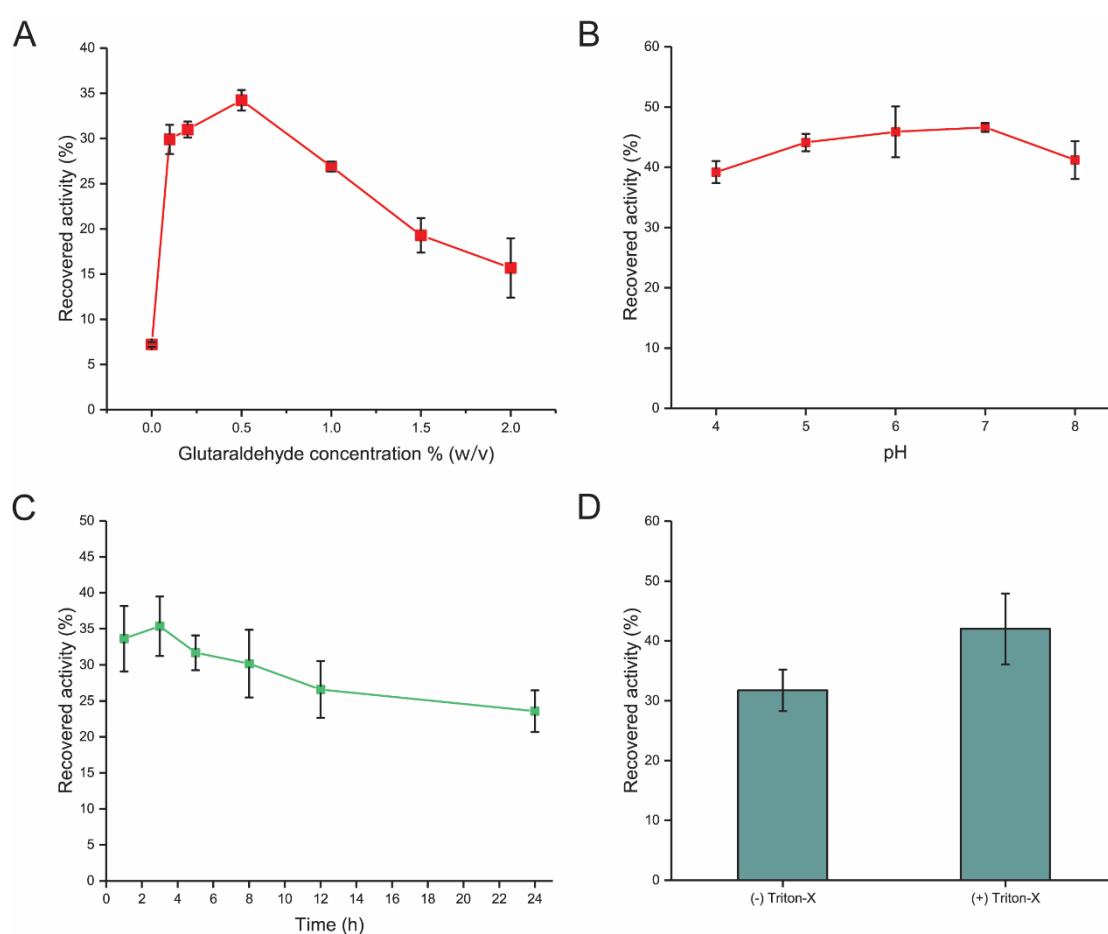


Figure 38. Effect of (A) glutaraldehyde concentration, (B) pH, (C) incubation time and (D) Triton-X100 treatment on the recovered activity of CLEAs. The data represent means of three assays, and error bars represent the standard deviation.

5.4.2. Biochemical characterization of free and immobilized R483A-LrInu

The optimum pH and temperature of the R483A-LrInu CLEAs were determined and compared to those of the free enzyme. The result demonstrated that the optimum pH of CLEAs was shifted to 4.0. The optimum pH of free inulosucrase was at pH 5.0, which was consistent with previous report [73]. The pH profile showed that CLEAs exhibited 20 – 60% relative activity in the alkaline range (pH 8.0–10.0), whereas the free enzyme completely lost its activity (< 5% relative activity) (Figure 39A). The shift of optimum pH might result from the change in ionization of amino acid residues in the microenvironment around the active site. This finding has been described for α -amylase [95], tyrosinase [99, 100] and lipase [98]. The optimum temperature for free and immobilized R483A-LrInu was found to be the same at 50°C. However, the temperature profile of the CLEAs format was broader than the free enzyme. CLEAs still exhibited 15-35% of inulosucrase relative activity at 60-70°C, while the free inulosucrase was inactive (< 5% relative activity) (Figure 39B). This finding suggested that the immobilization of inulosucrase in a CLEA format was able to preserve activity and increase the stability of the enzyme, resulting in a catalyst that is active in a wider range of conditions.

The pH stability of free and CLEA R483A-LrInu was investigated in the buffer pH range 3.0–8.0, reflecting the high stability of the enzyme in this range (>50% relative activity). As shown in Figure 40A, both free and CLEAs of R483A-LrInu are stable in a broad pH range (3.0–8.0). Nonetheless, the CLEAs are more stable than the free inulosucrase, retaining essentially 100% of its initial activity in the pH range of 6.0 – 8.0, while the free inulosucrase retained only 80% (Figure 40A). This result suggested that the preparation of inulosucrase as a CLEA has the potential to prevent the degradation or denaturation of inulosucrase during a pH change in the solution. For thermostability, both free and CLEA forms of R483A-LrInu were incubated at 50°C for 9 h. Under these conditions, the CLEAs retained activity as high as 70% of its initial activity, whereas the free R483A-LrInu retained only 50% at the same temperature (Figure 40B). The cross-linking approach could prevent the denaturation of enzyme molecules and stabilize the active conformation of the enzyme at high temperature.

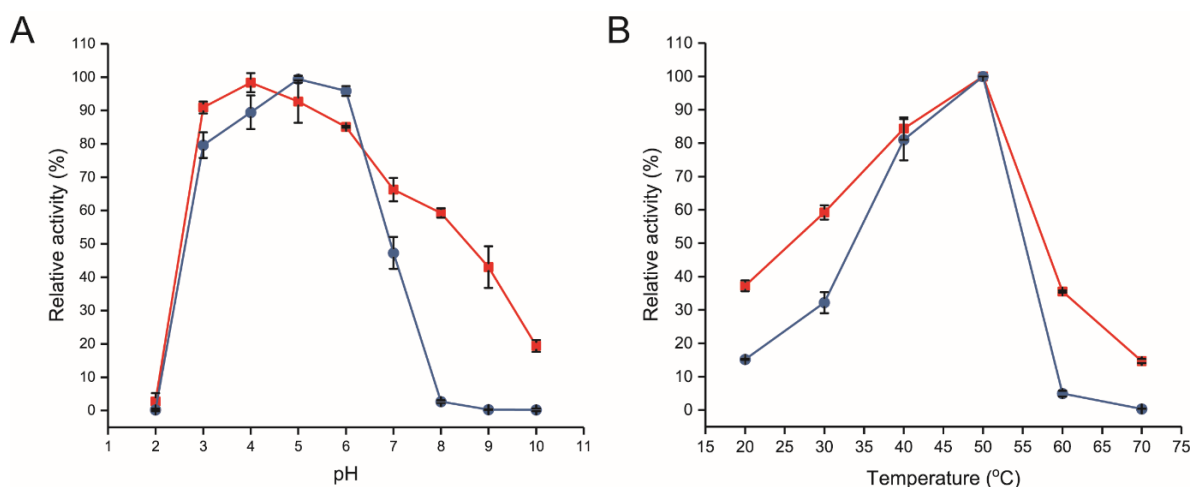


Figure 39. Effect of (A) pH and (B) temperature on the activity of free (blue line) and CLEAs R483A-Lrlnu (red line).

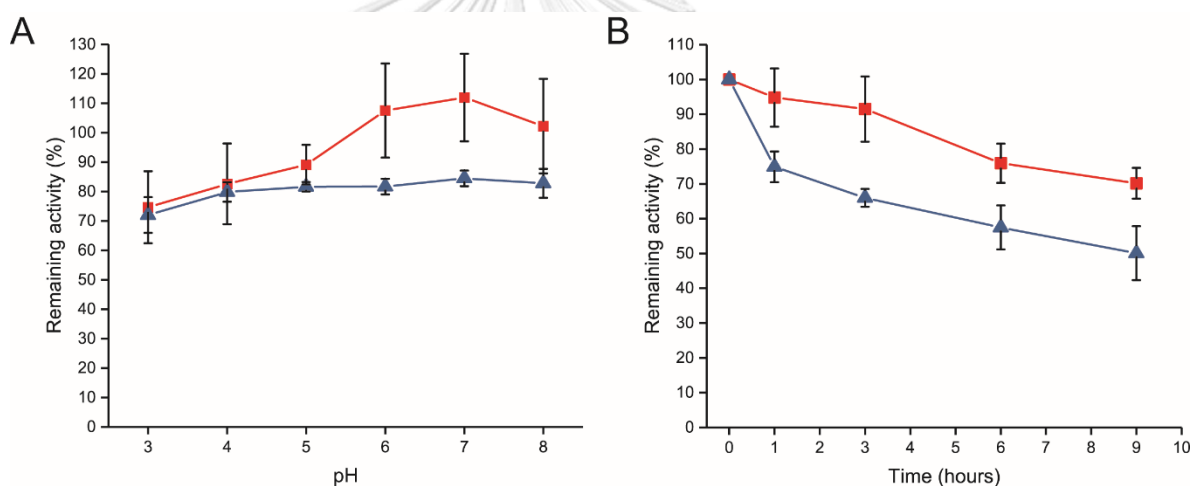


Figure 40. Effect of (A) pH and (B) temperature on the stability of free (blue line) and CLEAs R483A-Lrlnu (red line).

5.4.3. IFOS synthesis using free and immobilized R483A-Lrlnu

Enzyme immobilization is a technique that provides a microenvironment which prevents, or at least reduces, enzyme inactivation. Multiple covalent linkages might result in conformational changes of protein and may affect the product specificity. To explore the influence of immobilization on the IFOS product profile, thin layer chromatography (TLC) analysis of IFOS derived from free and immobilized R483A-Lrlnu was employed. The result demonstrated that the patterns of IFOS synthesized from free and immobilized R483A-Lrlnu were significantly different (Figure 41A). MALDI-TOF

analysis showed that The CLEAs synthesized shorter chain of IFOS, with degree of polymerization (DP) ranging from 3–8, while the soluble R483A-LrInu synthesized somewhat longer IFOS, with DP up to 13 (Figure 42). The change of the IFOS pattern produced by R483A-LrInu CLEAs suggested that they may provide a microenvironment for enzyme molecules which allowed only specific acceptors to diffuse into the enzyme active site, increasing product specificity. This finding was reported for other immobilized fructosyltransferase, such as levansucrase immobilized on vinyl sulfone-activated silica which selectively produced levan-type fructooligosaccharides (LFOs), while soluble levansucrase produced both LFOs and levan [43].

High performance liquid chromatography with pulsed amperometric detector (HPAEC-PAD) was also performed to confirm the findings of TLC analysis. The HPAEC result indicated that immobilization did not affect the linkage type of IFOS produced by R483A-LrInu, because all peaks observed on HPAEC profiles of both free and immobilized enzymes were located at the same position (Figure 41B). Quantitative analysis of IFOS produced by free and immobilized enzymes were also performed by HPLC with amino column (Figure 41C) (Asahipak NH2P-50 4E™ column, Shodex). The result showed that R483A-LrInu CLEAs produced higher amount of GF2-GF3, and lower amount of GF4-GF7 in comparison with the free enzyme. This finding indicated that preparation of inulosucrase as CLEAs can regulate the size of IFOS synthesized. Many studies showed that the biological activity of inulin is strongly dependent on its degree of polymerization. For example, IFOS with DP 2 – 8 show higher prebiotic activity than DP > 9 [53]. IFOS with DP 4 increased immunoglobulin A (IgA) secretion and enhanced IFN- γ and IL-10 production in the cecal CD4⁺ T cells in the rat [5]. Moreover, IFOS with DP 4-7 also had modest anti-oxidant activity [105]. Therefore, the R483A-LrInu CLEAs might be useful for the synthesis of bioactive oligosaccharides.

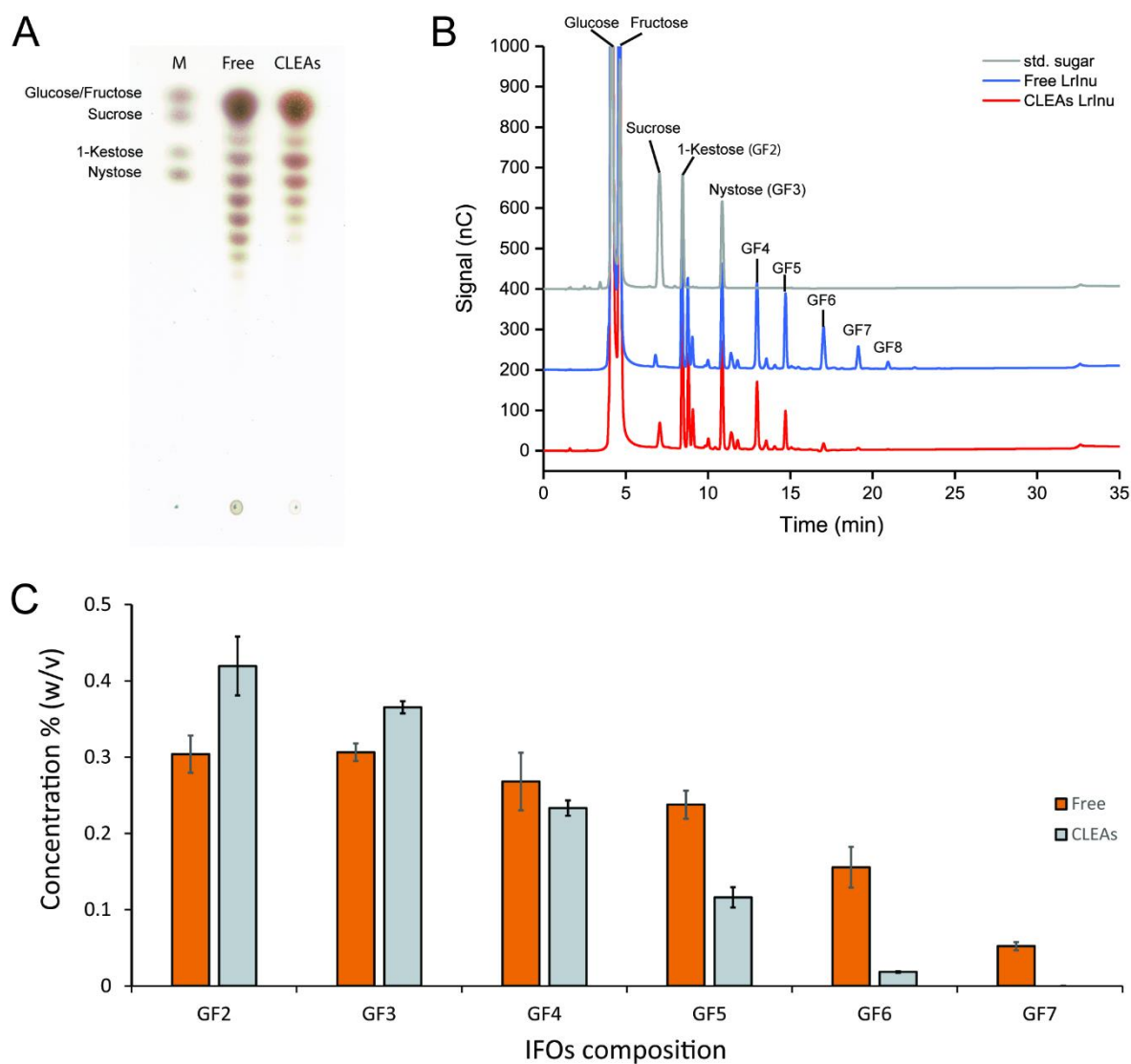


Figure 41. (A) TLC analysis of IFOS profiles synthesized by free and immobilized inulosucrase; lane M indicated the standard sugar. (B) HPAEC chromatogram of standard sugars and IFOS synthesized by free and immobilized inulosucrase. (C) IFOS compositions analyzed by HPLC with Asahipak NH2P-50 4E column.

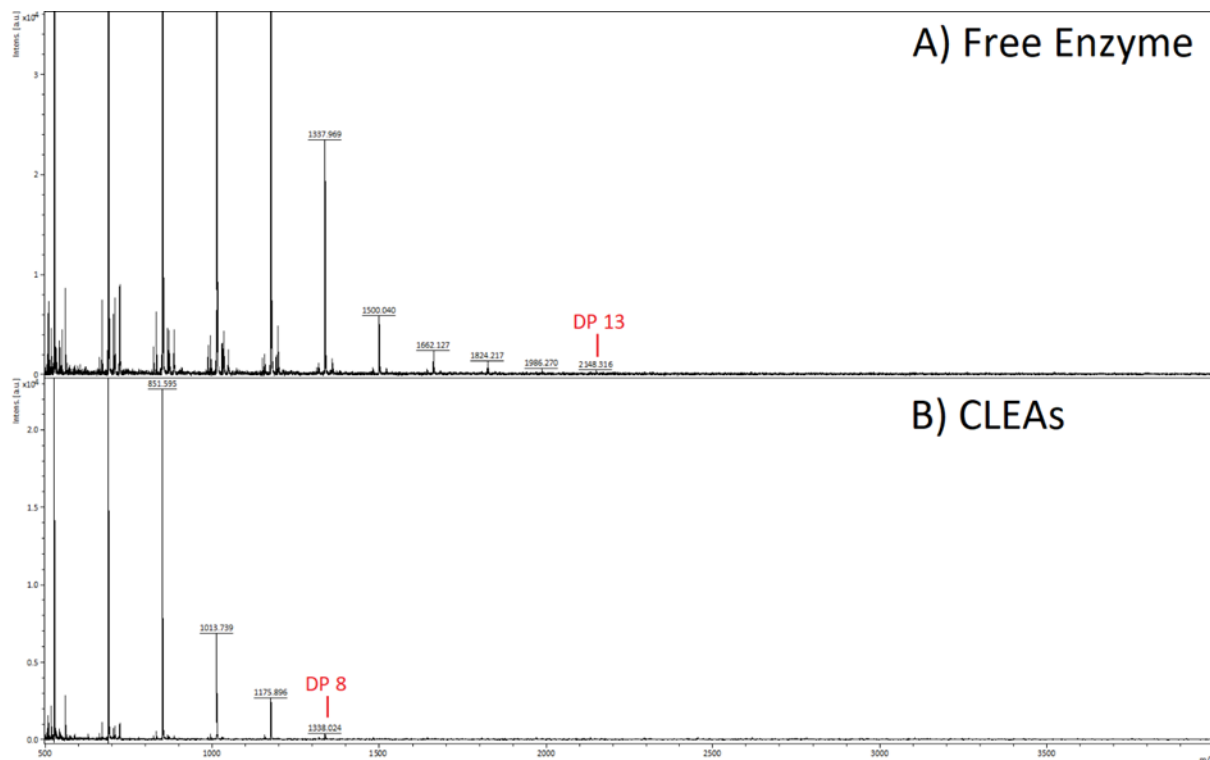


Figure 42. MALDI-TOF analysis of IFOS synthesized by free and immobilized inulosucrase.

Furthermore, the total IFOS produced by R483A-LrInu CLEAs was quantified using HPLC with Sugar-Pak™ column (Water) (Figure 43). The result showed that R483A-LrInu CLEAs could synthesize the total IFOS up to 1.2% (w/v) after incubating with 5% (w/v) sucrose for 4 h. After that, the amount of IFOS slightly decreased, and seemed to be constant at approximately of 1% (w/v) although the reaction was performed for 30 h.

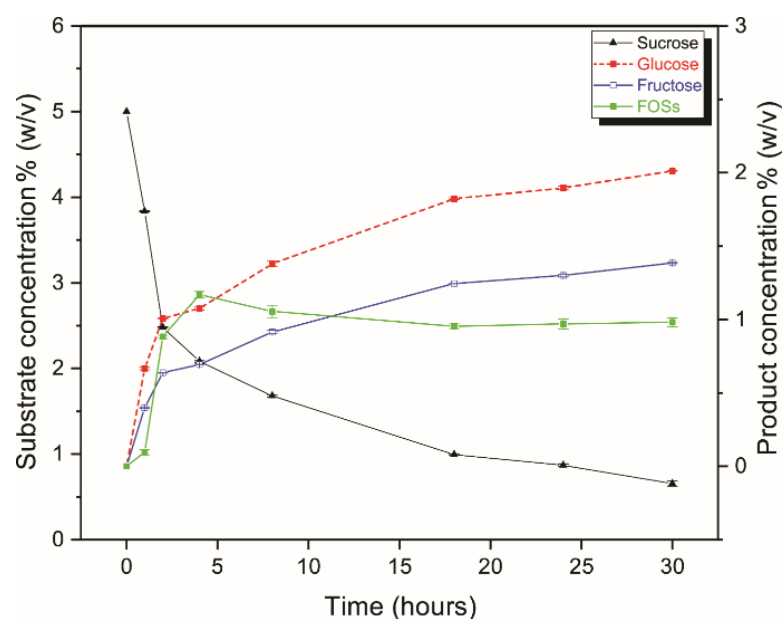


Figure 43. Production of IFOS by R483A-LrInu CLEAs. Reaction condition: 5 U/mL R483A-LrInu CLEAs, 5% (w/v) sucrose, 50 mM acetate buffer (pH 5.5) at 30°C. The sugar content was analyzed by HPLC with Sugar-Pak™ column.

5.4.4 Operational stability of R483A-LrInu CLEAs

Besides the increase in enzyme stability, the immobilized enzymes are also reusable [106, 107]. The operational stability of R483A-LrInu CLEAs was evaluated in a series of batch reactions. As presented in Figure 44, the activity of CLEAs reduced after four cycles of reuse and then remained constant at approximately 45% of the original activity. The reduction of CLEAs activity in early cycles might result from the more compact nature of CLEAs or desorption of non-covalently bound enzyme molecules after recycling of biocatalyst. This phenomenon was also found in other covalently immobilized enzymes, such as levansucrase immobilized on vinyl sulfone-activated silica [43] and inulosucrase immobilized on core-shell chitosan beads [82].

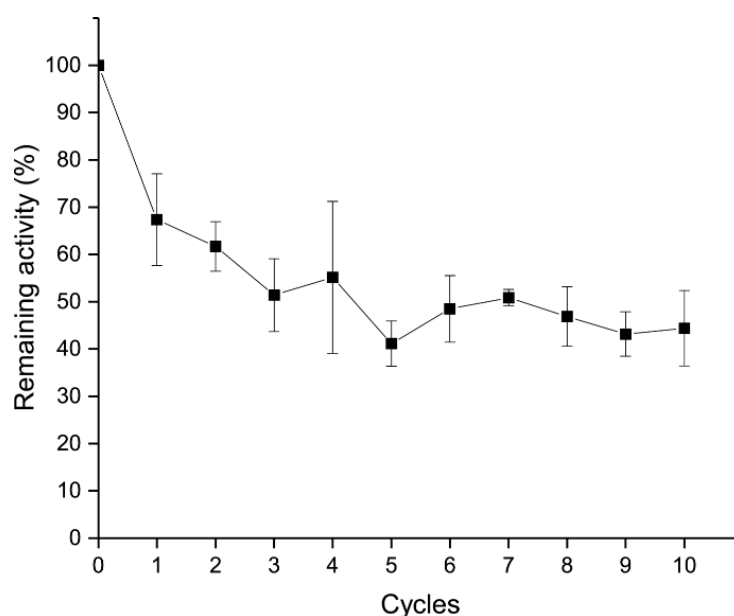


Figure 44. Operational stability of R483A-LrInu CLEAs.

5.5 Conclusion

The generation and characterization of CLEAs of *L. reuteri* inulosucrase mutant (R483A-LrInu) is first reported in this study. In comparison with the soluble inulosucrase, the CLEA-immobilized enzyme has higher pH stability and thermostability, as well as the promising operational stability for batch production of IFOS. Furthermore, the immobilization also increases the product specificity. Biedrzycka and Bielecka [41] reported that the prebiotic activity of IFOS is mainly dependent on their degree of polymerization, DP 2 – 8 showing higher prebiotic activity than DP > 9 [41]. Hence, the IFOS produced by R483A-LrInu CLEAs may be expected to have a higher prebiotic activity than the IFOS produced by soluble R483A-LrInu. Hence the overall properties of R483A-LrInu CLEAs make them very attractive as a biocatalyst for the synthesis of prebiotic IFOS.

CHAPTER VI

CONCLUSION

In present study, the combination of enzyme immobilization and enzyme engineering was used to improve the properties of inulosucrase. The immobilized inulosucrase from *Lactobacillus reuteri* 121 was firstly reported in this study. The wild-type inulosucrase was immobilized onto the novel, high capacity, core-shell chitosan beads (CSB) using glutaraldehyde. It was found that pH, glutaraldehyde concentration and protein concentration affects the immobilization efficiency and activity of immobilized enzyme. Biochemical characterization indicated that immobilized inulosucrase on CSB (INU-CSB) possessed excellent stability compared with the free enzyme. The INU-CSB was also used for fructooligosaccharide (FOS) synthesis, in both batch and continuous processes. The result analyzed by HPAEC indicated that the patterns of FOS synthesized from free and immobilized enzymes were comparable. Moreover, INU-CSB can be reused for the synthesis of IFOS at least 12 cycles, indicating that this immobilized biocatalyst has promising operational stability for batch and continuous production of IFOSs.

Nevertheless, the immobilization of inulosucrase on core-shell chitosan still had some limitations. Wild-type inulosucrase synthesized both oligosaccharide and fructan polymer, which possibly trapped in the pore of chitosan beads during the reactions. Therefore, the product pattern of inulosucrase should be engineered by rational site-directed mutagenesis. Initially, the oligosaccharides binding track of inulosucrase was unraveled by using structural-based prediction and alanine screening methodology. HPAEC-PAD, MALDI-TOF MS and molecular docking showed that oligosaccharides binding residues of inulosucrase located on different position from levansucrase. This is a first report that provides insight into the product binding motif of *Lactobacillus reuteri* inulosucrase.

After the oligosaccharide binding residues of inulosucrase was discovered, we attempt to engineer the size of FOS by blocking this oligosaccharide binding track using genetic engineering. Some amino acid residues were substituted by some bulky amino acid residues, such as phenylalanine, tyrosine and tryptophan. Computational

software, Rosetta, was used to predict the binding conformation, and calculated binding energy ($\Delta G_{\text{binding}}$) of oligosaccharide and enzyme. This study demonstrated the success of using aromatic amino acids to block the oligosaccharide binding track of inulosucrase in order to controlling the size of oligosaccharide synthesized.

Then, the stability and reusability of mutant enzyme was improved by enzyme immobilization. R483A mutant of inulosucrase was immobilized using cross-linked enzyme aggregates (CLEAs) under optimum conditions. It was found that glutaraldehyde concentration, pH and incubation time affected the activity of the CLEAs. Biochemical characterization indicated that the immobilization can improve pH and thermal stability of inulosucrase. Furthermore, the product specificity of inulosucrase was also improved by increasing the yield of GF2 and GF3.

Overall, this study showed the success of using enzyme immobilization and enzyme engineering techniques to improve the specificity and stability of inulosucrase. To the best of our knowledge, this is a first report on immobilization of inulosucrase. Moreover, enzyme engineering study not only offers a novel mutant enzyme that can synthesize different chain length of FOS, but also provides insight into the product binding motif of *Lactobacillus reuteri* 121 inulosucrase.

REFERENCES

1. Daudé, D., M. Remaud-Siméon, and I. André, *Sucrose analogs: an attractive (bio)source for glycodiversification*. Natural Product Reports, 2012. **29**(9): p. 945-960.
2. van Hijum, S.A.F.T., et al., *Characterization of a Novel Fructosyltransferase from Lactobacillus reuteri That Synthesizes High-Molecular-Weight Inulin and Inulin Oligosaccharides*. Applied and Environmental Microbiology, 2002. **68**(9): p. 4390-4398.
3. MACFARLANE, S., G.T. MACFARLANE, and J.H. CUMMINGS, *Review article: prebiotics in the gastrointestinal tract*. Alimentary Pharmacology & Therapeutics, 2006. **24**(5): p. 701-714.
4. Mabel, M.J., et al., *Physicochemical characterization of fructooligosaccharides and evaluation of their suitability as a potential sweetener for diabetics*. Carbohydrate Research, 2008. **343**(1): p. 56-66.
5. Ito, H., et al., *Degree of Polymerization of Inulin-Type Fructans Differentially Affects Number of Lactic Acid Bacteria, Intestinal Immune Functions, and Immunoglobulin A Secretion in the Rat Cecum*. Journal of Agricultural and Food Chemistry, 2011. **59**(10): p. 5771-5778.
6. Peshev, D. and W. Van den Ende, *Fructans: Prebiotics and immunomodulators*. Journal of Functional Foods, 2014. **8**: p. 348-357.
7. Pang, D.-J., et al., *Characterization of Inulin-Type Fructan from Platycodon grandiflorus and Study on Its Prebiotic and Immunomodulating Activity*. 2019. **24**(7): p. 1199.
8. Scholz-Ahrens, K.E. and J.r. Schrezenmeir, *Inulin and Oligofructose and Mineral Metabolism: The Evidence from Animal Trials*. The Journal of Nutrition, 2007. **137**(11): p. 2513S-2523S.
9. Fiordaliso, M., et al., *Dietary oligofructose lowers triglycerides, phospholipids and cholesterol in serum and very low density lipoproteins of rats*. 1995. **30**(2): p. 163-167.

10. Yanai, K., et al., *Molecular Cloning and Characterization of the Fructooligosaccharide-Producing β -Fructofuranosidase Gene from Aspergillus niger ATCC 20611*. *Bioscience, Biotechnology, and Biochemistry*, 2001. **65**(4): p. 766-773.
11. Goosen, C., et al., *Molecular and Biochemical Characterization of a Novel Intracellular Invertase from Aspergillus niger with Transfructosylating Activity*. *Eukaryotic Cell*, 2007. **6**(4): p. 674-681.
12. Mussatto, S.I., et al., *Fructooligosaccharides and β -fructofuranosidase production by Aspergillus japonicus immobilized on lignocellulosic materials*. *Journal of Molecular Catalysis B: Enzymatic*, 2009. **59**(1): p. 76-81.
13. Yang, Y.-l., et al., *Preparation of High-Purity Fructo-oligosaccharides by Aspergillus japonicus β -Fructofuranosidase and Successive Cultivation with Yeast*. *Journal of Agricultural and Food Chemistry*, 2008. **56**(8): p. 2805-2809.
14. Cheng, T.-C., K.-J. Duan, and D.-C. Sheu, *Immobilization of β -fructofuranosidase from Aspergillus japonicus on chitosan using tris(hydroxymethyl)phosphine or glutaraldehyde as a coupling agent*. *Biotechnology Letters*, 2005. **27**(5): p. 335.
15. Nagaya, M., et al., *Crystal structure of a β -fructofuranosidase with high transfructosylation activity from Aspergillus kawachii*. *Bioscience, Biotechnology, and Biochemistry*, 2017. **81**(9): p. 1786-1795.
16. Kurakake, M., et al., *Production of Fructooligosaccharides by β -Fructofuranosidases from Aspergillus oryzae KB*. *Journal of Agricultural and Food Chemistry*, 2010. **58**(1): p. 488-492.
17. Ortiz-Soto, M.E., V. Olivares-Illana, and A. López-Munguía, *Biochemical properties of inulosucrase from Leuconostoc citreum CW28 used for inulin synthesis*. *Biocatalysis and Biotransformation*, 2004. **22**(4): p. 275-281.
18. Anwar, M.A., et al., *The Probiotic Lactobacillus johnsonii NCC 533 Produces High-Molecular-Mass Inulin from Sucrose by Using an Inulosucrase Enzyme*. *Applied and Environmental Microbiology*, 2008. **74**(11): p. 3426-3433.

19. Anwar, M.A., et al., *Inulin and levan synthesis by probiotic Lactobacillus gasseri strains: characterization of three novel fructansucrase enzymes and their fructan products*. Microbiology, 2010. **156**(4): p. 1264-1274.
20. Díez-Municio, M., et al., *Enzymatic Synthesis and Characterization of Fructooligosaccharides and Novel Maltosylfructosides by Inulosucrase from Lactobacillus gasseri DSM 20604*. Applied and Environmental Microbiology, 2013. **79**(13): p. 4129-4140.
21. Ni, D., et al., *Biosynthesis of inulin from sucrose using inulosucrase from Lactobacillus gasseri DSM 20604*. International Journal of Biological Macromolecules, 2018. **109**: p. 1209-1218.
22. Frasch, H.-J., S.S.v. Leeuwen, and L. Dijkhuizen, *Molecular and biochemical characteristics of the inulosucrase HugO from Streptomyces viridochromogenes DSM40736 (Tü494)*. Microbiology, 2017. **163**(7): p. 1030-1041.
23. Charoenwongpaiboon, T., et al., *Preparation of Cross-Linked Enzyme Aggregates (CLEAs) of an Inulosucrase Mutant for the Enzymatic Synthesis of Inulin-Type Fructooligosaccharides*. 2019. **9**(8): p. 641.
24. Steiner, K. and H. Schwab, *RECENT ADVANCES IN RATIONAL APPROACHES FOR ENZYME ENGINEERING*. Computational and Structural Biotechnology Journal, 2012. **2**(3): p. e201209010.
25. Lorenzoni, A.S.G., et al., *Fructooligosaccharides synthesis by highly stable immobilized β -fructofuranosidase from Aspergillus aculeatus*. Carbohydrate Polymers, 2014. **103**: p. 193-197.
26. Fernandez-Arrojo, L., et al., *Dried alginate-entrapped enzymes (DALGEEs) and their application to the production of fructooligosaccharides*. Process Biochemistry, 2013. **48**(4): p. 677-682.
27. Smaali, I., et al., *Production of high-fructose syrup from date by-products in a packed bed bioreactor using a novel thermostable invertase from Aspergillus awamori*. Biocatalysis and Biotransformation, 2011. **29**(6): p. 253-261.

28. López-Gallego, F., J.M. Guisán, and L. Betancor, *Glutaraldehyde-Mediated Protein Immobilization*, in *Immobilization of Enzymes and Cells: Third Edition*, J.M. Guisan, Editor. 2013, Humana Press: Totowa, NJ. p. 33-41.
29. Krajewska, B., *Application of chitin- and chitosan-based materials for enzyme immobilizations: a review*. *Enzyme and Microbial Technology*, 2004. **35**(2): p. 126-139.
30. Budnyak, T.M., et al., *Synthesis and adsorption properties of chitosan-silica nanocomposite prepared by sol-gel method*. *Nanoscale Research Letters*, 2015. **10**(1): p. 87.
31. Yang, W.-Y., et al., *Development of Silica Gel-Supported Modified Macroporous Chitosan Membranes for Enzyme Immobilization and Their Characterization Analyses*. *The Journal of Membrane Biology*, 2014. **247**(7): p. 549-559.
32. Lei, Z. and S. Bi, *The silica-coated chitosan particle from a layer-by-layer approach for pectinase immobilization*. *Enzyme and Microbial Technology*, 2007. **40**(5): p. 1442-1447.
33. Ye, N., et al., *Synthesis of magnetite/graphene oxide/chitosan composite and its application for protein adsorption*. *Materials Science and Engineering: C*, 2014. **45**: p. 8-14.
34. Wang, J., et al., *Facile self-assembly of magnetite nanoparticles on three-dimensional graphene oxide-chitosan composite for lipase immobilization*. *Biochemical Engineering Journal*, 2015. **98**: p. 75-83.
35. Li, G.-y., et al., *Surface functionalization of chitosan-coated magnetic nanoparticles for covalent immobilization of yeast alcohol dehydrogenase from *Saccharomyces cerevisiae**. *Journal of Magnetism and Magnetic Materials*, 2010. **322**(24): p. 3862-3868.
36. Kuo, C.-H., et al., *Optimum conditions for lipase immobilization on chitosan-coated Fe₃O₄ nanoparticles*. *Carbohydrate Polymers*, 2012. **87**(4): p. 2538-2545.
37. Plou, F.J., et al., *Application of Immobilized Enzymes for the Synthesis of Bioactive Fructooligosaccharides*, in *Food Oligosaccharides*. 2014. p. 200-216.

38. Bradford, M.M., *A rapid and sensitive method for the quantitation of microgram quantities of protein utilizing the principle of protein-dye binding*. Analytical biochemistry, 1976. **72**(1): p. 248-254.
39. Miller, G.L., *Use of dinitrosalicylic acid reagent for determination of reducing sugar*. Analytical chemistry, 1959. **31**(3): p. 426-428.
40. Betancor, L., et al., *Glutaraldehyde in Protein Immobilization*, in *Immobilization of Enzymes and Cells*, J.M. Guisan, Editor. 2006, Humana Press: Totowa, NJ. p. 57-64.
41. Migneault, I., et al., *Glutaraldehyde: behavior in aqueous solution, reaction with proteins, and application to enzyme crosslinking*. Biotechniques, 2004. **37**(5): p. 790-802.
42. Okuda, K., et al., *Reaction of glutaraldehyde with amino and thiol compounds*. Journal of Fermentation and Bioengineering, 1991. **71**(2): p. 100-105.
43. Santos-Moriano, P., et al., *Vinyl sulfone-activated silica for efficient covalent immobilization of alkaline unstable enzymes: application to levansucrase for fructooligosaccharide synthesis*. RSC Advances, 2016. **6**(69): p. 64175-64181.
44. Illanes, A., et al., *Heterogeneous Enzyme Kinetics*, in *Enzyme Biocatalysis: Principles and Applications*, A. Illanes, Editor. 2008, Springer Netherlands: Dordrecht. p. 155-203.
45. Bissett, F. and D. Sternberg, *Immobilization of Aspergillus beta-glucosidase on chitosan*. Applied and environmental microbiology, 1978. **35**(4): p. 750-755.
46. Reshmi, R., G. Sanjay, and S. Sugunan, *Enhanced activity and stability of α -amylase immobilized on alumina*. Catalysis Communications, 2006. **7**(7): p. 460-465.
47. Abdel-Naby, M.A., et al., *Immobilization of Aspergillus oryzae tannase and properties of the immobilized enzyme*. 1999. **87**(1): p. 108-114.
48. Schmitt, M., U. Schuler-Schmid, and W. Schmidt-Lorenz, *Temperature limits of growth, TNase and enterotoxin production of Staphylococcus aureus strains isolated from foods*. International Journal of Food Microbiology, 1990. **11**(1): p. 1-19.

49. Secundo, F., *Conformational changes of enzymes upon immobilisation*. Chemical Society Reviews, 2013. **42**(15): p. 6250-6261.
50. Sangmanee, S., et al., *Production and immobilization of levansucrase*. Chiang Mai Journal of Science, 2015. **42**(1): p. 44-51.
51. Cantarel, B.L., et al., *The Carbohydrate-Active EnZymes database (CAZy): an expert resource for Glycogenomics*. Nucleic Acids Research, 2008. **37**(suppl_1): p. D233-D238.
52. Ozimek, L.K., et al., *The levansucrase and inulosucrase enzymes of Lactobacillus reuteri 121 catalyse processive and non-processive transglycosylation reactions*. 2006. **152**(4): p. 1187-1196.
53. Biedrzycka, E. and M. Bielecka, *Prebiotic effectiveness of fructans of different degrees of polymerization*. Trends in Food Science & Technology, 2004. **15**(3): p. 170-175.
54. Meng, G. and K. Fütterer, *Structural framework of fructosyl transfer in Bacillus subtilis levansucrase*. Nature Structural & Molecular Biology, 2003. **10**(11): p. 935-941.
55. Homann, A., et al., *Insights into polymer versus oligosaccharide synthesis: mutagenesis and mechanistic studies of a novel levansucrase from Bacillus megaterium*. Biochemical Journal, 2007. **407**(2): p. 189-198.
56. Liu, C., et al., *Isolation, structural characterization and immunological activity of an exopolysaccharide produced by Bacillus licheniformis 8-37-0-1*. Bioresource Technology, 2010. **101**(14): p. 5528-5533.
57. Caputi, L., et al., *Biomolecular Characterization of the Levansucrase of Erwinia amylovora, a Promising Biocatalyst for the Synthesis of Fructooligosaccharides*. Journal of Agricultural and Food Chemistry, 2013. **61**(50): p. 12265-12273.
58. Yanase, H., et al., *Identification of Functionally Important Amino Acid Residues in Zymomonas mobilis Levansucrase*. The Journal of Biochemistry, 2002. **132**(4): p. 565-572.
59. Strube, C.P., et al., *Polysaccharide Synthesis of the Levansucrase SacB from Bacillus megaterium Is Controlled by Distinct Surface Motifs*. 2011. **286**(20): p. 17593-17600.

60. Anwar, M.A., et al., *The role of conserved inulosucrase residues in the reaction and product specificity of Lactobacillus reuteri inulosucrase*. 2012. **279**(19): p. 3612-3621.
61. Meng, G. and K. Fütterer, *Donor substrate recognition in the raffinose-bound E342A mutant of fructosyltransferase Bacillus subtilis levansucrase*. BMC Structural Biology, 2008. **8**(1): p. 16.
62. Martínez-Fleites, C., et al., *Crystal structure of levansucrase from the Gram-negative bacterium Gluconacetobacter diazotrophicus*. Biochemical Journal, 2005. **390**(1): p. 19-27.
63. Wuerges, J., et al., *The crystal structure of Erwinia amylovora levansucrase provides a snapshot of the products of sucrose hydrolysis trapped into the active site*. Journal of Structural Biology, 2015. **191**(3): p. 290-298.
64. Pijning, T., et al., *Crystal Structure of Inulosucrase from Lactobacillus: Insights into the Substrate Specificity and Product Specificity of GH68 Fructansucrases*. Journal of Molecular Biology, 2011. **412**(1): p. 80-93.
65. Heckman, K.L. and L.R. Pease, *Gene splicing and mutagenesis by PCR-driven overlap extension*. Nature Protocols, 2007. **2**: p. 924.
66. Case, D.A., et al., *Amber 14*. 2014.
67. Schwede, T., et al., *SWISS-MODEL: an automated protein homology-modeling server*. Nucleic Acids Research, 2003. **31**(13): p. 3381-3385.
68. Gordon, J.C., et al., *H++: a server for estimating pKa's and adding missing hydrogens to macromolecules*. Nucleic Acids Research, 2005. **33**(suppl_2): p. W368-W371.
69. Guex, N. and M.C. Peitsch, *SWISS-MODEL and the Swiss-Pdb Viewer: An environment for comparative protein modeling*. ELECTROPHORESIS, 1997. **18**(15): p. 2714-2723.
70. Frisch, M., et al., *Gaussian 09, revision a. 02, gaussian. Inc.*, Wallingford, CT, 2009. **200**.
71. Trott, O. and A.J. Olson, *AutoDock Vina: Improving the speed and accuracy of docking with a new scoring function, efficient optimization, and multithreading*. Journal of Computational Chemistry, 2010. **31**(2): p. 455-461.

72. Davies, G.J., K.S. Wilson, and B. Henrissat, *Nomenclature for sugar-binding subsites in glycosyl hydrolases*. The Biochemical journal, 1997. **321 (Pt 2)**(Pt 2): p. 557-559.
73. van Hijum, S.A.F.T., M.J.E.C. van der Maarel, and L. Dijkhuizen, *Kinetic properties of an inulosucrase from Lactobacillus reuteri 121*. 2003. **534**(1-3): p. 207-210.
74. Sitthiyotha, T., R. Pichyangkura, and S. Chunsrivirod, *Molecular dynamics provides insight into how N251A and N251Y mutations in the active site of Bacillus licheniformis RN-01 levansucrase disrupt production of long-chain levan*. PLOS ONE, 2018. **13**(10): p. e0204915.
75. He, C., et al., *Rational designed mutagenesis of levansucrase from Bacillus licheniformis 8-37-0-1 for product specificity study*. 2018. **102**(7): p. 3217-3228.
76. Charoenwongpaiboon, T., et al., *Modulation of fructooligosaccharide chain length and insight into the product binding motif of Lactobacillus reuteri 121 inulosucrase*. Carbohydrate Polymers, 2019. **209**: p. 111-121.
77. Bhardwaj, G., et al., *Accurate de novo design of hyperstable constrained peptides*. Nature, 2016. **538**: p. 329.
78. Leaver-Fay, A., et al., *Chapter nineteen - Rosetta3: An Object-Oriented Software Suite for the Simulation and Design of Macromolecules*, in *Methods in Enzymology*, M.L. Johnson and L. Brand, Editors. 2011, Academic Press. p. 545-574.
79. O'Meara, M.J., et al., *Combined Covalent-Electrostatic Model of Hydrogen Bonding Improves Structure Prediction with Rosetta*. Journal of Chemical Theory and Computation, 2015. **11**(2): p. 609-622.
80. Bazzoli, A., S.P. Kelow, and J. Karanicolas, *Enhancements to the Rosetta Energy Function Enable Improved Identification of Small Molecules that Inhibit Protein-Protein Interactions*. PLOS ONE, 2015. **10**(10): p. e0140359.
81. Poultney, C.S., et al., *Rational Design of Temperature-Sensitive Alleles Using Computational Structure Prediction*. PLOS ONE, 2011. **6**(9): p. e23947.
82. Charoenwongpaiboon, T., et al., *Highly porous core-shell chitosan beads with superb immobilization efficiency for Lactobacillus reuteri 121 inulosucrase and*

- production of inulin-type fructooligosaccharides*. RSC Advances, 2018. **8**(30): p. 17008-17016.
83. Ozimek, L.K., et al., *Single amino acid residue changes in subsite – 1 of inulosucrase from Lactobacillus reuteri 121 strongly influence the size of products synthesized*. 2006. **273**(17): p. 4104-4113.
84. Kanjanatanin, P., et al., *Computational design of Bacillus licheniformis RN-01 levansucrase for control of the chain length of levan-type fructooligosaccharides*. International Journal of Biological Macromolecules, 2019. **140**: p. 1239-1248.
85. Miklos, Aleksandr E., et al., *Structure-Based Design of Supercharged, Highly Thermoresistant Antibodies*. Chemistry & Biology, 2012. **19**(4): p. 449-455.
86. Xia, Y., et al., *Improving the Thermostability and Catalytic Efficiency of the Subunit-Fused Nitrile Hydratase by Semi-Rational Engineering*. 2018. **10**(6): p. 1370-1375.
87. Jiang, R., et al., *One-Step Bioprocess of Inulin to Product Inulo-Oligosaccharides Using Bacillus subtilis Secreting an Extracellular Endo-Inulinase*. 2019. **187**(1): p. 116-128.
88. Hyun Kim, D., et al., *Production of inulo-oligosaccharides using endo-inulinase from a pseudomonas sp.* 1997. **19**(4): p. 369-372.
89. Kralj, S., et al., *Synthesis of fructooligosaccharides (FosA) and inulin (InuO) by GH68 fructosyltransferases from Bacillus agaradhaerens strain WDG185*. Carbohydrate Polymers, 2018. **179**: p. 350-359.
90. Cai, Q., et al., *Enhanced activity and stability of industrial lipases immobilized onto spherelike bacterial cellulose*. International Journal of Biological Macromolecules, 2018. **109**: p. 1174-1181.
91. Fernandez-Lopez, L., et al., *Effect of protein load on stability of immobilized enzymes*. Enzyme and Microbial Technology, 2017. **98**: p. 18-25.
92. Silva, C., et al., *Practical insights on enzyme stabilization*. Critical Reviews in Biotechnology, 2018. **38**(3): p. 335-350.

93. Schoevaart, R., et al., *Preparation, optimization, and structures of cross-linked enzyme aggregates (CLEAs)*. 2004. **87**(6): p. 754-762.
94. Talekar, S., et al., *Parameters in preparation and characterization of cross linked enzyme aggregates (CLEAs)*. RSC Advances, 2013. **3**(31): p. 12485-12511.
95. Talekar, S., et al., *Novel magnetic cross-linked enzyme aggregates (magnetic CLEAs) of alpha amylase*. Bioresource Technology, 2012. **123**: p. 542-547.
96. Ortiz-Soto, M.E., et al., *Evaluation of cross-linked aggregates from purified Bacillus subtilis levansucrase mutants for transfructosylation reactions*. BMC Biotechnology, 2009. **9**(1): p. 68.
97. Britton, H.T.S. and R.A. Robinson, *CXCVIII.—Universal buffer solutions and the dissociation constant of veronal*. Journal of the Chemical Society (Resumed), 1931(0): p. 1456-1462.
98. Yu, H.W., et al., *Cross-linked enzyme aggregates (CLEAs) with controlled particles: Application to Candida rugosa lipase*. Journal of Molecular Catalysis B: Enzymatic, 2006. **43**(1): p. 124-127.
99. Aytar, B.S. and U. Bakir, *Preparation of cross-linked tyrosinase aggregates*. Process Biochemistry, 2008. **43**(2): p. 125-131.
100. Xu, D.-Y., Y. Yang, and Z. Yang, *Activity and stability of cross-linked tyrosinase aggregates in aqueous and nonaqueous media*. Journal of Biotechnology, 2011. **152**(1): p. 30-36.
101. Sangeetha, K. and T. Emilia Abraham, *Preparation and characterization of cross-linked enzyme aggregates (CLEA) of Subtilisin for controlled release applications*. International Journal of Biological Macromolecules, 2008. **43**(3): p. 314-319.
102. Correia, I., et al., *Vanadate substituted phytase: Immobilization, structural characterization and performance for sulfoxidations*. Journal of Inorganic Biochemistry, 2008. **102**(2): p. 318-329.
103. Fazary, A.E., S. Ismadji, and Y.-H. Ju, *Biochemical studies on native and cross-linked aggregates of Aspergillus awamori feruloyl esterase*. International Journal of Biological Macromolecules, 2009. **44**(3): p. 240-248.

104. Talekar, S., et al., *Porous cross linked enzyme aggregates (p-CLEAs) of Saccharomyces cerevisiae invertase*. 2012. **2**(8): p. 1575-1579.
105. Cha, X., et al., *Inulin with a low degree of polymerization protects human umbilical vein endothelial cells from hypoxia/reoxygenation-induced injury*. *Carbohydrate Polymers*, 2019. **216**: p. 97-106.
106. Garcia-Galan, C., et al., *Potential of Different Enzyme Immobilization Strategies to Improve Enzyme Performance*. 2011. **353**(16): p. 2885-2904.
107. Datta, S., L.R. Christena, and Y.R.S. Rajaram, *Enzyme immobilization: an overview on techniques and support materials*. *3 Biotech*, 2013. **3**(1): p. 1-9.





จุฬาลงกรณ์มหาวิทยาลัย
CHULALONGKORN UNIVERSITY

APPENDIX

Supporting information

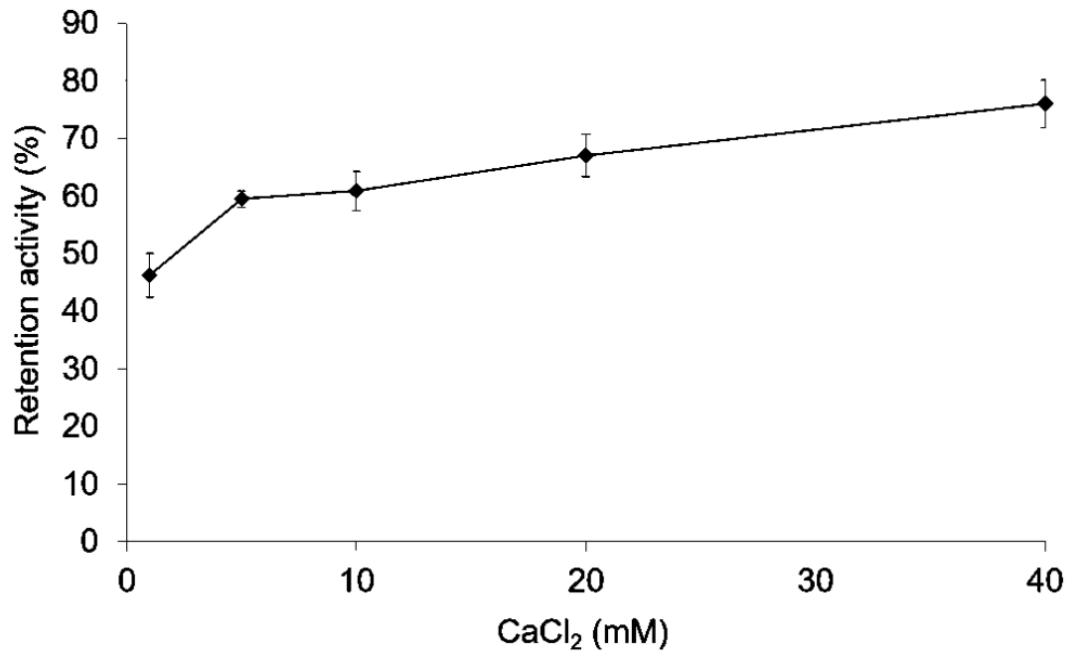


Figure S 1 Effect of CaCl₂ concentration on INU-CSBs stability



Table S 1 List of oligonucleotide primer for site-directed mutagenesis

Primer name	Sequence (5' - 3')
F_Ndel	GGTACATATGCTAGAACGCAAGGAACATAAAAAAAT
R_699HIS	GGTGCTCGAGTTTTAATCCATAACCAATTAAG
F_D478A	CTTTCCAATGCGGATATTAAGAGTCGG
R_D478A	CCGACTCTTAATATCCGCATTGGAAAG
F_D479A	CTTTCCAATGATGCGATTAAGAGTCGG
R_D479A	CCGACTCTTAATCGCATCATTGGAAAG
F_S482A	CAATGATGATATTAAGGCGCGGGCAACTTGG
R_S482A	CCCAAGTTGCCGCGCCTTAATATCATCATTGG
F_R483A	CCAATGATGATATTAAGAGTGC GGCAACTTGGG
R_R483A	CCCAAGTTGCCGCACTCTTAATATCATCATTGG
F_N543A	ACCCGTTTAGCGCGAGGAAGT
R_N543A	ACTTCCTCGCGCTAAACGGGT
F_W551A	TGATGATGCTGCGATGAATGCTAAT
R_W551A	ATTAGCATTATCGCAGCATCATCA
F_N555A	GGATGAATGCTGCGTATGCCGTTGG
R_N555A	CCAACGGCATACGCAGCATTATCC
F_N561A	CCGTTGGTGATGCGGTTGCAATGGTCGG
R_N561A	CCGACCATTGCAACCGCATCACCAACGG
F_D689A	CGTGATAAACCTGTTGCGTGGGACTTAATTGG
R_D689A	CCAATTAAGTCCCACGCAACAGGTTTATCACG
F_R483F	CCAATGATGATATTAAGAGTTTCGCAACTTGGG
R_R483F	CCCAAGTTGCGAACTCTTAATATCATCATTGG
F_R483Y	CCAATGATGATATTAAGAGTTACGCAACTTGGG
R_R483Y	CCCAAGTTGCGTAACTCTTAATATCATCATTGG
F_R483W	CCAATGATGATATTAAGAGTTCCGCAACTTGGG
R_R483W C	CCCAAGTTGCGGAACTCTTAATATCATCATTGG

Table S 2 List of amino acid residues found in the carbohydrate binding site

PDB code	Residues
Levansucrase & Inulosucrase	
1PT2	Glu340, Arg360, Asp86, Trp85, Ser164, Asp247, Arg246
3BYN	Trp85, Ser164, Asp247, Arg246, Asp86, Arg360, Glu340
2YFT	Arg424, Asp425, Ser340, Trp271, Glu522, Arg542, Asp272
β-Fructofuranosidase	
3U14	Trp76, Asn49, Gln68, Asp179, Ser111, Arg178, Glu230, Trp314, Asn254, Ser434, Gln435
5FK7, 5FK8, 5FKB, 5FKC, 5FMD	Gln97, Trp105, Asn79, Asp221, Asp146, Arg220, Glu303, His343, Glu334, Leu170
2OXB	Gln203, Gln39, Ser83, Asp149
2QQU	Asp23, Trp47, Gln39, Ser83, Arg148, Asp149, Glu203, Asp239, Asn22
Fructosyltransferase	
3LDR, 3LEM, 3LIH	Tyr404, Asp60, Arg190, Asp119, Glu292, Ile143, Glu318, Glu405
3UGG, 3UGH	Asp33, Asn60, Trp57, Asp157, Ser93, Glu211, Arg156, Asp244, Gln49, Gln247
Glucansucrase	
3HZ3, 3KLL	Gln1140, Asp1136, Arg1023, His1135, Asp1458, Gln1509, Asn1025, Glu1063, Asn1029, Glu1063, Ser1137
5JBE, 5JBF	Ser1440, Glu1437, Lys1128, Asp112, Ser1577, Asn974, Gly1487, Gly919
Mannanase	
2MAN, 3MAN	Gly260, Asn259, His86, Trp59, Trp30
2VX6, 2VX7	Gln385, Arg374, Trp373, Asp130, His156, His220, Glu338, Glu221, Trp167, Ser268, Tyr297
2WHL, 2WHM	Asn256, Ser257, Trp31, Glu212, His143, His377, Arg361, Trp360, Tyr285
5JU9	Glu45, Ala63, Lys59, Asn126, Ser129, Ala128, Ile173, Arg125
4Y7E	Trp80, Tyr246, Glu178, Gln217, Asn182, Trp215, Thr309, Asn308
1ODZ	Glu212, His143, His377, Arg361, Glu121, Trp360, Tyr285
4CD7	Asn182, His183, Glu151, Asn97, Arg104, Glu231, Glu151, Tyr299, Trp245, Glu282
5AGD	Arg229, Asp239, Asn181, Asp228, Tyr243, Leu295, Asp71, Asp294, Asn125, Asp124, Trp128
4BOJ	Asn181, Asp228, Tyr243, Arg229, Asp239
1PMH	Asn110, Gln161, Lys106
2YIH	Glu187, Thr194, Arg295, Gln243, Glu288
Amylase	
1PIG	Val163, Trp59, Gln63, Leu165, His299, Asp300, Glu240, Lys200, His201, Glu233, His101, His305
1UA3	Val163, Gln63, Trp59, Leu165, Arg195, Glu233, Asp300, Asp197, His101
3L2L	Gly106, Gln63, Glu233, Trp59

Figure S 2 (continued)

1RP8	Val47, His45, Met53, Ala96, Cys95, Ala146, Gln296, His290, Asp291, Arg178, Glu205
1UH2, 1UH3	Asp516, Arg520, His267, Asn356, Arg354, His471, Asp472, Gln396, Asn3, Asp75, Asn68, Thr44
2D0F	Arg520, Asp516, His221, Asp180, Ser182, His267, Asn356, Glu395, Asp472
2BVW	Asp226, Asp180, His271, Asn280, Asn234, Asn310
2FH8,2FHB,2FHC,2FHF	Asp834, Asp890, Thr642, Glu706, Asp677, Asp560, His833, Arg675, Cys643, Arg889, Asn835, Arg737, Asp734, His607, Ser640
1CXL	Arg47, Asp371, Arg375, Asp328, His327, Arg227, Gln257, Trp101
1WO2	His299, Val163, Leu165, Gln63, Trp59, Asp197, Glu233, Ala198, Asp300, Arg195
1MW1	Ser508, Tyr438, Gln437, Asp231
1EO5, 1EO7	Trp101, Arg227, His327, Asp328, Arg375, Ser145, Asp371, Asp147, Ser146, Asn193, Tyr195
1ZS2	Asp394, Arg446, Asp286, His187, Arg509, Asp144, His392, Arg284, Asp393, Gln328
Cellulase	
3QXQ	Asp116, Tyr182, Ser113, Asp110, Asn112, Gly169
3AMM, 3AMP	Trp26, Lys73, Arg60, Asn24, Glu134, Glu231, Tyr180, Thr145, Glu116, Cys134
4M24	Glu135, Arg176, Asp205, Ala206
1CEN	Gln16, His207, Gln140, Glu280, His90, Met318, Trp313, Asp319
2A3H	Trp262, Glu269, His35, Tyr40, Lys267, Tyr66
3CUG, 3CUJ	Glu43, Trp273, Glu127, Glu233, Lys47, His80, Asn44, Gln87, Gln203, Asn172, Arg237, His205
3A3H	Glu139, Tyr202, Asn179, Glu228, Tyr66, Tyr40, Lys267, His35, Glu269, Trp262, Ala234
5OFL, 5OFK	Trp297, His87, Glu46, Gln248, Asn139, Gln140, Asn220, Asn47, Asn186, His218, Lys50, Gln216
1HF6	His101, Tyr66, Asn138, Glu228, Tyr202, Lys267, Tyr40, His35, Glu269, Trp262, Ala234
2CKR	Trp389, Gln355, Tyr330, Glu263, His334, Tyr338, Asp394, Glu192, Arg396, Tyr189
4JCW	Gly21, Glu116, Lys115, Gly117
2WAB, 2WAO	His310, Gln299, Met263
3AZT	Asn20, Trp286, His205, Tyr198, Asn135, His95, Trp30
4D5O, 4D5P, 4D5Q	Asn103, Val104, Asp179, Asn37, Trp38
5CVY	Gln214, Gln219, Glu212, Tyr296, Lys267, Tyr268, Tyr403, Tyr322, Asn224, Thr223, Gln177, Thr106, Glu49, Trp684, Glu38, Asp534
1UU6	Asn22, Asn155, Glu205, Glu120, Tyr132, Trp24

Figure S 2 (continued)	
4B4F	Lys509, Asp176, Lys491, Asn366, Asp497, Glu495, Gly328, His326, Asn282, Asp226, Ser232
β-Galactosidase	
5IHR, 5JUV	Glu200, Gln298, Asn199, Tyr96, Ala141, Asn140, Glu142, Tyr364, Ala237
4DUW	Asp201, His391, Asn460, Glu537, Ser796, Tyr503
1JYN	Asn102, His540, Asp201, Gln537, Glu461
1JZ8	Asn102, His540, Asp201, Glu461, Gln537
Chitinase	
1NH6	Thr276, Trp167, Lys369, Arg446, Trp275, Trp539, Arg172, Glu473
3B9A	Arg173, Trp570, Trp275, Thr276, Trp168, Asp392, Lys370
5GQB	Thr269, Trp268, Trp532, Glu306
4MNK	Asp117, Tyr191, Glu119, Gln331, Trp327



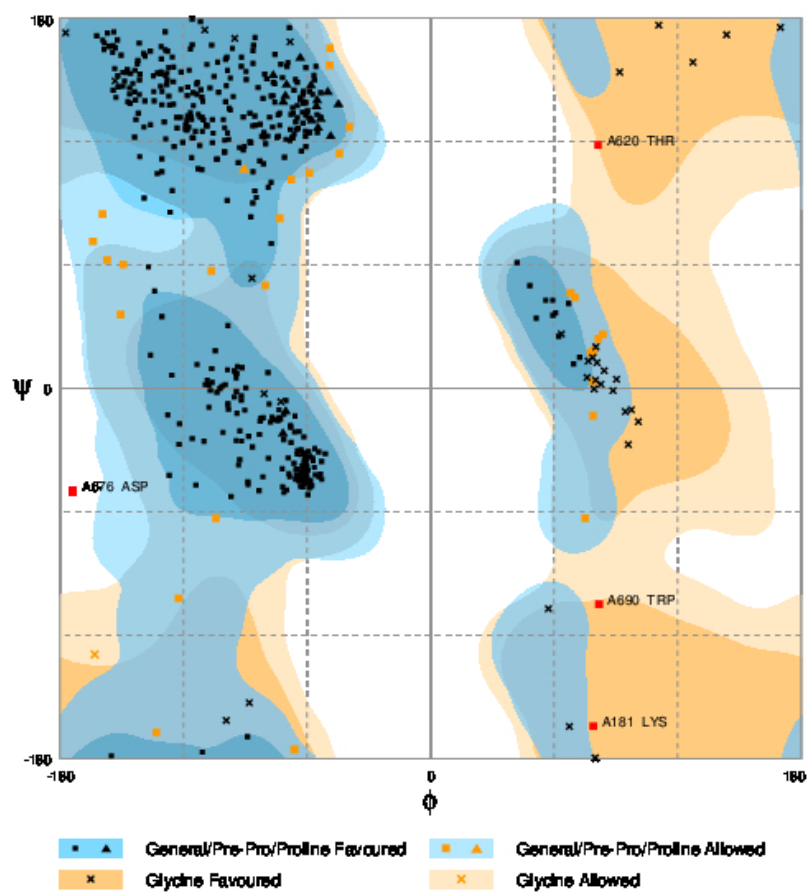


Figure S 2 Ramachandran plot of the homology model of *Lactobacillus reuteri* 121 inulosucrase.



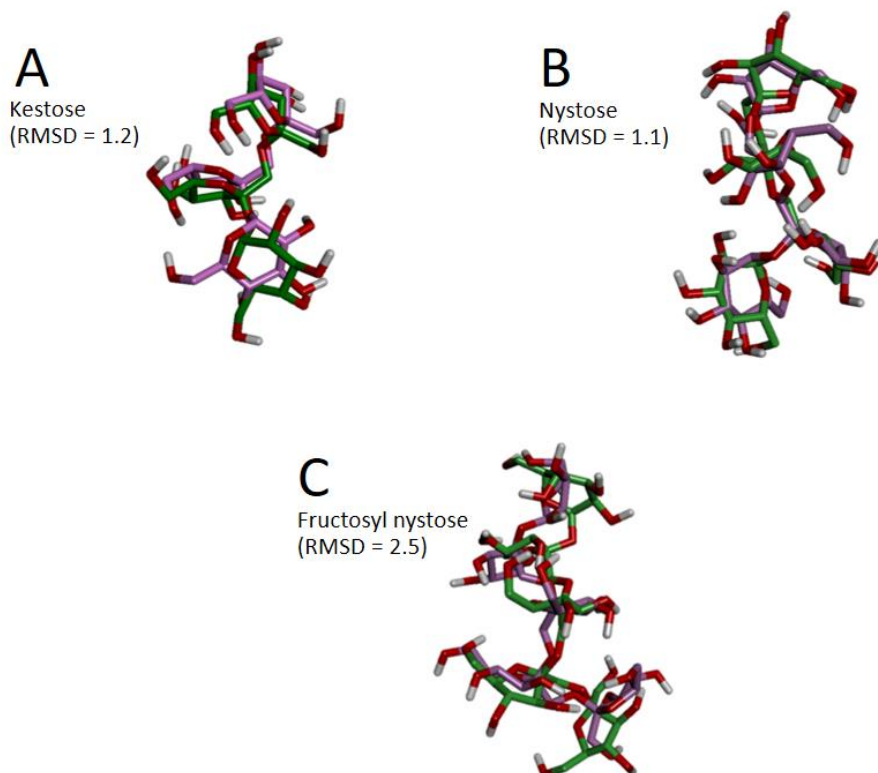


Figure S 3 Superimpositions of the crystal binding conformation (purple) and best docked conformation (green) of GF_2 (A), GF_3 (B) and GF_4 (C).

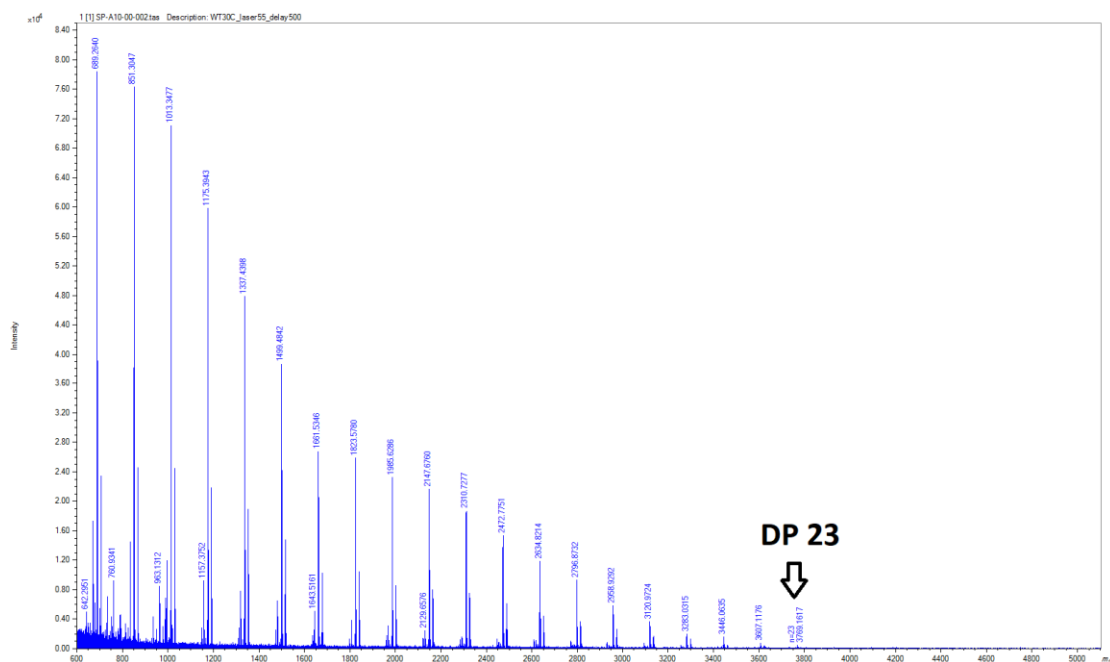


Figure S 4 MALDI-TOF MS analysis of WT inulosucrase oligosaccharide products synthesized at 30°C.

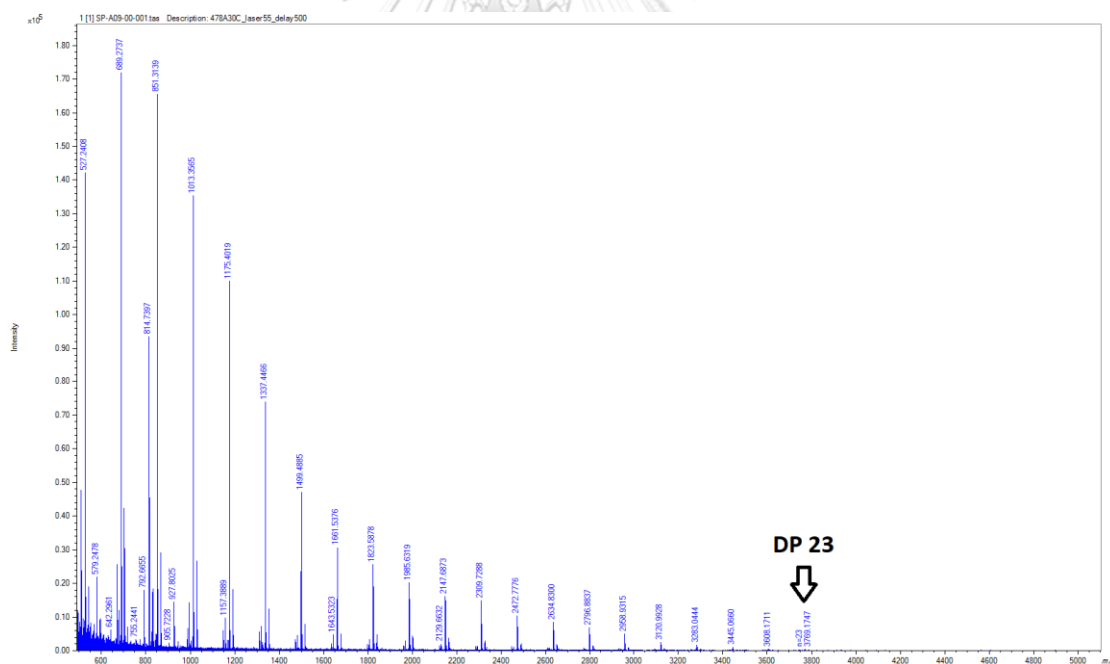


Figure S 5 MALDI-TOF MS analysis of D478A inulosucrase oligosaccharide products synthesized at 30°C.

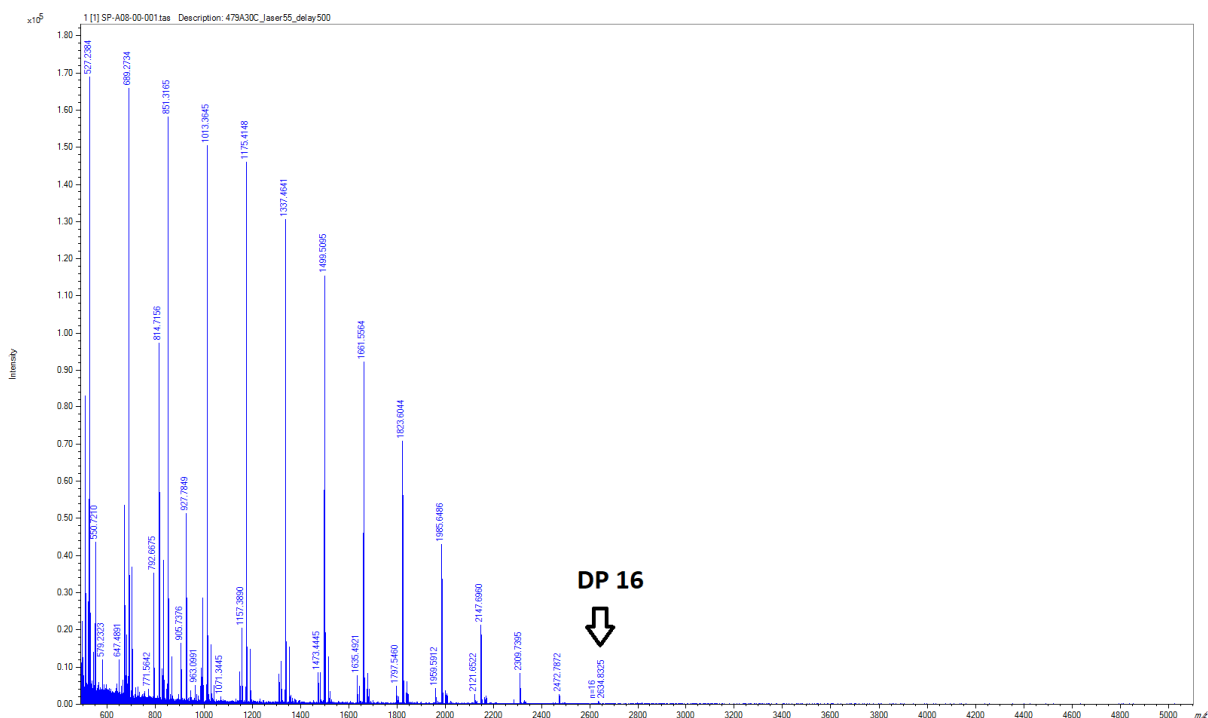


Figure S 6 MALDI-TOF MS analysis of D479A inulosucrase oligosaccharide products synthesized at 30°C.

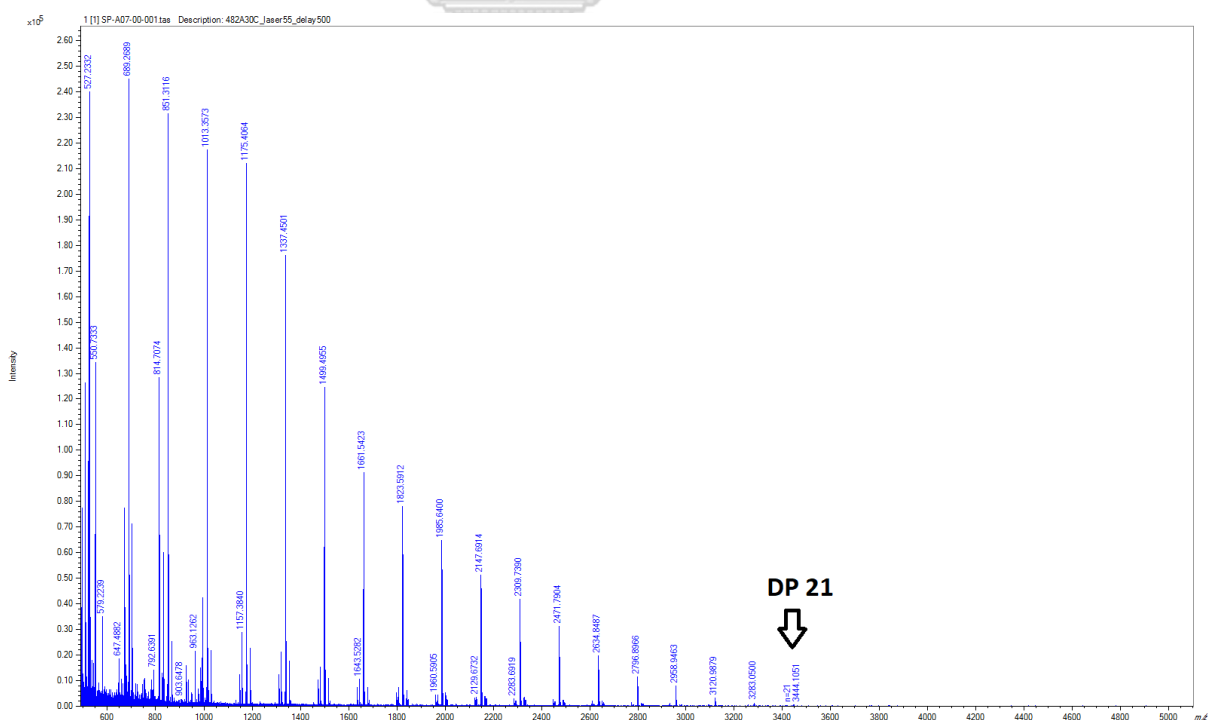


Figure S 7 MALDI-TOF MS analysis of S482A inulosucrase oligosaccharide products synthesized at 30°C.

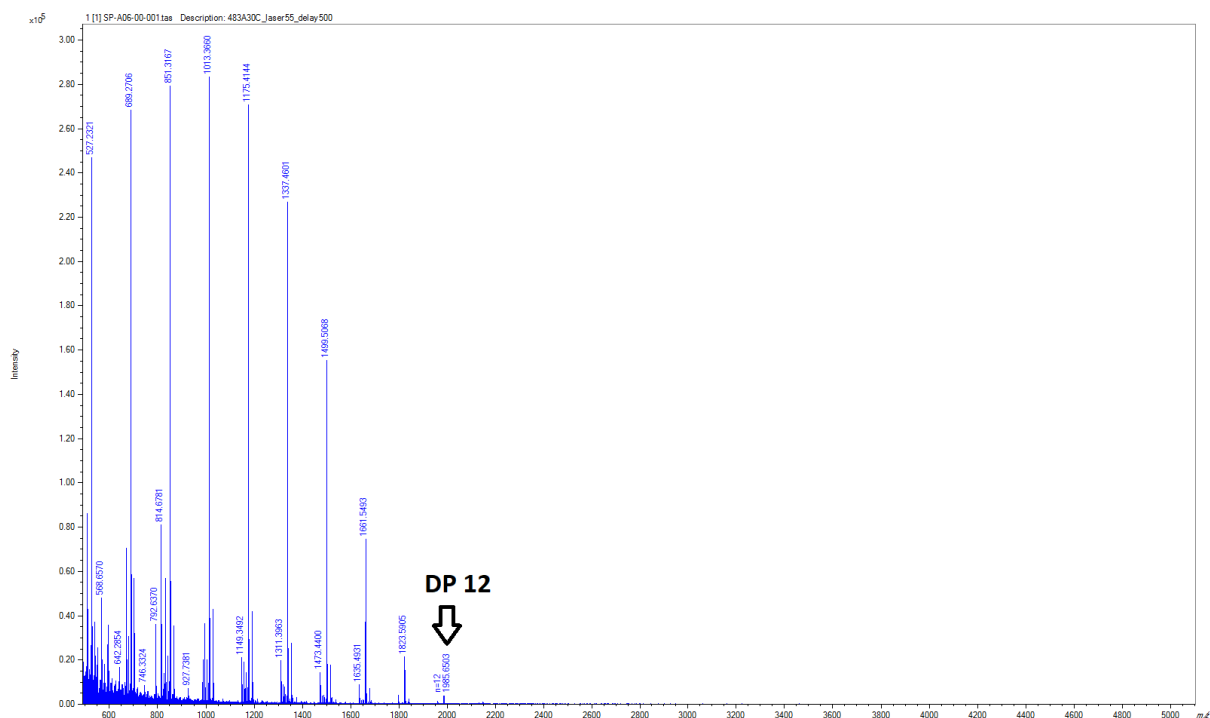


Figure S 8 MALDI-TOF MS analysis of R483A inulosucrase oligosaccharide products synthesized at 30°C

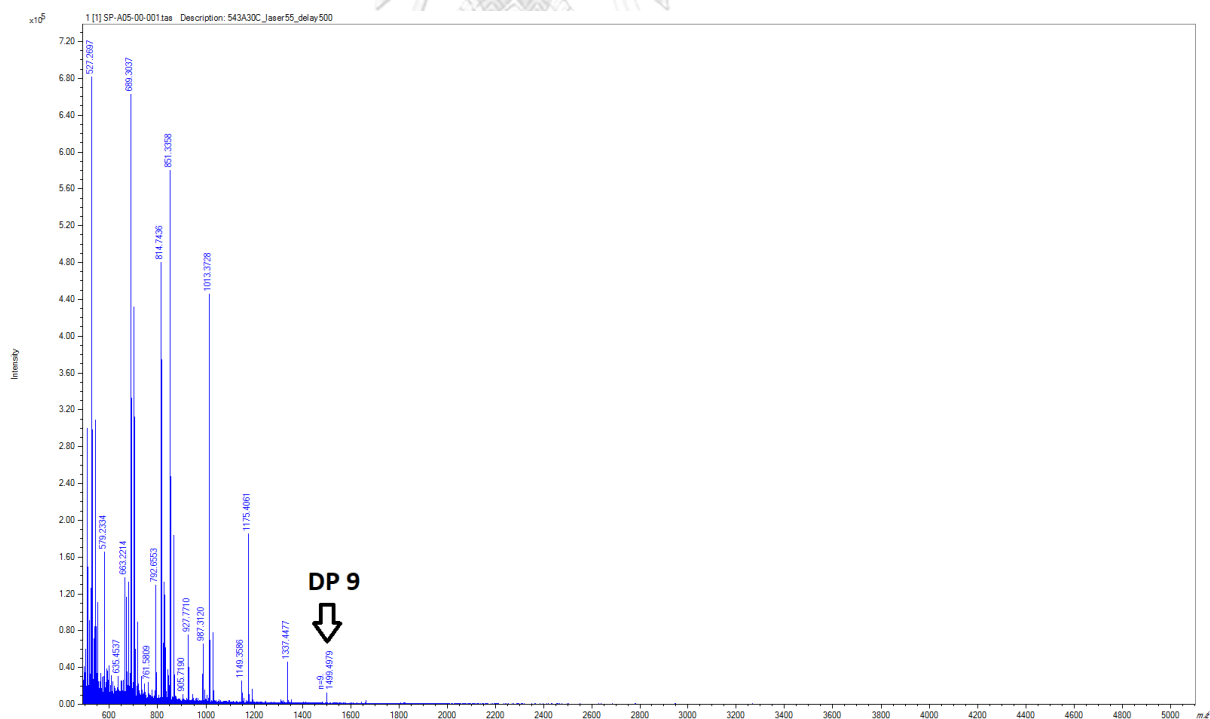


Figure S 9 MALDI-TOF MS analysis of N543A inulosucrase oligosaccharide products synthesized at 30°C

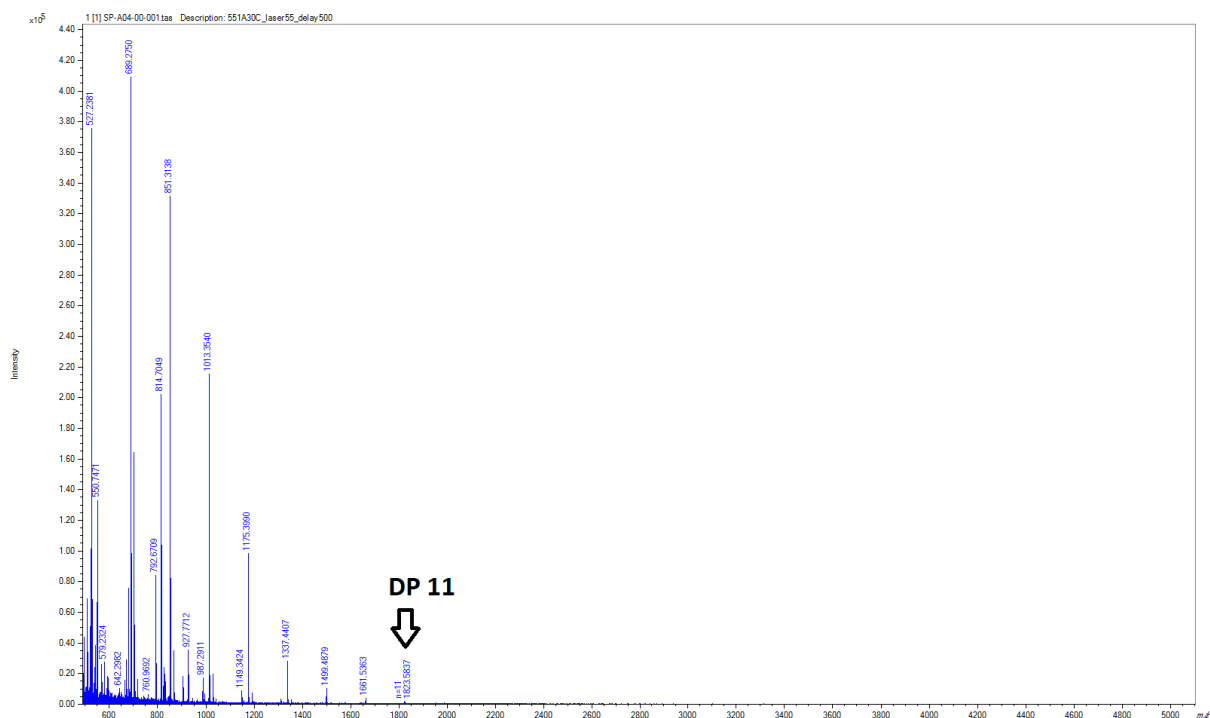


Figure S 10 MALDI-TOF MS analysis of W551A inulosucrase oligosaccharide products synthesized at 30°C

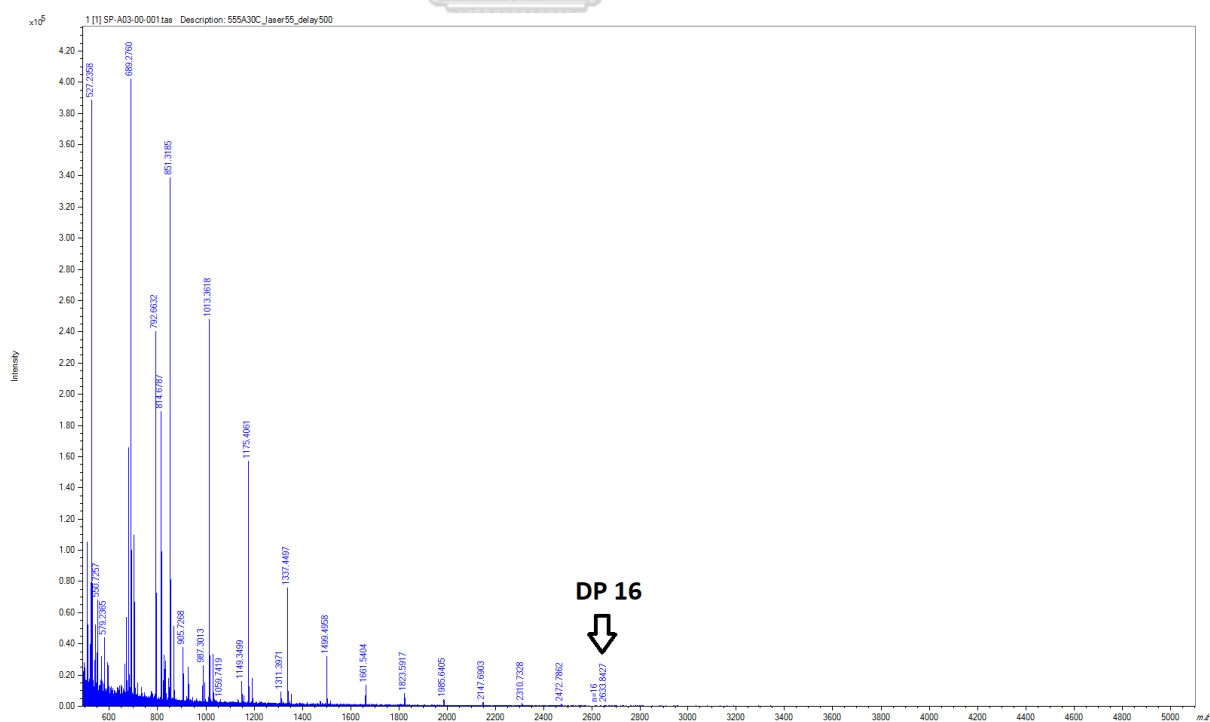


Figure S 11 MALDI-TOF MS analysis of N555A inulosucrase oligosaccharide products synthesized at 30°C

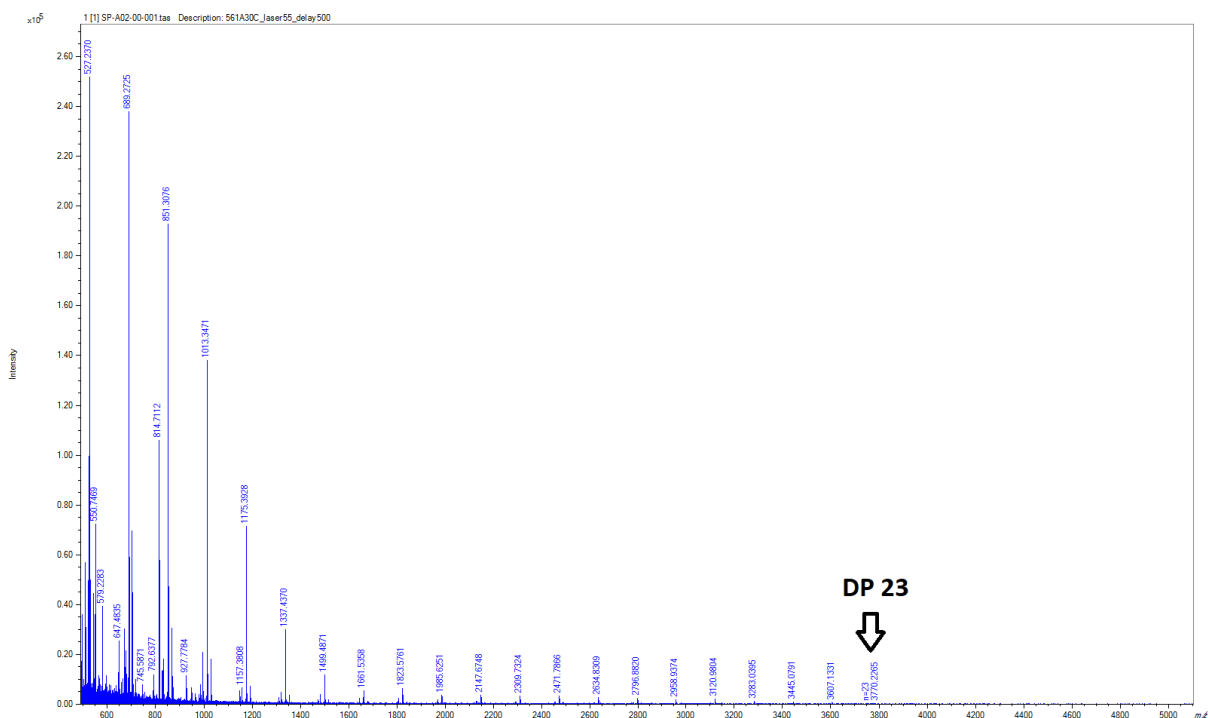


Figure S 12 MALDI-TOF MS analysis of N561A inulosucrase oligosaccharide products synthesized at 30°C

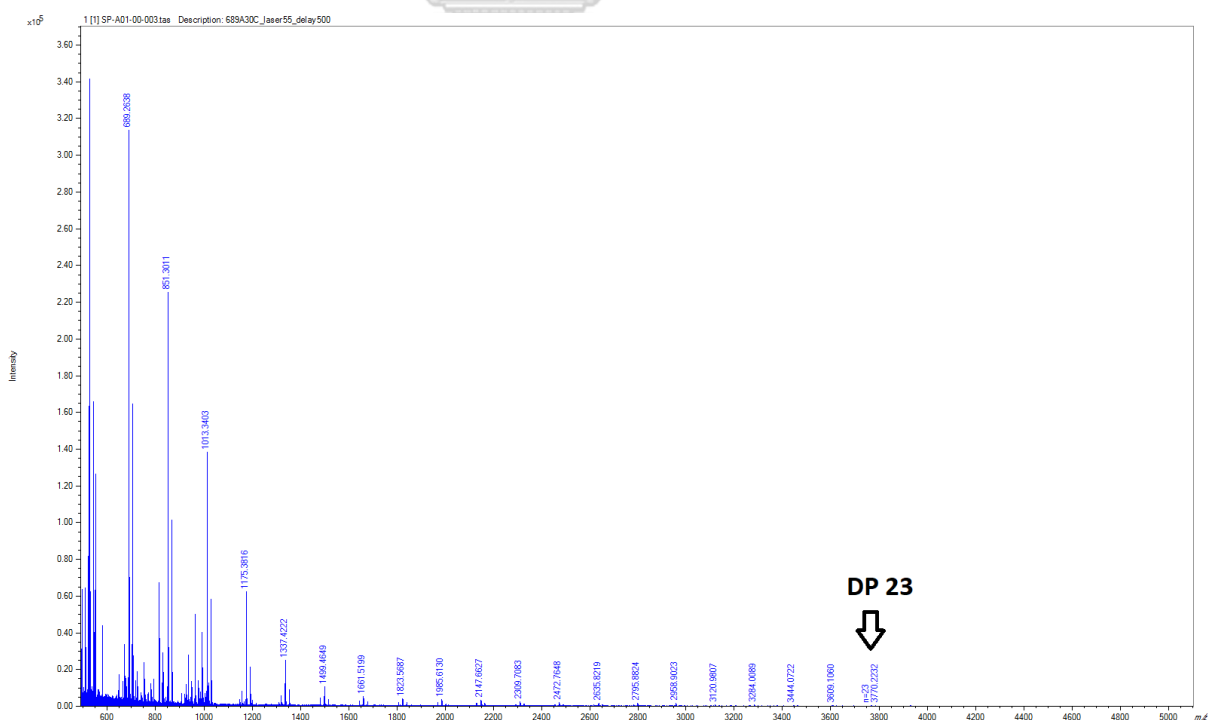


Figure S 13 MALDI-TOF MS analysis of D689A inulosucrase oligosaccharide products synthesized at 30°C

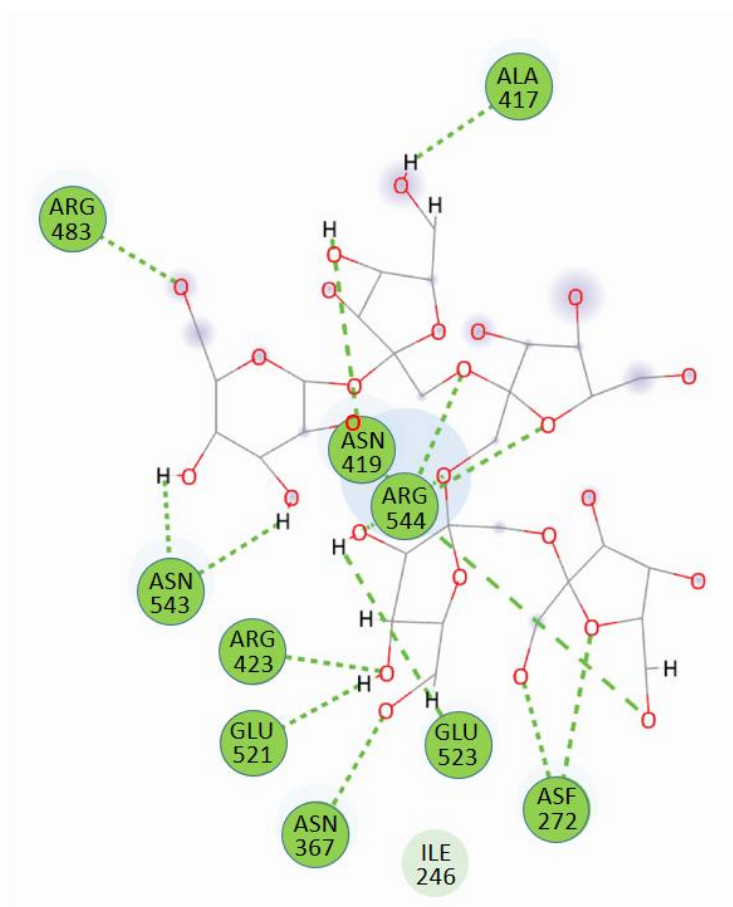


Figure S 14 The interactions between the binding residues of *L. reuteri* 121 inulosucrase and GF4 derived from docking result. ASF is fructosyl-D272 (*fru*-D272).

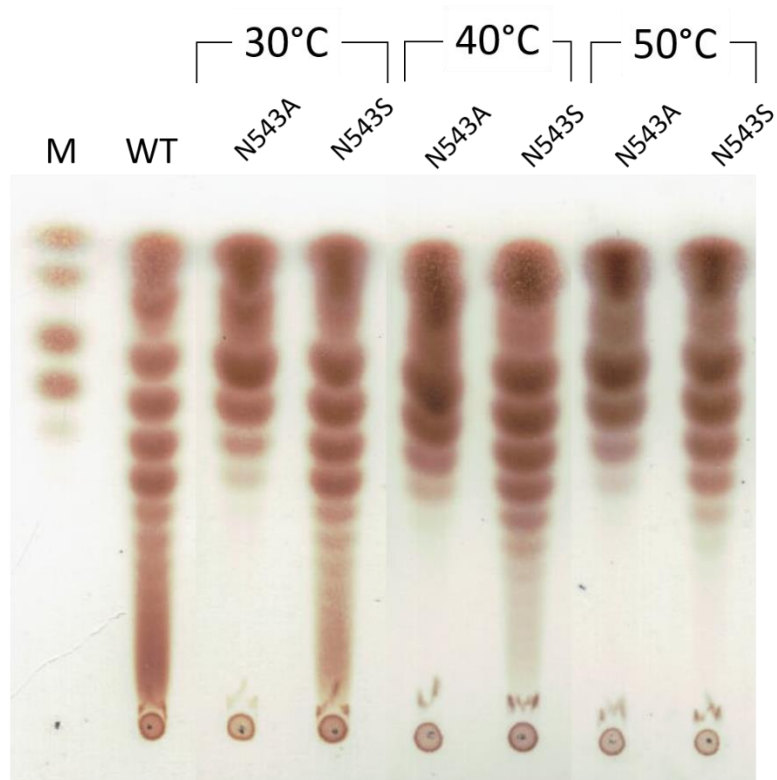


Figure S 15 TLC of FOS products synthesized from N543A and N543S inulosucrase

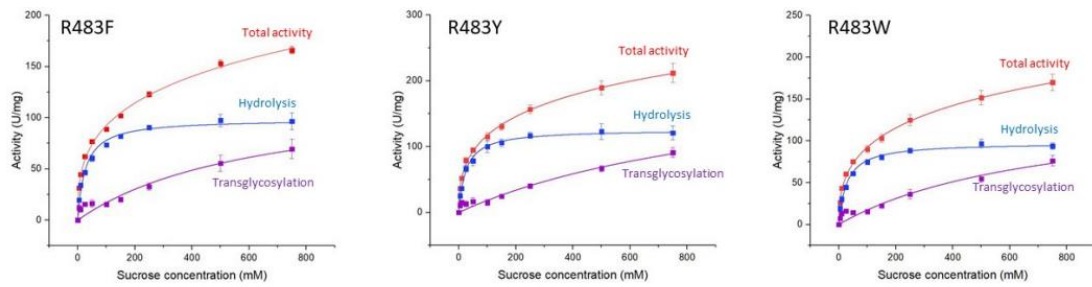


Figure S 16 Graphs of relationship between initial velocity (V) and sucrose concentration for wild-type and mutant inulosucrase. The kinetic parameters were determined based on activity versus sucrose concentration curve, using 'OriginPro' as curve fitting software.



VITA

NAME Thanapon Charoenwongpaiboon

DATE OF BIRTH 23 November 1991

PLACE OF BIRTH Ban Pong, Ratchaburi

INSTITUTIONS ATTENDED B.Sc., (Chemistry) Silpakorn University
Ph.D., (Biochemistry and molecular biology) Chulalongkorn University

HOME ADDRESS 408/37 Village No. 4, Pak Raet Sub-district, Ban Pong District, Ratchaburi Province

PUBLICATION

- Mahalapbutr, P., Wonganan, P., Charoenwongpaiboon, T., Prousoontorn, M. H., Chavasiri, W., & Rungrotmongkol, T. (2019). Enhanced solubility and anticancer potential of mansonone G by β -cyclodextrin-based host-guest complexation: A computational and experimental study. *Biomolecules*, 9(10), 545.
- Kanjanatanin, P., Pichyangkura, R., Sitthiyotha, T., Charoenwongpaiboon, T., Wangpaiboon, K., & Chunsrivirod, S. (2019). Computational design of *Bacillus licheniformis* RN-01 levansucrase for control of the chain length of levan-type fructooligosaccharides. *International Journal of Biological Macromolecules*, 140, 1239-1248.
- Charoenwongpaiboon, T., Pichyangkura, R., Field, R. A., & Prousoontorn, M. H. (2019). Preparation of cross-linked enzyme aggregates (CLEAs) of an inulosucrase mutant for the enzymatic synthesis of inulin-type fructooligosaccharides. *Catalysts*, 9(8), 641.
- Charoenwongpaiboon, T., Wangpaiboon, K., Panpetch, P., Field, R. A., Barclay, J. E., Pichyangkura, R., & Kuttiyawong,

K (2019). Temperature-dependent inulin nanoparticles synthesized by *Lactobacillus reuteri* 121 inulosucrase and complex formation with flavonoids. *Carbohydrate Polymers*, 223, 115044.

- Nopvichai, C., Charoenwongpaiboon, T., Luengluepunya, N., Ito, K., Muanprasat, C., & Pichyangkura, R. (2019). Production and purification of mannan oligosaccharide with epithelial tight junction enhancing activity. *PeerJ*, 7, e7206.

- Wangpaiboon, K., Pitakchatwong, C., Panpetch, P., Charoenwongpaiboon, T., Field, R. A., & Pichyangkura, R. (2019). Modified properties of alternan polymers arising from deletion of SH3-like motifs in *Leuconostoc citreum* ABK-1 alternansucrase. *Carbohydrate Polymers*, 220, 103-109.

- Charoenwongpaiboon, T., Klaewkla, M., Chunsriviro, S., Wangpaiboon, K., Pichyangkura, R., Field, R. A., & Prousoontorn, M. H. (2019). Rational re-design of *Lactobacillus reuteri* 121 inulosucrase for product chain length control. *RSC Advances*, 9(26), 14957-14965.

- Charonwongpaiboon, T., Supraditaporn, K., Klaimon, P., Wangpaiboon, K., Pichyangkura, R., Issaragrisil, S., & Lorthongpanich, C. (2019). Effect of alternan versus chitosan on the biological properties of human mesenchymal stem cells. *RSC Advances*, 9(8), 4370-4379.

- Charoenwongpaiboon, T., Sitthiyotha, T., Ayutthaya, P. P. N., Wangpaiboon, K., Chunsriviro, S., Prousoontorn, M. H., & Pichyangkura, R. (2019). Modulation of fructooligosaccharides chain length and insight into the product binding motif of *Lactobacillus reuteri* 121 Inulosucrase. *Carbohydrate Polymers*, 209, 111-121.

- Wangpaiboon, K., Padungros, P., Nakapong, S., Charoenwongpaiboon, T., Rejzek, M., Field, R. A., & Pichyangkura, R. (2018). An α -1, 6-and α -1, 3-linked glucan produced by *Leuconostoc citreum* ABK-1 alternansucrase with nanoparticle and film-forming properties. *Scientific reports*, 8(1), 8340.

- Charoenwongpaiboon, T., Wangpaiboon, K., Pichyangkura, R., & Prousoontorn, M. H. (2018). Highly porous core-shell chitosan beads with superb immobilization efficiency for *Lactobacillus reuteri* 121 inulosucrase and production of inulin-type fructooligosaccharides. *RSC Advances*, 8(30), 17008-17016.

